

The influence of population size on host-parasite coevolution



Dissertation

in fulfillment of the requirements for the degree *Doctor rerum naturalium*
of the Faculty of Mathematics and Natural Sciences at Kiel University

Submitted by Andrei Papkou

Department of Evolutionary Ecology and Genetics

Zoological Institute, Kiel University

Kiel, 2014

First referee – Prof. Dr. Hinrich Schulenburg

Second referee – Prof. Dr. Joachim Kurtz

Date of oral examination: 3.07.2014

Approved for publication: 3.07.2014

Signed:

Contents

Declaration	iv
Contribution of authors	v
Summary	vii
Zusammenfassung	viii
Introduction	1
I The importance of fluctuations in population size for host-parasite coevolutionary dynamics	8
II Lotka–Volterra dynamics kills the Red Queen	29
III Population size influences the evolutionary trajectories of host-parasite interactions	40
IV The selective benefit of toxins during pathogen coevolution with a host	78
Curriculum vitae	135
Acknowledgments	136

Declaration

I, Andrei Papkou, declare that:

- Apart from my supervisor's guidance the content and design of the thesis is all my own work;
- Specific aspects of my thesis were supported by colleagues; their contribution is specified in detail in the Chapter "Contribution of authors" at the beginning of the thesis;
- The thesis has not already been submitted neither partially nor wholly as part of a doctoral degree to another examining body. Apart from the included published paper no other part of the thesis has been published nor submitted for publishing;
- The thesis has been prepared subject to the Rules of Good Scientific Practice of the German Research Foundation.

Contribution of authors

This thesis consists of four chapters, each represented by a publication or unpublished manuscript. Andrei Papkou developed original ideas and wrote the manuscripts with major contribution for CHAPTER I and CHAPTER III, and on collaborative basis for CHAPTER II. For the unpublished study in CHAPTER IV, Andrei Papkou exclusively developed tools and performed the functional analysis of the candidate genes. Hinrich Schulenburg developed original ideas and supervised research in all manuscripts.

CHAPTER I: **Andrei Papkou**, Chaitanya S. Gokhale, Arne Traulsen, Hinrich Schulenburg. “**The importance of fluctuations in population size for host-parasite coevolutionary dynamics**”, unpublished review paper

AP and **HS** conceived the idea. **AP** reviewed the relevant literature and wrote the manuscript. **HS** read and improved the manuscript. **CSG** and **AT** advised the writing but have not seen the final manuscript yet.

CHAPTER II: Chaitanya S. Gokhale, **Andrei Papkou**, Arne Traulsen, Hinrich Schulenburg. “**Lotka-Volterra Dynamics Kills the Red Queen: Population Size Fluctuations and Associated Stochasticity Dramatically Change Host-Parasite Coevolution**”. *BMC Evolutionary Biology* 13 (2013): 254.

HS and **AP** conceived the project. **CSG** and **AT** developed the model and performed simulations. All authors analysed the results and wrote the manuscript. All authors read and approved the final manuscript.

CHAPTER III: **Andrei Papkou**, Rebecca Schalkowski, Mike-Christoph Barg, Ines Braker, Hinrich Schulenburg. “**Population size influences the evolutionary trajectories of host-parasite interactions**”, unpublished manuscript

AP conceived the project, developed original methods, performed the evolution experiment and phenotypical analysis, analysed data and wrote the manuscript. **RS**, **MCB**, **IB** supported the performance of evolution experiment and phenotypical tests. **HS** conceived and supervised the project, analysed data, read and improved the manuscript.

CHAPTER IV: Leila Masri, Antoine Branca, Anna E. Sheppard, **Andrei Papkou**, David Laehnemann, Patrick S. Günther, Swantje Prah, Manja Saebelfeld, Philip R. Crain, Jakob Strauß, Jacqueline Hollensteiner, Heiko Liesegang, Elzbieta Brzuszkiewicz, Rolf Daniel, Nicolaas K. Michiels, Rebecca D. Schulte, Joachim Kurtz, Philip Rosenstiel, Arndt Telschow, Erich Bornberg-Bauer, Hinrich Schulenburg. “**The selective benefit of toxins during pathogen coevolution with a host, unpublished manuscript**”. Part of the manuscript is based on **LEILA MASRI**’s PhD Thesis “Experimental test of the consequences of host-

parasite coevolution of the nematode *Caenorhabditis elegans* and its microparasite *Bacillus thuringiensis*” Kiel 2012

LM conceived, performed, and analysed the evolution experiment, and drafted the manuscript. AB conceived and performed genomic analysis of evolved pathogens, and drafted the manuscript. AES conceived and performed pathogen toxin analysis, and drafted the manuscript. DL, PSG, SP supported performance and analysis of evolution experiment. MS supported pathogen toxin analysis. **AP**, JH performed functional analysis of pathogen toxins. PRC, JS, AT developed, implemented, and analysed the mathematical model. EB, HL, RD supported pathogen whole genome analysis. NKM, RDS, JK contributed to design and analysis of evolution experiment. PR, EBB contributed to genome data analysis. HS conceived and supervised the study, contributed to data analysis, and drafted the manuscript. All authors read and approved the final manuscript.

Hiermit bestätige ich als Betreuer der Arbeit die oben stehenden Angaben

Summary

Host-parasite coevolution is defined as reciprocal adaptation between coexisting hosts and parasites. It associates with strong antagonistic selection, leading to fast changes in fitness-related traits, such as host resistance or parasite virulence, which in turn affects overall host population performance and parasite prevalence. The resulting dynamics of the interaction inherently causes population size fluctuations. Infection outbreaks followed by parasite disappearance, host mass extinctions and periodic oscillations in host and parasite abundance are all examples of changes in population size under natural conditions. These demographic variations enhance stochasticity and affect the process of evolution. Despite a large body of evidence suggesting that fluctuating population size is an inevitable consequence of host-parasite interplay, population size is usually assumed to be constant or infinite (ignoring stochasticity) in current studies on coevolution (CHAPTER I). The main goal of this thesis is to enhance a more realistic view on host-parasite coevolution by theoretically and experimentally testing the influence of fluctuating population size and associated stochasticity. First, together with colleagues, I examined the consequences of changing population size in a theoretical model by relaxing conventionally made assumptions of infinite and constant population size (CHAPTER II). We found that fluctuating population size combined with stochasticity dramatically changed host-parasite coevolution dynamics by (i) greatly increasing fixation rates and, therefore, (ii) preventing continuous genotype oscillations, which in case of infinite or constant population size would sustain (in accordance with negative-frequency dependent selection). As an experimental approach, central for this thesis, I carried out an evolution experiment with two interacting model organisms - the nematode *Caenorhabditis elegans* and the pathogenic bacterium *Bacillus thuringiensis* (CHAPTER III). I developed for this purpose a high-throughput protocol, which allowed propagation of many replicate populations for 23 host generations under three different demographic regimes: small populations (increased stochasticity), large populations (“deterministic” situation), and populations periodically forced to bottlenecks (fluctuating population size). After the experiment, I phenotypically characterized evolved host and parasite populations by exposing them to the ancestral antagonist and found the following evolutionary changes in fitness related-traits: (i) an increase in host fecundity, (ii) a decrease in host survival, and (iii) the accumulation of population divergence in parasite virulence. Additionally, I performed a time-shift experiment by confronting coevolved host and parasite populations from three different time points of the coevolution experiment in all possible combinations in order to infer the temporal dynamics of coevolution. The time-shift experiment revealed (iv) a striking pattern of negative frequency-dependent selection providing the first experimental demonstration of this type of dynamics for experimentally coevolved host and parasite. Moreover, (v) negative frequency-dependent selection was found in large populations and only partially in populations subjected to bottlenecks but not in small populations, suggesting that fluctuating population size and increased stochasticity can alter coevolutionary dynamics, in accordance with the results of the theoretical model. Finally, I performed a functional analysis of two toxin genes of *B. thuringiensis*, which had been identified as candidate genes in a separate evolution experiment, and confirmed their contribution to the pathogenicity of this bacterium (CHAPTER IV). Taken together, my PhD project emphasizes the selective impact of coevolution on trait evolution in both antagonists, especially under large population sizes.

Zusammenfassung

Die Koevolution zwischen Wirt und Parasit stellt einen Prozess reziproker Anpassungen zwischen einem Wirt und einem mit ihm koexistierenden Parasiten dar. Die assoziierte antagonistische Selektion führt im Laufe der Koevolution zu schnellen Veränderungen in Fitness-bestimmenden Merkmalen, beispielsweise der Resistenz des Wirtes oder der Virulenz des Parasiten, was sich auf die Entwicklung der gesamten Wirtspopulation wie auch die Verbreitung des Parasiten auswirkt. Daraus resultierende Dynamik der Interaktion führt nahezu unausweichlich zu einer Veränderung von Populationsgrößen. Der Ausbruch einer Infektionskrankheit gefolgt von einem völligen Verschwinden des Parasiten, Massensterben der Wirtsorganismen und periodische Oszillationen in der Häufigkeit des Parasiten sind Beispiele für sich verändernde Populationsgrößen, wie sie in natürlichen Wirt-Parasit-Interaktionen auftreten. Derart extreme Schwankungen in der Populationsgröße können das Auftreten stochastischer Prozesse steigern und evolutionäre Prozesse beeinflussen. Trotz einer großen Fülle von Indizien, die fluktuierende Populationsgrößen als unausweichliche Folge von Wirt-Parasit-Wechselbeziehungen belegen, wird in derzeitigen Studien zur Koevolution meist eine konstante oder unbegrenzte Populationsgröße ohne stochastische Prozesse angenommen (KAPITEL I). Das vorrangige Ziel dieser Arbeit war es, die Wirt-Parasit-Koevolution unter realitätsnäheren Bedingungen zu betrachten, indem der Einfluss fluktuierender Populationsgrößen und damit verbundener stochastischer Prozesse theoretisch und experimentell getestet wurde. Zunächst untersuchte ich zusammen mit Kooperationspartnern die Auswirkungen sich verändernder Populationsgrößen in einem theoretischen Modell, in welchem wirkklassische Annahmen einer unbegrenzten und konstanten Populationsgröße aufgehoben haben (KAPITEL II). Hierbei kam heraus, dass fluktuierende Populationsgrößen in Verbindung mit stochastischen Prozessen zu einer dramatischen Veränderung der koevolutionären Dynamik führen können und zwar aufgrund: (i) einer stark gesteigerten Fixierungsrate, und daraus folgend (ii) einer Aufhebung kontinuierlicher Genotyp-Oszillationen, wie sie für unbegrenzte oder kontante Populationsgrößen typisch sind (übereinstimmend mit negativ frequenzabhängiger Selektion). Im Zentrum dieser Arbeit stand vor allem ein experimenteller Untersuchungsansatz. Konkret habe ich dabei ein Evolutionsexperiment mit zwei interagierenden Modellorganismen, dem Nematoden *Caenorhabditis elegans* und dem pathogenen Bakterium *Bacillus thuringiensis*, durchgeführt habe (KAPITEL III). Für diesen Ansatz habe ich ein "High-throughput"-Protokoll entwickelt, welches es mir ermöglichte, zahlreiche replikaten Populationen über 23 Wirtsgenerationen unter verschiedenen demographischen Regimen zu untersuchen, inklusive: Kleine Populationen (erhöhte Stochastizität), große Populationen ("deterministische" Situation), und Populationen, die periodische "Bottlenecks" durchliefen (fluktuierende Populationsgröße). Nach Ablauf des Experiments charakterisierte ich phänotypische Eigenschaften der evolvierten Wirts- und Parasitenpopulationen, indem ich sie jeweils mit dem ancestralen Stammes Antagonisten konfrontierte. Ich konnte die folgenden evolutionären Veränderungen Fitness-bestimmender Merkmale aufdecken: (i) Gesteigerte Fekundität des Wirtes, (ii) verringertes Überleben des Wirtes und (iii) gehäufte Divergenz in Virulenz der Par-

asitenpopulationen. Daneben führte ich ein „time-shift“-Experiment durch, indem ich koevolvierte Wirts- und Parasitpopulationen aus von drei verschiedenen Zeitpunkten der Koevolution in allen Kombinationen miteinander konfrontierte, um daraus die zeitliche Evolutionsdynamik abzuleiten. Mit Hilfe dieses “time-shift“-Experiments konnte ich ein auffälliges Muster negativ frequenzabhängiger Selektion aufdecken, und erhielt somit den ersten experimentellen Beweis für diese Art von Selektionsdynamik in experimentell koevolvierten Wirten und Parasiten. Darüber hinaus wurde (v) negativ frequenzabhängige Selektion in großen Populationen gefunden, und nur teilweise in Populationen, welche Bottlenecks ausgesetzt waren, jedoch nicht in kleinen Populationen. Dieses Ergebnis deutet darauf hin, dass fluktuierende Populationsgrößen und erhöhte Stochastizität die evolutionäre Dynamik verändern können, in Übereinstimmung mit den Ergebnissen des theoretischen Modells. Zum Abschluss führte ich eine funktionelle Analyse zweier Toxin-kodierender Gene von *B. thuringiensis* durch, die in einem separaten Evolutionsexperiment als Kandidaten-Gene identifiziert worden waren, und konnte deren Beitrag zur Pathogenität des Bakteriums bestätigen (KAPITEL IV). Insgesamt gesehen belegt meine Doktorarbeit die enorme Selektionsdynamik von Wirt-Parasit Koevolution auf die Veränderung von Merkmalseigenschaften in beiden Antagonisten, insbesondere bei erhöhter Populationsgröße.

Introduction

Parasites are species which inflict harm on other species by living at their expense. Parasites are usually found inside or on the surface of their hosts. They are present in a very wide range of taxonomic groups, including microscopic viruses, bacteria, unicellular eukaryotes and larger organisms like flatworms, nematodes, arthropods and even plants. Almost every free-living species on earth suffers from more than one parasitic species. Such an extreme diversity of parasites and their abundance in nature are the results of many million years of evolution, during which parasites sophisticated their host exploitation strategies. However parasite evolution did not go unreciprocated, because their very high cost on host fitness with host death as an extreme, forced hosts to evolve efficient defense mechanisms. Examples of specialized defenses range from the adaptive immune system of vertebrates[15], R proteins in plants[16], complex immune signaling in invertebrates [9] and the recently discovered antiviral CRISPR/Cas complex in bacteria[17]. In the process of antagonistic evolution, even a small improvement in host resistance would automatically disfavour a certain parasite and promote counter-adaptations. Similarly, increased parasite infectivity would enhance selection for novel host resistance traits. The process of continuous adaptations and counter-adaptations between coexisting host and parasite is referred to as coevolution[1].

Because host-parasite interactions are ubiquitous and associated with high selection pressures, host-parasite coevolution is believed to be one of the main driving forces in biological evolution[1]. Coevolution favours genetic diversity[18, 6] and sexual reproduction[25, 5, 13], accelerates geographical dispersal[10, 4] and adaptation rates[19]. Therefore, understanding of the exact mechanisms involved represents one of the main aims of modern evolutionary biology. However, the highly dynamic and complex nature of antagonistic interaction makes studies of coevolution a particularly challenge. The combination of different evolutionary research approaches proved to be of particular value. Field studies provide essential knowledge about most common but also most striking patterns found in natural host-parasite interactions, serving as a solid basis for building theory on host-parasite coevolution[2, 11, 12]. A modeling approach helps to identify general principles of coevolutionary interactions and formulate falsifiable hypotheses, which can be tested in field studies and controlled laboratory experiments[22, 20]. Though any simulation of biological processes either in laboratory experiments or *in silico* implies reduction of real complexity found in nature, the degree of simplification should not interfere with the research question and generality of obtained results. In this thesis, I tried to highlight one potential gap in our current view on host-parasite coevolution (CHAPTER I), namely, changing population size, and then present first steps towards a better understanding of its role in coevolution using a modelling approach (CHAPTER II) and also experimental evolution (CHAPTER III). As an addition to the latter experimental work, I also

present my contribution to a separate evolution experiment, which was based on a similar evolution experiment and for which I established and applied methods to test the functional relevance of toxin genes identified to be favoured during coevolution using genomic analysis (CHAPTER IV).

As mentioned above, host-parasite coevolution is very dynamic, meaning that evolutionary success of one particular host or parasite genotype can quickly turn into its defeat or even extinction[21]. One of the inevitable consequences of these dynamics is that host and parasite population size are not constant. Instead, coevolving host and parasite rather undergo rapid and dramatic changes in population size[14]. Moreover, even in the absence of evolutionary change, interactions on the ecological level is very likely to result in population size oscillations, similar to predator-prey dynamics described by the classical Lotka-Volterra model. Another important source of population size variation is parasitic life history involving many transmission events, combined with spatial and temporal dynamics in prevalence[24, 23]. Further population size variations may be induced by additional environmental variation, such as that related to food availability or the presence of environmental stressors. Surprisingly, despite many empirical examples documenting population size fluctuations in host-parasite interactions, population size is largely neglected in the current literature on the topic. In CHAPTER I, the most relevant examples are described, followed by a discussion on the potential influence of such fluctuating population sizes on host-parasite coevolutionary dynamics. The most obvious effects of fluctuating population size are reduction in genetic diversity and increased randomness, which can interfere with selection (especially during bottlenecks). Other important consequences of changing population size for coevolution, like changes in fixation probabilities or eco-evolutionary feedback, are more difficult to predict. Therefore, we suggest that additional theoretical and experimental efforts are needed to investigate the role of population size in reciprocal adaptation. While the assumption of constant or infinite population size is very convenient for experimental and theoretical work, a more general and realistic view on natural host-parasite coevolution requires consideration of dynamically changing population size.

CHAPTER II uses a mathematical modelling approach to demonstrate that different assumptions about population size lead to fundamentally different allele fixation rates and, thus, different evolutionary outcomes. Two types of selection dynamics, which are currently used to explain coevolutionary adaptation, have different predictions about fixation rate[1]. One of them, recurrent selective sweeps dynamics, is characterized by fast repeated fixation of alleles in the coevolving species. Host and parasite constantly improve their fitness (and associated traits like resistance and infectivity, respectively) via accumulation of adaptive mutations, resembling an arms race (i.e., arm race dynamics). The second type of dynamics, negative frequency-dependent dynamics, does not lead to fast fixations, as there is no superior parasite mutant which can efficiently infect all host genotypes. Instead, there is always a set of parasite genotypes present, which vary in their abilities to infect host genotypes. Under this scenario, a parasite genotype which is the best in infecting the most common host genotype would temporally prevail. This automatically gives an advantage to rare host genotypes which would, consequently, increase in frequency, favouring

different parasite types. In the long run, negative frequency-dependent dynamics (often termed Red Queen dynamics) results in continuous oscillations of host and parasite genotype frequencies without fixations. In CHAPTER II different mathematical models which vary in the assumptions about population size fluctuations, are used to examine the resulting coevolutionary dynamics. The basic model is identical to most current models used for simulation of negative frequency-dependent dynamics and assumes infinite population size (deterministic model). Additionally we produced two analogous stochastic models, where either constant or changing host and parasite population size was implemented. Deterministic model and stochastic simulations with a constant population size produced negative frequency-dependent genotype oscillations, as expected. In contrast, a more realistic model where population size was allowed to change as a consequence of the antagonistic interaction led to very fast genotype fixation and termination of the frequency oscillations. Interestingly, in the latter case, the fixation probability was higher for an originally rare host genotype under a wide parameter space, suggesting a negative frequency-dependent mode of selection (i.e., a selective advantage of rare genotypes). This finding confirms our original idea that fluctuating population size can alter host-parasite coevolution and emphasizes that the frequently made assumption of constant or infinite population size may be misleading.

Similar to the situation in theoretical research, experimental host-parasite studies usually rely on constant population size. Biological host-parasite systems are getting increasingly popular, as they allow us to connect natural processes and theoretical models by controlling for crucial factors in a laboratory set-up. Forcing host and parasite laboratory species to interact for many generations leads to their reciprocal adaptation. Such experiments, known as experimental coevolution, have been successfully applied to confirm a number of predictions about host-parasite coevolution, for example, evolutionary changes in interaction-relevant traits like host resistance or parasite virulence, increased rates of evolution, local adaptation and rare advantage[3, 7]. However, in coevolution experiments, population size is usually kept constant and often chosen to be large enough to avoid genetic drift, leaving unanswered the question about the impact of extreme variation in population size on coevolutionary dynamics. The central goal of CHAPTER III was to test the influence of population size on antagonistic adaptation by the means of experimental evolution.

In this evolution experiment the impact of increased randomness and strong genetic drift is assessed by comparing evolution in small (100 individuals) and large host populations (3000 host individuals) exposed to a co-adapting or non-changing pathogen. Additionally, as a first step to understanding coevolution under complex demographic dynamics, we simulated fluctuating population size by artificially imposing bottlenecks on the evolving populations. Carrying out experimental coevolution under such different demographic regimes in a consistent and comparable way was based on the versatile and well established *Caenorhabditis elegans* - *Bacillus thuringiensis* host-parasite interaction system[6, 13]. Both model organisms can be easily maintained in the laboratory, purified from mixed cultures, cryopreserved and manipulated genetically. Importantly, the bacterium *B. thuringiensis* is able to infect and multiply inside *C. elegans*, ultimately causing

host death. During my project I improved the available methods for this system by introducing a novel viscous medium, which permitted to perform experimental evolution in microtiter plates in a high-throughput manner.

In CHAPTER III I present the experimental design for the coevolution experiment and detailed phenotypic analysis that allows us to assess temporal dynamics of antagonistic adaptation in the relevant host and parasite traits. The approach used revealed rapid changes in reproduction and survival of coevolved hosts, and an increased differentiation of parasite populations across different demographic regimes. Based on a time-shift exposure of coevolved antagonists from different time points, host and parasite interaction patterns strongly suggest that coevolution has been determined by negative frequency-dependent selection. To my knowledge, these results represent the first demonstration of this type of coevolutionary dynamics for both antagonists. The only previously published empirical example of negative frequency-dependent selection was obtained in a naturally coevolving system for the parasite only[11]. Intriguingly, the negative frequency-dependent selection dynamics are found by us in the large host populations and only partially in the fluctuating populations, but not in small populations. This finding is consistent with the result of stochastic simulations in CHAPTER II, suggesting that increased randomness and changing population size would prevent continuous genotype oscillations induced by negative frequency-dependent selection.

The ultimate goal of any experimental coevolution is to explain observed phenotypic changes by underlying genetic processes. With the development of next-generation sequencing in recent years, it is possible to detect the signatures of selection via population genomic analysis of experimentally evolved lines[9, 8]. Then, if candidate genes are found, they need to be tested in functional analysis, for example by gene knock-out or overexpression. The material generated in the current coevolution experiment has not yet been analyzed genetically, but to illustrate the applicability of genomic and functional analyses, in CHAPTER IV, I report of my contribution to a separate evolution experiment, similarly based on the *B. thuringiensis*-*C. elegans* interaction model. In this particular experiment performed by Leila Masri, coevolution with the host was found to favour the maintenance of one parasite plasmid encoding virulence factors. My contribution to this study was to assess the functional relevance of the two toxin genes located on the plasmid. For this purpose, the virulence of *B. thuringiensis* either genetically modified to express these toxins or supplemented with heterologously expressed toxins was compared to strains lacking the toxins. The results demonstrated that these genes indeed represent important virulence factors for this bacterial pathogen. A similar strategy can be used for analysis and validation of the genetic basis of coevolved *B. thuringiensis* from other evolution experiments.

References

- [1] Mark E. J. Woolhouse, Joanne P. Webster, Esteban Domingo, Brian Charlesworth, and Bruce R. Levin. Biological and biomedical implications of the co-evolution of pathogens and their hosts. *Nature Genetics*, 32(4):569–577, December 2002.
- [2] Frank Fenner and Bernardino Fantini. *Biological Control of Vertebrate Pests: The History of Myxomatosis - an Experiment in Evolution*. CABI, New York, NY, USA, first edition, December 1999.
- [3] Tadeusz J. Kawecki, Richard E. Lenski, Dieter Ebert, Brian Hollis, Isabelle Olivieri, and Michael C. Whitlock. Experimental evolution. *Trends in Ecology & Evolution*, 27(10):547–560, October 2012.
- [4] Michael A Brockhurst, Andrew D Morgan, Andrew Fenton, and Angus Buckling. Experimental coevolution with bacteria and phage: the pseudomonas fluorescens–phi2 model system. *Infection, Genetics and Evolution: Journal of Molecular Epidemiology and Evolutionary Genetics in Infectious Diseases*, 7(4):547–552, July 2007.
- [5] Levi T. Morran, Olivia G. Schmidt, Ian A. Gelarden, Raymond C. Parrish, and Curtis M. Lively. Running with the red queen: Host-parasite coevolution selects for biparental sex. *Science*, 333(6039):216–218, July 2011.
- [6] Rebecca D. Schulte, Carsten Makus, Barbara Hasert, Nico K. Michiels, and Hinrich Schulenburg. Multiple reciprocal adaptations and rapid genetic change upon experimental coevolution of an animal host and its microbial parasite. *Proceedings of the National Academy of Sciences*, 107(16):7359–7364, April 2010.
- [7] Michael A. Brockhurst and Britt Koskella. Experimental coevolution of species interactions. *Trends in Ecology & Evolution*, 28(6):367–375, June 2013.
- [8] Nelson E. Martins, Vítor G. Faria, Viola Nolte, Christian Schlötterer, Luis Teixeira, Élio Sucena, and Sara Magalhães. Host adaptation to viruses relies on few genes with different cross-resistance properties. *Proceedings of the National Academy of Sciences*, page 201400378, April 2014.
- [9] Justin R. Meyer, Devin T. Dobias, Joshua S. Weitz, Jeffrey E. Barrick, Ryan T. Quick, and Richard E. Lenski. Repeatability and contingency in the evolution of a key innovation in phage lambda. *Science*, 335(6067):428–432, January 2012. PMID: PMC3306806.
- [10] A. Buckling and P. B. Rainey. Antagonistic coevolution between a bacterium and a bacteriophage. *Proceedings of the Royal Society of London. Series B: Biological Sciences*, 269(1494):931–936, May 2002.
- [11] Ellen Decaestecker, Sabrina Gaba, Joost A. M. Raeymaekers, Robby Stoks, Liesbeth Van Kerckhoven, Dieter Ebert, and Luc De Meester. Host–parasite

- ‘Red Queen’ dynamics archived in pond sediment. *Nature*, 450(7171):870–873, November 2007.
- [12] Dieter Ebert. Host-parasite coevolution: Insights from the daphnia-parasite model system. *Current Opinion in Microbiology*, 11(3):290–301, June 2008.
- [13] Leila Masri, Rebecca D. Schulte, Nadine Timmermeyer, Stefanie Thanisch, Lena Luise Crummenerl, Gunther Jansen, Nico K. Michiels, and Hinrich Schulenburg. Sex differences in host defence interfere with parasite-mediated selection for outcrossing during host–parasite coevolution. *Ecology Letters*, 16(4):461–468, April 2013.
- [14] R. M. May and R. M. Anderson. Epidemiology and genetics in the coevolution of parasites and hosts. *Proceedings of the Royal Society B: Biological Sciences*, 219(1216):281–313, October 1983.
Cell counter.
- [15] Max D. Cooper and Matthew N. Alder. The evolution of adaptive immune systems. *Cell*, 124(4):815–822, February 2006.
- [16] Peter N. Dodds and John P. Rathjen. Plant immunity: towards an integrated view of plant–pathogen interactions. *Nature Reviews Genetics*, 11(8):539–548, August 2010.
- [17] Philippe Horvath and Rodolphe Barrangou. CRISPR/Cas, the immune system of bacteria and archaea. *Science*, 327(5962):167–170, January 2010.
- [18] K. M. Wegner, T. B. H. Reusch, and M. Kalbe. Multiple parasites are driving major histocompatibility complex polymorphism in the wild. *Journal of Evolutionary Biology*, 16(2):224–232, March 2003.
- [19] Steve Paterson, Tom Vogwill, Angus Buckling, Rebecca Benmayor, Andrew J Spiers, Nicholas R Thomson, Mike Quail, Frances Smith, Danielle Walker, Ben Libberton, Andrew Fenton, Neil Hall, and Michael A Brockhurst. Antagonistic coevolution accelerates molecular evolution. *Nature*, 464(7286):275–278, March 2010.
- [20] S. Gandon, A. Buckling, E. Decaestecker, and T. Day. Host–parasite coevolution and patterns of adaptation across time and space. *Journal of Evolutionary Biology*, 21(6):1861–1866, 2008.
- [21] Sonia Altizer, Drew Harvell, and Elizabeth Friedle. Rapid evolutionary dynamics and disease threats to biodiversity. *Trends in Ecology & Evolution*, 18(11):589–596, November 2003.
- [22] Anil Agrawal and Curtis M. Lively. Infection genetics: gene-for-gene versus matching-alleles models and all points in between. *Evolutionary Ecology Research*, 4(1):79–90, 2002.
- [23] Mark E. J. Woolhouse, Louise H. Taylor, and Daniel T. Haydon. Population biology of multihost pathogens. *Science*, 292(5519):1109–1112, May 2001.

References

- [24] Bryan T. Grenfell, Oliver G. Pybus, Julia R. Gog, James L. N. Wood, Janet M. Daly, Jenny A. Mumford, and Edward C. Holmes. Unifying the epidemiological and evolutionary dynamics of pathogens. *Science*, 303(5656):327–332, January 2004.
- [25] Curtis M. Lively and Jukka Jokela. Temporal and spatial distributions of parasites and sex in a freshwater snail. *Evolutionary ecology research*, 4(2):219–226, 2002.

Part I.
The importance of fluctuations
in population size for
host-parasite coevolutionary
dynamics

Andrei Papkou, Chaitanya Gokhale, Arne Traulsen, Hinrich Schulenburg

Host-parasite coevolution is widely believed to have a major influence on biological evolution, especially as these interactions impose high selective pressure on the reciprocally interacting antagonists. The exact nature of the underlying dynamics are yet under debate and may be determined by recurrent selective sweeps (i.e., arms race dynamics), negative frequency-dependent selection, overdominant selection, or a combination thereof. In all cases, the interactions are inherently associated with reciprocally induced changes in population size, which should have a major impact on co-adaptation processes, yet are neglected in almost all current work at both empirical and theoretical levels. We here suggest that the consideration of these population size fluctuations is key for full appreciation of the coevolutionary dynamics and, thus, a more realistic view on the complex nature of species interactions.

Introduction

Over past decades host-parasite coevolution has received particular scientific interest because it associates with high selective constraints, resulting in very fast and complex dynamics, influencing the evolution of a variety of trait functions[1]. On the one hand, dramatic reduction in host fitness due to infection ensures strong selection for a more resistant host[64]. On the other hand, different host defence strategies impose high selection pressure on a parasite. Genetic variants (alleles) conferring an advantage in the antagonistic interaction can be rapidly fixed[45, 65]. A series of fixation events occurring in parallel in host and parasite populations results in recurrent selective sweeps (RSS) or arms race dynamics. Alternatively, a beneficial allele is not readily fixed because it either has an additional adverse effect (cost) or provides an advantage exclusively when facing a specific antagonist genotype. In this case, several alleles can coexist over a longer time period. A shift in genetic composition of the host would cause an adequate change in the parasite population and vice versa, leading to continuous negative frequency-dependent allele oscillations (i.e, negative frequency-dependent selection, NFDS), which are often referred to as Red Queen dynamics [46, 47].

Both types of selection dynamics, RSS and NFDS, are supported by empirical studies[45, 46], but their exact role in natural host-parasite interactions is not fully understood. Different factors have been proposed to shape the coevolutionary dynamics[84], such as genetic diversity[73], the genetic system of the interaction[74], different aspects of life history[66], metapopulation structure[71, 72], and fluctuating environmental changes[57]. Paradoxically, one fundamental outcome of host-parasite interaction, namely continuously changing population size, is usually not taken into account. In fact, allele frequencies and a number of individuals change simultaneously, as part of the integral process of host-parasite coevolution, generating a shift in the genetic composition as well as population size. Temporal fluctuations in population size should have a strong effect on density-dependent parameters of infection, genetic diversity, selection-drift interplay and, ultimately, on coevolution dynamics.

Considering that host-parasite interactions are inherently associated with dramatic changes in population size (SECTION 1), and that such changes are often additionally an intrinsic part of epidemiological processes (e.g., transmission bottleneck, SECTION 2), it is extremely important to elucidate their role in reciprocal adaptation between host and parasite. Surprisingly, the effect of population size is usually neglected in theoretical models of coevolution and kept constant, where possible, in experimental systems. In this paper, we review the evidence for population size fluctuations during host-parasite interactions and discuss their

consequences for coevolution (SECTION 3). We argue that considering population size variation as a part of host-parasite interactions will facilitate a better understanding of the underlying dynamics and the resulting changes at both phenotypic and genetics levels (SECTION 4).

1 Population size fluctuations are a direct consequence of reciprocal host-parasite interactions

By definition, a parasite reduces host fitness through its negative effect on host survival and reproduction[64, 75, 76]. Therefore, host exploitation leads to a decrease in host population size. At the same time, a reduction in host abundance automatically leads to shrinkage of the niche (resources) for the parasite. The principle of mutual dependence of population sizes among antagonistically interacting species was formalized by Lotka and Volterra almost 90 years ago as a set of differential equations (known as the Lotka-Volterra model)[43, 44]. The Lotka-Volterra model produces periodic cycles in host (prey) population size tracked by cycles in parasite (predator) abundance (Figure 1A). In accordance with theoretical predictions, comprehensive evidence from field studies show temporally cycling patterns in host and parasite population sizes[50, 25, 28]. Some examples are listed in Table 1 and more can be found elsewhere[50, 75, 76].

Activity of parasites is considered to be one of the determinants of species abundance [29]. However, in practice it is often difficult to disentangle the effect caused by parasites from those produced by other factors, like random and seasonal changes in environment, density regulation, interactions with other species. Thus, proof-of-principle experiments in controlled settings were carried out previously (see Table 1). In Utida's classical experiment, the host azuki bean weevil and its parasitoid wasp were propagated in a laboratory for many generations with characteristic cyclic oscillations in population size (Figure 1B)[23]. Another type of experiment was performed in wild populations of red grouse where anthelmintic treatment succeeded in removing the population cycles, which are otherwise induced by the parasitic nematode (Figure 1C)[30]. This particular result demonstrates that host population size can be regulated by parasites, but generalizations to a broader context are still being discussed (see[29, 92]).

Host-parasite interactions are not uniform in time and space, as acknowledged by the geographic mosaic theory of coevolution[77]. The above examples may thus refer to only a very specific, endemic situation within the geographic mosaic, which is characterized by the continuous presence of a particular parasite in a particular host population and infection of a considerable proportion of host individuals. In reality, however, a parasite can be absent or present at very low numbers (for example, if only a small proportion of hosts is susceptible) and only occasionally invade host populations, possibly resulting in a dramatic spread of the parasite (i.e., an epidemic). Such infectious dynamics are commonly described by epidemiological models[78], and their predicted consequences range from a parasite failure to host extinction and from sustained oscillations to chaos dynamics[41, 42, 81, 79]. A similarly wide variety of outcomes has also been reported in empirical studies (see Table 1). Importantly, in case of a dramatic impact, the reduction in host abundance is likely to coincide with the highest selection intensities (e.g., in a coevolutionary 'hot spots'). In contrast, when only

few hosts are infected or host performance is not strongly compromised, the epidemic would not affect host allele frequencies (coevolution 'cold spot'). Similarly, in situations with spatial heterogeneity, localities with high parasitic prevalence are more likely to be an arena of evolutionary as well as demographic changes.

We conclude that host-parasite interactions inherently generate population size perturbations, and that the geographic mosaic is expected to encompass a potentially complex network of populations with either high or low rates of allele frequency as well as population size changes.

2 Bottlenecks as components of a parasite's life cycle

Parasites are commonly viewed as having superior adaptive potential in comparison to their hosts due to their larger population size, shorter generation time, often haploid genome, and usually high frequencies of horizontal gene transfer[1]. However, parasite abundance is usually subjected to rapid changes during the interaction with hosts. An event of a dramatic decline in population size followed by recovery is called a bottleneck and can take place at different stages of the parasite life cycle.

A new infection in a host organism can be initiated from as low as 1-10 infectious particles or cells[6, 8, 7]. During within-host proliferation, a parasite, especially viruses or bacteria, multiplies reaching quantities which are many times larger than the original inoculum. In turn, a host organism may counteract parasite replication via diverse defence mechanisms. Host immune system can operate in a highly specific manner simultaneously reducing the overall parasite load and selecting for a more persistent genotype[86]. Next, new infectious stages are shed into the environment, where the probability to be transmitted greatly depends on various factors, including host density, a proportion of susceptible host and persistence of transmissible stages[78, 85]. A combination of these factors determines the extent of the experienced transmission bottleneck, which, thus, represents a crucial factor that determines parasite fitness. In addition, many parasites possess a complex life cycle involving intermediate hosts or vector species, potentially resulting in a very heterogeneous environment for the parasite that can produce extremely complex patterns of demographic changes[80, 93].

Contrary to their host, parasites usually do not show continuously high abundance at a certain geographic location or time period. Instead, numerous examples document unexpected frequency fluctuations during an epidemic, parasite emergence and complete extinction, invasions to new ranges and host shifts[87]. For instance, the long-term fluctuations in the incidence of measles, mumps and pertussis were observed in human populations before the introduction of mass vaccination[101]. Another example of complex spatio-temporal parasite occurrence is travelling infection waves, described for raccoon rabies spreading across the eastern USA [102]

Taken together, the temporally and spatially variable nature of parasitism and the numerous constraints during the parasite life cycle strongly suggest that extreme variation in population size represents a universal characteristic of parasite biology with a high potential influence on its evolution.

3 Varying population size does influence reciprocal adaptation

Population size is one of the key parameters determining the availability of genetic diversity and also the intensity of genetic drift and selection. Classical population genetics explicitly defines the relationship between population size and different evolutionary forces. Yet, the specific effect of temporal variation in population size on the adaptation process is largely unexplored and thus, to date, only poorly understood. Many basic assumption underlying classical theory are often violated in real populations making any extrapolations less straightforward. Nevertheless, some studies, theoretical and empirical, strongly suggest that population size fluctuations can affect reciprocal host-parasite co-adaptations.

3.1 Genetic diversity in fluctuating populations

Population size variation may affect genetic diversity in two ways: (i) by scaling the rate of producing novel variants (effective mutation/recombination rate), or (ii) by influencing the maintenance of genetic diversity already present in a population. The number of mutations produced *de novo* is proportional to the population size, thus small populations would almost exclusively rely on standing genetic variation. If a host population has low genetic diversity, it would suffer from high parasitic prevalence due to the inability to counter-adapt. This situation is frequently observed in endangered species where low diversity correlates with high parasitic load[2, 11]. Increases in genetic diversity are often observed in growing parasite populations, especially during an outbreak, when a parasite may increase its adaptive potential[88]. For example, the peaks in the genetic diversity of A/H3N2 and A/H1N1 influenza viruses coincide with annual outbreaks in winter season [3]. The diversification in some virus phylogeny trees has been shown to correlate with onset of epidemics[61, 4]. Within-host proliferation of a parasite can also lead to accumulation of genetic diversity, as documented for HIV in recently infected patients[5].

Genetic diversity can be vastly reduced by bottlenecks encountered during host-parasite interaction. Among the well known examples is an isolated population of African lion in the Ngorongoro Crater, which preserved only 30% of its original diversity after the severe bottleneck caused by the epizootic of biting flies[10, 9]. Bottlenecks experienced by parasites in the course of repeated infection cycles lead to founding effects, which, in some cases, can play the dominant role for parasite evolution[12, 18, 19, 21]. For example, HIV demonstrates a substantially higher adaptation rate at the intra-host level compared to the inter-host level, which was suggested to be a consequence of strong founding effects combined with only a minor role of selection during transmission[13, 14].

Parasitic pressure is considered to be one of the prime forces in the evolution of sex[82]. Sexual reproduction and recombination can generate additional genetic diversity, which is of most importance to eukaryotic hosts with small population sizes. Thus, even if genetic diversity is limited, sexual reproduction would help small host populations to combat parasites. The empirical studies confirmed the advantage of sex and outcrossing for most host-parasite systems[100, 99, 60, 67]. Other examples suggest potentially complex relationships between sex differences in fitness upon parasite exposure and long-term adaptive benefits due to sexual

reproduction and outcrossing[68], where various factors including population size can play an important role[69]. In addition, small population size would lead to an elevated inbreeding rate diminishing the advantage of sex. On the other hand, it has been proposed that small populations would respond to strong genetic drift by evolving higher recombination rates [70].

3.2 Selection and genetic drift under fluctuating population size

Apart from affecting genetic diversity, variation in population size can determine the efficiency of selection. According to Kimura, the time to fixation of neutral or nearly neutral loci is proportional to the effective population size[20]. Upon a bottleneck random genetic drift becomes very strong and therefore interferes with selection. Elevated strength of random genetic drift may favor the accumulation of deleterious mutations and result in fitness decline[33, 48], as known for many viruses[15, 17, 16]. In contrast, it has been suggested that extreme bottlenecks can facilitate purging selection operating during transmission in plant viruses[98, 18].

As for beneficial alleles, fixation probability of a new mutation is usually predicted by a proportion of effective population size (N_e) to census sizes (N) and a selection coefficient (s): $\pi = 2s\frac{N_e}{N}$ [37, 36]. Effective population size N_e of a fluctuating population is approximated by a harmonic mean of census sizes. Accordingly, high fluctuation amplitudes would reduce fixation probabilities by decreasing $\frac{N_e}{N}$, as a harmonic mean is stronger influenced by small numbers[35]. As illustrated above, fixation probabilities of beneficial alleles in changing populations can be calculated by assuming constant effective population size, which, therefore, has often been taken as a proxy to predict the behavior of real populations. This view has recently been challenged with the development of new approaches and the employment of stochastic models[34]. In particular, the probability of fixation was shown to vary in dependence on the exact demographic scenario, for example, when comparing exponential and logistic growth or decline, when considering single changes in population size (such as a bottleneck), or when populations have a constant size versus regular size fluctuations[38]. The approximation given above holds true only under specific assumptions and may under- or overestimate fixation probability[38, 39, 34, 40]. Forcing the population size to a fixed value can introduce a bias in inferring adaptation rates, albeit it is very convenient because of equivalence of the population size and density. For example, when competition of two mutants, which differ in their growth rate, is modelled under constant population size, then this would result in negative growth for the slow mutant, even though its number is increasing in reality[39]. In this case, the estimation can be biased, as fixation probability appears to differ among growing and declining populations[38, 39].

3.3 Eco-evo feedback

Variation in population size during host-parasite coevolution is usually not independent of selection, as outlined above. This implies that strong reciprocal selection and extreme changes in population size can interact. The consequences of this interaction are not yet clear. It has been suggested that the adaptive response can buffer population size fluctuations, because at least some individuals

in the host population would acquire resistance[59]. For example, after introducing the Myxoma virus to the rabbit populations of Australia in 1950, the first epidemic was characterized by high mortality and had a devastating effect on the host[58]. In the following years, however, the rabbits developed resistance and the virus decreased its virulence, which eventually led to recovery of host abundance. In contrast, rapid evolution was also proposed to cause an increase of virulence and thus destabilize host populations[87], as it has been found for the bacterial pathogen *Mycoplasma gallisepticum* emerging in house finch populations[103]. The pathogen emergence followed by evolution of increased virulence has resulted in 60% decline of the previously prospering host populations.

Yet another fascinating consequence of the combined action of demographic variations and coevolutionary selection is that it should potentially favour a much larger variety of evolutionary pathways than similar selective constraints in populations with constant size. Wright's shifting balance theory predicts that a population can move away from sub-optimal peak on the fitness landscape as a result of genetic drift during a bottleneck[89]. A new position can offer different evolutionary opportunities overcoming constraints imposed by epistatic interactions or trade-offs.

In summary, fluctuations encountered by host and parasite populations are shown to have a strong effect on genetic diversity, drift and selection, as well as, they may be involved in eco-evolutionary feedback. Therefore, host-parasite coevolution would have different dynamics under fluctuating and constant population size, making the latter not an accurate assumption for simulating coevolution in real populations.

4 Future directions in studying host-parasite coevolution

Key questions for our understanding of host-parasite coevolution regard the exact traits and underlying molecular mechanisms that mediate reciprocal adaptation in natural populations and the exact underlying selection dynamics involved. Future research at both theoretical and empirical/experimental level should address these questions taking into account population size fluctuations, as briefly illustrated below.

In particular, most current models assume constant or infinite population size, under which coevolutionary selection may be shaped by either an RSS or NFDS. These two selection dynamics produce fundamentally different predictions on fixation rates[1]. RSS is characterized by rapid selective sweeps, while NFDS prevents fixation through negative frequency-dependence. Different factors, including genetic architecture[74], life history[66], and spatial structure[71], are likely to promote or impede allele segregation rate. We suggest that population size variation, as an inherent property of host-parasite interactions with a high impact on fixation rates can play a crucial role in shaping selection dynamics. Interestingly, a few epidemiological models have already been extended to allow for population size fluctuations[41, 42], but they are rarely considered in a coevolutionary context[49, 56, 81, 90, 71]. It was even proposed that demographic parameters might have a stronger influence on coevolution compared to genetic factors[81]. Similarly, the recognition of demographic history as an essential element for phy-

lognetic analysis has led to novel insights in virus evolution[52, 14, 88], whereas population size fluctuations are usually neglected in models which are aimed at uncovering the mechanisms of coevolution.

Modelling approaches should additionally consider stochastic processes in the context of population size variations, especially as the commonly used deterministic modelling methods are unlikely to capture the true dynamics in small populations[91]. It is necessary to note here, that stochasticity can influence various aspects of host-parasite interactions, like fecundity rates and prevalence levels, mutational processes and genetic drift, and also fluctuations in the environment[53]. To our opinion, random genetic drift and variation in the life-history (demographic stochasticity) are essential for full understanding of the coevolutionary dynamics, as these two factors have a critical influence on allele frequency changes. Unfortunately, to date, very few attempts have been undertaken to characterize host-parasite coevolution with changing population size using mathematical models that explicitly allow for stochastic processes[54, 55]. In a recent study, we have found a dramatic effect of changing population size on the coevolution[55]. In particular, the combination of stochasticity and changing population size leads to fast fixations (consistent with RSS dynamics), while the same model with constant population size or the deterministic version result in the pattern typical for NFDS dynamics. In the former case, the fixation events coincided with strong antagonist-mediated selection during a population bottleneck, suggesting a strong role of the interaction between selection and population size variation.

There is an urgent need for more empirical data, which simultaneously evaluates demographic history and evolutionary changes in a host-parasite system. One of the few available examples concerns the detailed long-term data set on the introduction of the Myxoma virus into rabbit populations in Australia[58]. The unavoidable complexity of such long-term field studies can be overcome by experimental coevolution, which provides a powerful tool for testing specific hypotheses under controlled settings, as demonstrated in several model systems, most often consisting of bacteria-phage interactions[83]. Interestingly, a thorough theoretical framework that considers periodic bottlenecks has already been developed to describe adaptation rates in serial passage experiments[94, 95, 96, 34]. This framework could be expanded to capture the dynamics in coevolution experiments, thus possibly helping design of future experiments, for example, by choosing “optimal ratio” of bottlenecks (i.e. providing faster adaptation rates) [97].

Ideally, future experimental approaches should directly test the consequences of fluctuating versus non-fluctuating population sizes. The effect of self-governed fluctuations on coevolution could be assessed experimentally by comparing a treatment where population size is externally controlled and a treatment where demographic dynamics is determined directly by the reciprocity of the host-parasite interaction. Although particularly challenging, such an experiment should still be realistic, especially when considering that previous experiments succeeded in coevolution between host and parasite and also their long-term coexistence[23, 51, 83]. Interestingly, the effect of genetic feedback on ecological interactions was noticed already in early coexistence experiments[23, 24].

Conclusion

Host and parasite species interact at ecological and evolutionary levels. High variation in population size is an unavoidable consequence of host-parasite interaction and can strongly influence reciprocal adaptation. While such influence is strongly supported by empirical and theoretical studies, population size fluctuations are largely neglected in the debate about the exact nature of coevolution. Therefore, we suggest that for full appreciation of host-parasite coevolution further efforts are needed that specifically address the role of population size variation on the resulting reciprocal selection dynamics.

Figures

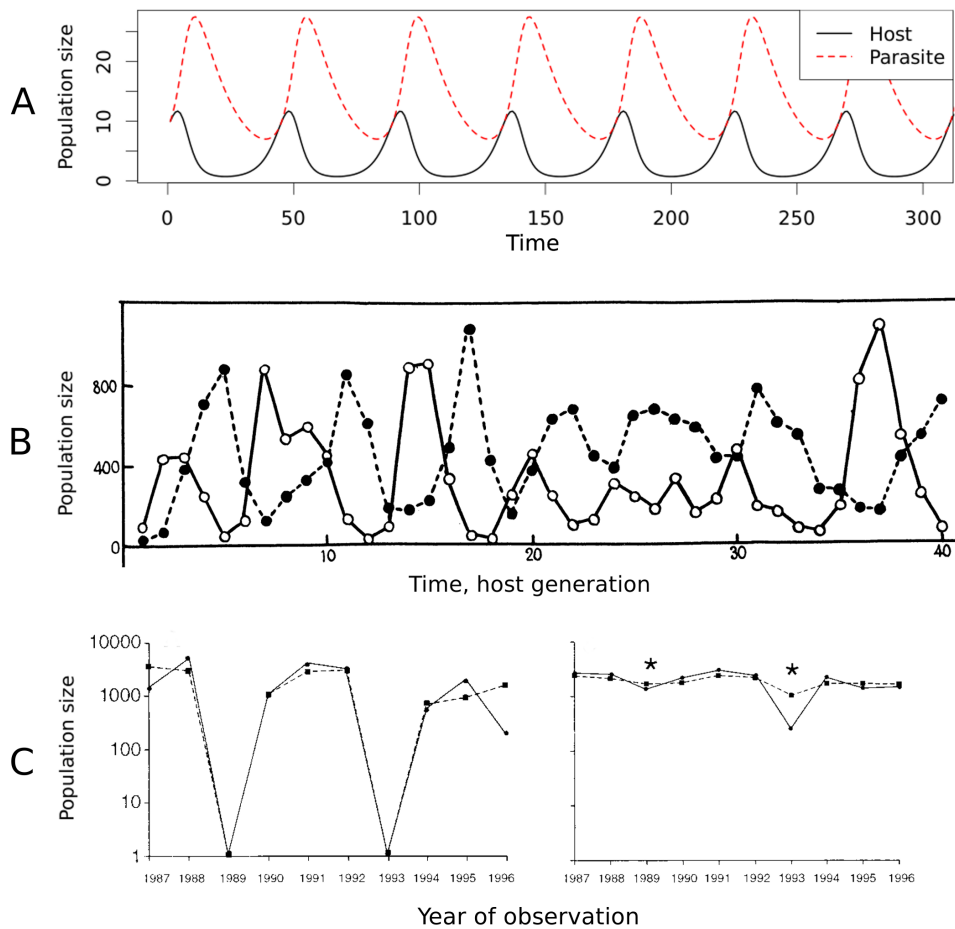


Figure 1: Population size fluctuations in host-parasite interaction

A. Hypothetical host-parasite population cycles produced by classical Lotka-Volterra equation. The solid black line shows a host and the red dashed line shows a parasite. **B.** Population cycles of azuki bean weevil *Callosobruchus chinensis* and its parasitoid wasp *Heterospilus prosopidis* in Utida experiment [23]. The solid line with open circles is for the host and the dashed line with filled circles is for the parasite **C.** Population cycles (left panel) in red grouse *Lagopus lagopus scoticus* caused by the nematode *Trichostrongylus tenuis* and their removal by anthelmintic treatment (right panel). Population size was estimated by number of animals shot each year. Different lines correspond to replicate populations. Modified from [30].

Tables

Table 1. Examples of variations in population size as a result of host-parasite interactions

Host	Parasite	Ref.	Pattern found	Time interval
Field observations				
diatom <i>Asterionella formosa</i>	chytrid fungus <i>Zygorhizidium planktonicum</i>	[25]	seasonal parasite outbreak followed by host decline, sometimes 2 cycles	1978-1980, Jan-May
	chytrid fungus <i>Rhizophyidium planktonicum</i>	[26]	2 epidemics coincide with host decline	1984, Apr-May, Jun-Jul
11 phytoplankton species	fungal infections, mainly <i>Rhizidiaceae</i>	[31]	diverse epidemic pattern, often strong effect on host density	1987-1989
red grouse, <i>Lagopus lagopus scoticus</i>	nematode <i>Trichostrongylus tenuis</i>	[28]	cyclic oscillations of host and parasite	1977-1989
European rabbit <i>Oryctolagus cuniculus</i>	myxoma virus	[58]	strong decline in host population followed by recovery as a result of emerged resistance	1950-1997
Laboratory experiments				
common housefly <i>Musca domestica</i>	parasitoid wasp <i>Mormoniella vitripennis</i>	[22]	1 cycle of change in host and parasite populations	7 host and parasite "generations"
	parasitoid wasp <i>Nasonia vitripennis</i>	[24]	cyclic oscillations in host and parasite	80 weeks

Host	Parasite	Ref.	Pattern found	Time interval
azuki bean weevil <i>Callosobruchus chinensis</i>	parasitoid wasp <i>Neocatolaccus mamezophagus</i>	[32, 23]	cyclic oscillations in host and parasite	51 host generations
moth <i>Plodia interpunctella</i>	parasitoid wasp <i>Heterospilus prosopidis</i>	[23]	cyclic oscillations in host and parasite	up to 112 host generations
water flea <i>Daphnia magna</i>	White Bacterial Disease, bacterium <i>Pasteuria ramosa</i> , ascomycete fungus <i>Metschnikowiella bicuspidata</i> , microsporidia <i>Glugoides intestinalis</i> , <i>Ordospora colligata</i> and <i>Flabelliforma magnivora</i>	[27]	diverse pattern ranging from extinction to coexistence	8-10 host generations
Mass extinction				
a variety of amphibian species from Mesoamerica	chytridiomycete fungus <i>Batrachochytrium dendrobatidis</i>	[62]	host decline coincides with an increase in the parasite prevalence	1964-1999
seal <i>Phoca vitulina</i>	phocine distemper virus	[63]	up to 60% extinction	1988, 2002

References

- [1] Mark E. J. Woolhouse, Joanne P. Webster, Esteban Domingo, Brian Charlesworth, and Bruce R. Levin. Biological and biomedical implications of the co-evolution of pathogens and their hosts. *Nat Genet*, 32(4):569–577, December 2002.
- [2] David W. Coltman, Jill G. Pilkington, Judith A. Smith, and Josephine M. Pemberton. Parasite-mediated selection against inbred soay sheep in a free-living, island population. *Evolution*, 53(4):1259, August 1999.
- [3] Andrew Rambaut, Oliver G. Pybus, Martha I. Nelson, Cecile Viboud, Jeffery K. Taubenberger, and Edward C. Holmes. The genomic and epidemiological dynamics of human influenza a virus. *Nature*, 453(7195):615–619, May 2008.
- [4] Kok Keng Tee, Tommy Tsan-Yuk Lam, Yoke Fun Chan, Jon M. Bible, Adeeba Kamarulzaman, C. Y. William Tong, Yutaka Takebe, and Oliver G. Pybus. Evolutionary genetics of human enterovirus 71: Origin, population dynamics, natural selection, and seasonal periodicity of the VP1 gene. *Journal of Virology*, 84(7):3339–3350, April 2010.
- [5] Frank Maldarelli, Mary Kearney, Sarah Palmer, Robert Stephens, JoAnn Mican, Michael A. Polis, Richard T. Davey, Joseph Kovacs, Wei Shao, Diane Rock-Kress, Julia A. Metcalf, Catherine Rehm, Sarah E. Greer, Daniel L. Lucey, Kristen Danley, Harvey Alter, John W. Mellors, and John M. Coffin. HIV populations are large and accumulate high genetic diversity in a nonlinear fashion. *Journal of Virology*, 87(18):10313–10323, September 2013.
- [6] Rachael M. Jones, Mark Nicas, Alan Hubbard, Matthew D. Sylvester, and Arthur Reingold. The infectious dose of francisella tularensis (tularemia). *Applied Biosafety*, 10(4):227, 2005.
- [7] Yutaka Komiya, Keiko Katayama, Hisao Yugi, Masaaki Mizui, Harumichi Matsukura, Tetsushi Tomoguri, Yuzo Miyakawa, Ayako Tabuchi, Junko Tanaka, and Hiroshi Yoshizawa. Minimum infectious dose of hepatitis b virus in chimpanzees and difference in the dynamics of viremia between genotype a and genotype c. *Transfusion*, 48(2):286–294, February 2008.
- [8] Paul Schmid-Hempel and Steven A Frank. Pathogenesis, virulence, and infective dose. *PLoS Pathogens*, 3(10), October 2007.
- [9] Stephen J. O’Brien and James F. Evermann. Interactive influence of infectious disease and genetic diversity in natural populations. *Trends in Ecology & Evolution*, 3(10):254–259, October 1988.
- [10] D. E. Wildt, M. Bush, K. L. Goodrowe, C. Packer, A. E. Pusey, J. L. Brown, P. Joslin, and S. J. O’Brien. Reproductive and genetic consequences of founding isolated lion populations. *Nature*, 329(6137):328–331, September 1987.

- [11] Joseph I. Hoffman, Fraser Simpson, Patrice David, Jolianne M. Rijks, Thijs Kuiken, Michael A. S. Thorne, Robert C. Lacy, and Kanchon K. Dasmahapatra. High-throughput sequencing reveals inbreeding depression in a natural population. *Proceedings of the National Academy of Sciences*, 111(10):3775–3780, March 2014.
- [12] Charles TT Edwards, Edward C. Holmes, Daniel J. Wilson, Raphael P. Viscidi, Elaine J. Abrams, Rodney E. Phillips, and Alexei J. Drummond. Population genetic estimation of the loss of genetic diversity during horizontal transmission of HIV-1. *BMC Evolutionary Biology*, 6(1):28, March 2006.
- [13] Philippe Lemey, Andrew Rambaut, and Oliver G Pybus. HIV evolutionary dynamics within and among hosts. *AIDS reviews*, 8(3):125–140, September 2006.
- [14] Oliver G. Pybus and Andrew Rambaut. Evolutionary analysis of the dynamics of viral infectious disease. *Nature Reviews Genetics*, 10(8):540–550, August 2009.
- [15] L Chao. Fitness of RNA virus decreased by muller’s ratchet. *Nature*, 348(6300):454–455, November 1990.
- [16] Cristina Escarmís, Mercedes Dávila, Nathalie Charpentier, Alma Bracho, Andrés Moya, and Esteban Domingo. Genetic lesions associated with muller’s ratchet in an RNA virus. *Journal of Molecular Biology*, 264(2):255–267, November 1996.
- [17] E Duarte, D Clarke, A Moya, E Domingo, and J Holland. Rapid fitness losses in mammalian RNA virus clones due to muller’s ratchet. *Proceedings of the National Academy of Sciences*, 89(13):6015 –6019, July 1992.
- [18] S. Miyashita and H. Kishino. Estimation of the size of genetic bottlenecks in cell-to-cell movement of soil-borne wheat mosaic virus and the possible role of the bottlenecks in speeding up selection of variations in trans-acting genes or elements. *Journal of virology*, 84(4):1828–1837, 2010.
- [19] Mark P. Zwart, José-Antonio Daròs, and Santiago F. Elena. One is enough: In vivo effective population size is dose-dependent for a plant RNA virus. *PLoS Pathog*, 7(7):e1002122, July 2011.
- [20] Motoo Kimura and Tomoko Ohta. The average number of generations until fixation of a mutant gene in a finite population. *Genetics*, 61(3):763–771, March 1969.
- [21] Serafín Gutiérrez, Yannis Michalakis, and Stéphane Blanc. Virus population bottlenecks during within-host progression and host-to-host transmission. *Current Opinion in Virology*, 2(5):546–555, October 2012.
- [22] Paul De Bach and Harry S. Smith. Are population oscillations inherent in the host-parasite relation? *Ecology*, 22(4):363–369, October 1941.

- [23] Syunro Utida. Cyclic fluctuations of population density intrinsic to the host-parasite system. *Ecology*, 38(3):442–449, July 1957.
- [24] David Pimentel. Population regulation and genetic feedback evolution provides foundation for control of herbivore, parasite, and predator numbers in nature. *Science*, 159(3822):1432–1437, March 1968.
- [25] Ellen Van Donk and J. Ringelberg. The effect of fungal parasitism on the succession of diatoms in lake maarsseveen i (the netherlands). *Freshwater Biology*, 13(3):241–251, June 1983.
- [26] Kees Bruning, Rob Lingeman, and Joop Ringelberg. Estimating the impact of fungal parasites on phytoplankton populations. *Limnology and Oceanography*, 37(2):252–260, 1992.
- [27] Dieter Ebert, Marc Lipsitch, and Katrina L. Mangin. The effect of parasites on host population density and extinction: Experimental epidemiology with daphnia and six microparasites. *The American Naturalist*, 156(5):459–477, November 2000.
- [28] Andrew P. Dobson and Peter J. Hudson. Regulation and stability of a free-living host-parasite system: *Trichostrongylus tenuis* in red grouse. II. population models. *Journal of Animal Ecology*, 61(2):487–498, June 1992.
- [29] D.M. Tompkins and M. Begon. Parasites can regulate wildlife populations. *Parasitology Today*, 15(8):311–313, August 1999.
- [30] Peter J. Hudson, Andy P. Dobson, and Dave Newborn. Prevention of population cycles by parasite removal. *Science*, 282(5397):2256–2258, December 1998.
- [31] Harald Holfeld. Fungal infections of the phytoplankton: seasonality, minimal host density, and specificity in a mesotrophic lake. *New Phytologist*, 138(3):507–517, March 1998.
- [32] Syunro Utida. On the equilibrium state of the interacting population of an insect and its parasite. *Ecology*, 31(2):165–175, April 1950.
- [33] M C Whitlock. Fixation of new alleles and the extinction of small populations: drift load, beneficial alleles, and sexual selection. *Evolution; International Journal of Organic Evolution*, 54(6):1855–1861, December 2000.
- [34] Z. Patwa and LM Wahl. The fixation probability of beneficial mutations. *Journal of The Royal Society Interface*, 5(28):1279–1289, 2008.
- [35] Motoo Kimura and Tomoko Ohta. Probability of gene fixation in an expanding finite population. *Proceedings of the National Academy of Sciences*, 71(9):3377–3379, September 1974.
- [36] M. Kimura. Stochastic processes in population genetics, with special reference to distribution of gene frequencies and probability of gene fixation. In Ken-ichi Kojima, editor, *Mathematical Topics in Population Genetics*,

- number 1 in *Biomathematics*, pages 178–209. Springer Berlin Heidelberg, January 1970.
- [37] W. J. Ewens. The probability of survival of a new mutant in a fluctuating environment. *Heredity*, 22:438–443, 1967.
- [38] S.P. Otto and M.C. Whitlock. The probability of fixation in populations of changing size. *Genetics*, 146(2):723, 1997.
- [39] Amaury Lambert. Probability of fixation under weak selection: a branching process unifying approach. *Theoretical Population Biology*, 69(4):419–441, June 2006.
- [40] T. L. Parsons, C. Quince, and J. B. Plotkin. Some consequences of demographic stochasticity in population genetics. *Genetics*, 185(4):1345–1354, May 2010.
- [41] Roy M. Anderson and Robert M. May. Regulation and stability of host-parasite population interactions: I. regulatory processes. *Journal of Animal Ecology*, 47(1):219–247, February 1978.
- [42] Robert M. May and Roy M. Anderson. Regulation and stability of host-parasite population interactions: II. destabilizing processes. *Journal of Animal Ecology*, 47(1):249–267, February 1978.
- [43] V. Volterra. Variations and fluctuations of the number of individuals in animal species living together. *Journal du Conseil*, 3(1):3, 1928.
- [44] A J Lotka. The growth of mixed populations: two species competing for a common food supply. *Journal of the Washington Academy of Sciences*, 22(461-469):461–469, 1932.
- [45] A. Buckling and P. B. Rainey. Antagonistic coevolution between a bacterium and a bacteriophage. *Proceedings of the Royal Society of London. Series B: Biological Sciences*, 269(1494):931–936, May 2002.
- [46] Ellen Decaestecker, Sabrina Gaba, Joost A. M. Raeymaekers, Robby Stoks, Liesbeth Van Kerckhoven, Dieter Ebert, and Luc De Meester. Host–parasite ‘Red queen’ dynamics archived in pond sediment. *Nature*, 450(7171):870–873, November 2007.
- [47] Dieter Ebert. Host-parasite coevolution: Insights from the daphnia-parasite model system. *Current Opinion in Microbiology*, 11(3):290–301, June 2008.
- [48] P.R.A. Campos and LM Wahl. The effects of population bottlenecks on clonal interference, and the adaptation effective population size. *Evolution*, 63(4):950–958, 2009.
- [49] R. M. May and R. M. Anderson. Epidemiology and genetics in the coevolution of parasites and hosts. *Proceedings of the Royal Society B: Biological Sciences*, 219(1216):281–313, October 1983.

- [50] Roy M. Anderson and Robert M. May. Infectious diseases and population cycles of forest insects. *Science*, 210(4470):658–661, 1980.
- [51] Ottar N. Bjørnstad, Steven M. Sait, Nils C. Stenseth, David J. Thompson, and Michael Begon. The impact of specialized enemies on the dimensionality of host dynamics. *Nature*, 409(6823):1001–1006, February 2001.
- [52] Bryan T. Grenfell, Oliver G. Pybus, Julia R. Gog, James L. N. Wood, Janet M. Daly, Jenny A. Mumford, and Edward C. Holmes. Unifying the epidemiological and evolutionary dynamics of pathogens. *Science*, 303(5656):327–332, January 2004.
- [53] Thomas Lenormand, Denis Roze, and François Rousset. Stochasticity in evolution. *Trends in Ecology & Evolution*, 24(3):157–165, March 2009.
- [54] Benjamin J. Z. Quigley, Diana García López, Angus Buckling, Alan J. McKane, and Sam P. Brown. The mode of host–parasite interaction shapes co-evolutionary dynamics and the fate of host cooperation. *Proceedings of the Royal Society B: Biological Sciences*, 279(1743):3742–3748, September 2012.
- [55] Chaitanya S Gokhale, Andrei Papkou, Arne Traulsen, and Hinrich Schulenburg. Lotka-volterra dynamics kills the red queen: population size fluctuations and associated stochasticity dramatically change host-parasite coevolution. *BMC evolutionary biology*, 13:254, 2013.
- [56] R. M. May and R. M. Anderson. Parasite—host coevolution. *Parasitology*, 100(Supplement S1):S89–S101, 1990.
- [57] Justyna Wolinska and Kayla C King. Environment can alter selection in host-parasite interactions. *Trends in Parasitology*, 25(5):236–244, May 2009.
- [58] Frank Fenner and Bernardino Fantini. *Biological Control of Vertebrate Pests: The History of Myxomatosis - an Experiment in Evolution*. CABI, Wallingford, Oxon, UK ; New York, NY, USA, first edition edition, December 1999.
- [59] Jennifer B.H. Martiny, Lasse Riemann, Marcia F. Marston, and Mathias Middelboe. Antagonistic coevolution of marine planktonic viruses and their hosts. *Annual Review of Marine Science*, 6(1):393–414, 2014.
- [60] Kayla C King, Lynda F Delph, Jukka Jokela, and Curtis M Lively. The geographic mosaic of sex and the red queen. *Current Biology: CB*, 19(17):1438–1441, September 2009.
- [61] Roman Biek, J. Caroline Henderson, Lance A. Waller, Charles E. Rupprecht, and Leslie A. Real. A high-resolution genetic signature of demographic and spatial expansion in epizootic rabies virus. *Proceedings of the National Academy of Sciences*, 104(19):7993–7998, May 2007.
- [62] Tina L. Cheng, Sean M. Rovito, David B. Wake, and Vance T. Vredenburg. Coincident mass extirpation of neotropical amphibians with the emergence of the infectious fungal pathogen *batrachochytrium dendrobatidis*. *Proceedings of the National Academy of Sciences*, 108(23):9502–9507, June 2011.

- [63] Tero Härkönen, Rune Dietz, Peter Reijnders, Jonas Teilmann, Karin Harding, Ailsa Hall, Sophie Brasseur, Ursula Siebert, Simon J. Goodman, and Paul D. Jepson. The 1988 and 2002 phocine distemper virus epidemics in european harbour seals. *Diseases of aquatic organisms*, 68(2):115–130, 2006.
- [64] F. M. D. Gulland. The impact of infectious diseases on wild animal populations: a review. In *Ecology of infectious diseases in natural populations*. Cambridge University Press, Cambridge, pages 20–51. 1995.
- [65] Michael A Brockhurst, Andrew D Morgan, Andrew Fenton, and Angus Buckling. Experimental coevolution with bacteria and phage. the pseudomonas fluorescens–phi2 model system. *Infection, Genetics and Evolution: Journal of Molecular Epidemiology and Evolutionary Genetics in Infectious Diseases*, 7(4):547–552, July 2007.
- [66] Luke G. Barrett, Peter H. Thrall, Jeremy J. Burdon, and Celeste C. Linde. Life history determines genetic structure and evolutionary potential of host–parasite interactions. *Trends in Ecology & Evolution*, 23(12):678–685, December 2008.
- [67] Levi T. Morran, Olivia G. Schmidt, Ian A. Gelarden, Raymond C. Parrish, and Curtis M. Lively. Running with the red queen: Host-parasite coevolution selects for biparental sex. *Science*, 333(6039):216–218, July 2011.
- [68] Leila Masri, Rebecca D. Schulte, Nadine Timmermeyer, Stefanie Thanisch, Lena Luise Crummenerl, Gunther Jansen, Nico K. Michiels, and Hinrich Schulenburg. Sex differences in host defence interfere with parasite-mediated selection for outcrossing during host–parasite coevolution. *Ecology Letters*, 16(4):461–468, April 2013.
- [69] Niels AG Kerstes, Camillo Bérénos, and Oliver Y. Martin. Coevolving parasites and population size shape the evolution of mating behaviour. *BMC Evolutionary Biology*, 13(1):29, February 2013.
- [70] Sarah P. Otto and Nick H. Barton. Selection for recombination in small populations. *Evolution*, 55(10):1921–1931, October 2001.
- [71] Sylvain Gandon, Yannis Michalakis, and Dieter Ebert. Temporal variability and local adaptation. *Trends in Ecology & Evolution*, 11(10):431, October 1996.
- [72] S. Gandon and Y. Michalakis. Local adaptation, evolutionary potential and host–parasite coevolution: interactions between migration, mutation, population size and generation time. *Journal of Evolutionary Biology*, 15(3):451–462, May 2002.
- [73] C. M. Lively and V. Apanius. Genetic diversity in host-parasite interactions. In *Ecology of infectious diseases in natural populations*, volume 7, page 421. 1995.

- [74] Aneil Agrawal and Curtis M. Lively. Infection genetics: gene-for-gene versus matching-alleles models and all points in between. *Evolutionary Ecology Research*, 4(1):79–90, 2002.
- [75] A. P. Dobson and P. J. Hudson. Microparasites: observed patterns in wild animal populations. In *Ecology of infectious diseases in natural populations*, volume 7, page 52. 1995.
- [76] P. J. Hudson and A. P. Dobson. Macroparasites: observed patterns in naturally fluctuating animal populations. In *Ecology of infectious diseases in natural populations*, volume 5, pages 144–176. 1995.
- [77] John N. Thompson. *The geographic mosaic of coevolution*. University of Chicago Press, 2005.
- [78] Roy M. Anderson, Robert M. May, B. Anderson, and & 0 more. *Infectious Diseases of Humans: Dynamics and Control*. Oxford University Press, USA, reprint edition edition, September 1992.
- [79] J. A. P. Heesterbeek and M. G. Roberts. Mathematical models for microparasites of wildlife. In *Ecology of infectious diseases in natural populations*, pages 90–122. 1995.
- [80] Robert M. May and Roy M. Anderson. Population biology of infectious diseases: Part II. *Nature*, 280(5722):455–461, August 1979.
- [81] Steven A. Frank. Ecological and genetic models of host-pathogen coevolution. *Heredity*, 67(1):73–83, 1991.
- [82] W. D. Hamilton, R. Axelrod, and R. Tanese. Sexual reproduction as an adaptation to resist parasites (a review). *Proceedings of the National Academy of Sciences*, 87(9):3566–3573, May 1990.
- [83] Michael A. Brockhurst and Britt Koskella. Experimental coevolution of species interactions. *Trends in Ecology & Evolution*, 28(6):367–375, June 2013.
- [84] James K M Brown and Aurélien Tellier. Plant-parasite coevolution: bridging the gap between genetics and ecology. *Annual review of phytopathology*, 49:345–367, 2011.
- [85] Hamish McCallum, Nigel Barlow, and Jim Hone. How should pathogen transmission be modelled? *Trends in Ecology & Evolution*, 16(6):295–300, June 2001.
- [86] Bruce R. Levin, Marc Lipsitch, and Sebastian Bonhoeffer. Population biology, evolution, and infectious disease: Convergence and synthesis. *Science*, 283(5403):806–809, February 1999. PMID: 9933155.
- [87] Sonia Altizer, Drew Harvell, and Elizabeth Friedle. Rapid evolutionary dynamics and disease threats to biodiversity. *Trends in Ecology & Evolution*, 18(11):589–596, November 2003.

- [88] Elizabeth A. Archie, Gordon Luikart, and Vanessa O. Ezenwa. Infecting epidemiology with genetics: a new frontier in disease ecology. *Trends in Ecology & Evolution*, 24(1):21–30, January 2009.
- [89] Sewall Wright. The shifting balance theory and macroevolution. *Annual Review of Genetics*, 16(1):1–20, 1982. PMID: 6760797.
- [90] Steven A. Frank. Coevolutionary genetics of plants and pathogens. *Evolutionary Ecology*, 7(1):45–75, 1993.
- [91] Andrew J. Black and Alan J. McKane. Stochastic formulation of ecological models and their applications. *Trends in Ecology & Evolution*, 27(6):337–345, June 2012.
- [92] Isabella M. Cattadori, Daniel T. Haydon, and Peter J. Hudson. Parasites and climate synchronize red grouse populations. *Nature*, 433(7027):737–741, February 2005.
- [93] Mark E. J. Woolhouse, Louise H. Taylor, and Daniel T. Haydon. Population biology of multihost pathogens. *Science*, 292(5519):1109–1112, May 2001.
- [94] L.M. Wahl and P.J. Gerrish. The probability that beneficial mutations are lost in populations with periodic bottlenecks. *Evolution*, 55(12):2606–2610, 2001.
- [95] J.M. Heffernan and L.M. Wahl. The effects of genetic drift in experimental evolution. *Theoretical population biology*, 62(4):349–356, 2002.
- [96] Lindi M Wahl, Philip J Gerrish, and Ivan Saika-Voivod. Evaluating the impact of population bottlenecks in experimental evolution. *Genetics*, 162(2):961–971, October 2002.
- [97] JE Hubbarde and LM Wahl. Estimating the optimal bottleneck ratio for experimental evolution: the burst-death model. *Mathematical biosciences*, 213(2):113–118, 2008.
- [98] Peter B. Visser, Derek J. F. Brown, Frans Th. Brederode, and John F. Bol. Nematode transmission of tobacco rattle virus serves as a bottleneck to clear the virus population from defective interfering RNAs. *Virology*, 263(1):155–165, October 1999.
- [99] Curtis M. Lively and Jukka Jokela. Temporal and spatial distributions of parasites and sex in a freshwater snail. *Evolutionary ecology research*, 4(2):219–226, 2002.
- [100] Mark F. Dybdahl and Curtis M. Lively. The geography of coevolution: Comparative population structures for a snail and its trematode parasite. *Evolution*, 50(6):2264, December 1996.
- [101] R. M. Anderson, B. T. Grenfell, and R. M. May. Oscillatory fluctuations in the incidence of infectious disease and the impact of vaccination: time series analysis. *The Journal of Hygiene*, 93(3):587–608, December 1984. PMID: 6512259 PMID: PMC2129464.

- [102] Colin A. Russell, David L. Smith, Lance A. Waller, James E. Childs, and Leslie A. Real. A priori prediction of disease invasion dynamics in a novel environment. *Proceedings of the Royal Society of London. Series B: Biological Sciences*, 271(1534):21–25, January 2004.
- [103] Dana M. Hawley, Erik E. Osnas, Andrew P. Dobson, Wesley M. Hochachka, David H. Ley, and André A. Dhondt. Parallel patterns of increased virulence in a recently emerged wildlife pathogen. *PLoS Biol*, 11(5):e1001570, May 2013.

Part II.

Lotka–Volterra dynamics kills the Red Queen

Chaitanya S Gokhale, Andrei Papkou, Arne Traulsen, and Hinrich Schulenburg. Lotka-Volterra dynamics kills the red queen: population size fluctuations and associated stochasticity dramatically change host-parasite coevolution. *BMC Evolutionary Biology*, 13:254, 2013.

RESEARCH ARTICLE

Open Access

Lotka–Volterra dynamics kills the Red Queen: population size fluctuations and associated stochasticity dramatically change host-parasite coevolution

Chaitanya S Gokhale^{1*}, Andrei Papkou², Arne Traulsen^{1†} and Hinrich Schulenburg^{2+*}

Abstract

Background: Host-parasite coevolution is generally believed to follow Red Queen dynamics consisting of ongoing oscillations in the frequencies of interacting host and parasite alleles. This belief is founded on previous theoretical work, which assumes infinite or constant population size. To what extent are such sustained oscillations realistic?

Results: Here, we use a related mathematical modeling approach to demonstrate that ongoing Red Queen dynamics is unlikely. In fact, they collapse rapidly when two critical pieces of realism are acknowledged: (i) population size fluctuations, caused by the antagonism of the interaction in concordance with the Lotka-Volterra relationship; and (ii) stochasticity, acting in any finite population. Together, these two factors cause fast allele fixation. Fixation is not restricted to common alleles, as expected from drift, but also seen for originally rare alleles under a wide parameter space, potentially facilitating spread of novel variants.

Conclusion: Our results call for a paradigm shift in our understanding of host-parasite coevolution, strongly suggesting that these are driven by recurrent selective sweeps rather than continuous allele oscillations.

Keywords: Host-parasite coevolution, Red Queen hypothesis, Lotka-Volterra dynamics, Genetic drift, Population bottleneck

Background

The Red Queen from Lewis Carroll's tale 'Through the looking glass' is commonly used as a metaphor for selection-induced rapid evolution [1-3]. It is based on the observation that persistence in an environment with changing selective constraints requires ongoing adaptations to the encountered challenges [4]. Host-parasite coevolution with antagonistic and inter-dependent interactions represents one of the role models for such rapid evolutionary change [5,6]. For instance, an increase in host resistance reduces parasite fitness, thus immediately favoring parasite varieties with altered virulence and/or

immune-evasion mechanisms. In turn, a novel parasite attack mechanism decreases host fitness, thus favoring host varieties with new counter-defenses. If the interaction persists, then it will lead to continuous parasite adaptations and host counter-adaptations. The rapid evolutionary dynamics associated with these interactions is very well documented in the literature, ranging from field studies on rabbits and their myxoma viruses [7], snails and their trematode parasites [8], *Daphnia magna* waterfleas and their bacterial parasites [9] to laboratory-based coevolution experiments between bacteria and their phages [10-12], the nematode *Caenorhabditis elegans* and bacterial parasites [13,14], or the red flour beetle *Tribolium castaneum* and its microsporidian parasite [15,16].

It is thus widely accepted that these interactions evolve fast and continuously. Yet, to date, the exact underlying selection dynamics are not always well understood.

*Correspondence: gokhale@evolbio.mpg.de;
hschulenburg@zoologie.uni-kiel.de

†Equal contributors

¹Evolutionary Theory Group, Max Planck Institute for Evolutionary Biology, August Thienemann Str-2, 24306, Plön, Germany

²Department of Evolutionary Ecology and Genetics, Christian-Albrechts-University of Kiel, 24098, Kiel, Germany

These dynamics can generally be influenced by metapopulation structure and environmental variation [17,18]. Within a particular population and specific environmental context, two main alternatives are thought to be of prime importance: recurrent selective sweeps and negative frequency-dependent selection [5,6,19-21]. Both alternatives are consistent with the above original definition of the Red Queen hypothesis by Van Valen [4], whereas, curiously, only the second alternative is referred to as Red Queen dynamics [5,6,20]. The two alternatives are closely related because both assume a selective advantage of a rare genotype, for example a novel host resistance variant. However, they differ fundamentally in the way in which the new variant originates and spreads within the population. The concept of recurrent selective sweeps (often termed *arms race dynamics*) consists of two steps: the *de novo* appearance of a beneficial allele (e.g., by mutation or immigration) and its subsequent spread through the population to fixation (i.e., the selective sweep). These sweeps occur repeatedly in host and parasite populations, usually each time with a new beneficial allele. They may only lead to fast changes in absolute time if at least one of the following factors applies: new alleles arise frequently, new alleles become immediately visible and thus selectable at the phenotypic level, the new alleles provide a high selective advantage, and/or the organisms have short generation times. This situation is best met in bacteriophage interactions, which are usually characterized by large population sizes (i.e., high likelihood of the occurrence of favorable mutations), short generation times, and haploid genomes (i.e., new mutations are immediately expressed phenotypically) [11,22-24] (but see also [25]).

In contrast, the dynamics for multicellular host systems are traditionally viewed to be determined by negative frequency-dependent selection leading to sustained oscillations of the same alleles (i.e., Red Queen dynamics [6,20]), but not to the fixation of single alleles. In this case, standing genetic variation is required, because the population sizes for these hosts are usually comparatively small, their generation times comparatively long, and their genomes diploid. As a consequence, recurrent selective sweeps are commonly thought to be rather slow in these systems. Instead, if standing genetic variation is available, then negative frequency-dependent selection can produce fast and continuous allele frequency changes even in these host systems. Such negative frequency-dependent dynamics seem to be present in some multicellular host systems, including the freshwater snail *Potamopyrgus antipodarum* [8,26] and the waterflea *Daphnia magna* [9].

Numerous theoretical models have been developed to study the underlying selection dynamics. Interestingly, the current models typically focus on evolutionary change (i.e., the rate of change in host and parasite allele frequencies in response to the type of interaction). These

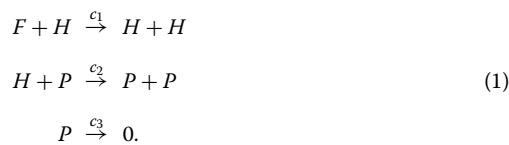
approaches have thus largely neglected ecological dynamics, which can have a huge impact on the evolutionary process. Population size fluctuations deserve particular attention in this context, because they are induced by reciprocal selection among the antagonists and, therefore, represent an inherent property of host-parasite coevolution - irrespective of additional environmental variation [7,10,27-30]. Since selection is reciprocal, population size fluctuations should be coupled between the antagonists, and generally follow Lotka-Volterra dynamics [31,32]. Such demographic variations have the potential to affect the dynamics of host-parasite allele frequency changes by introducing two important effects. Firstly, the rising and falling population sizes produce bottlenecks where selection favours a particular allele. The favored allele may thus reach comparatively high frequencies during the bottleneck, possibly enhancing its spread in the subsequently expanding population. Secondly, the elevated stochasticity during the bottleneck may lead to a further increase and thus spread of the favored allele.

In this manuscript, we aim at understanding in how far Lotka-Volterra population size fluctuations and the associated stochastic effects influence the dynamics of allele frequency changes during host-parasite coevolution. While several previous theoretical models have applied the Lotka-Volterra dynamics to host-parasite coevolution (e.g., [33-37]), their influence on the evolutionary dynamics has not yet been systematically explored by comparison with a model with constant population size. Similarly, stochastic effects during host-parasite coevolution have only been considered in a few theoretical studies (e.g., [38,39]), yet, to our knowledge, with a single exception [40] under constant population size and not in combination with Lotka-Volterra dynamics. Hence, while the previous studies have independently utilised stochastic effects or Lotka-Volterra dynamics, a systematic analysis of the consequences of each of these factors, either alone or in combination, is as yet missing - in spite of their potential importance. The novelty of our study lies in bringing together these two aspects and comparing their influence to the traditional model, in which Lotka-Volterra dynamics and stochastic effects are excluded. More specifically, we here use the standard matching-alleles host-parasite interaction model to assess allele frequency dynamics in the presence versus absence of Lotka-Volterra oscillations for a stochastic versus an analogous deterministic model.

Methods

Based on the Lotka-Volterra equations [31,32], we address the population dynamics of interacting hosts and parasites. The host corresponds to the prey in the original model, and the parasite to the predator. The host

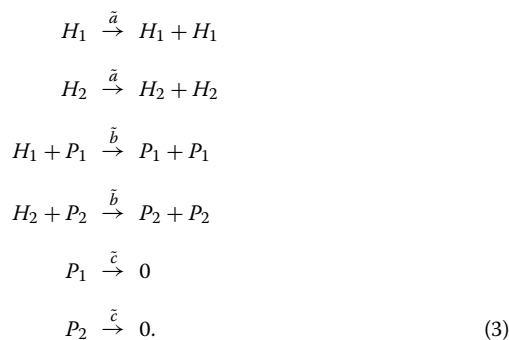
consumes a (constant) food supply F and reproduces at rate c_1 . Parasites infect hosts at rate c_2 , leading to elimination of a host and generation of an additional parasite. Parasites die at rate c_3 . The number of host and parasite individuals are given by H and P . In a stochastic system these interactions can be defined by the following reactions [41,42],



Usage of these specific reactions facilitates tracking of each unit of the interacting antagonists and, thus, it allows a more precise characterization of the resulting dynamics. These reactions can also be used directly for exact stochastic simulations based on the Gillespie algorithm. They further provide a microscopic dynamics from which the deterministic Lotka-Volterra equations emerge in the limit of infinite population size [42],

$$\begin{aligned} \dot{H} &= c_1FH - c_2HP \\ \dot{P} &= c_2HP - c_3P. \end{aligned} \quad (2)$$

Host-parasite coevolution is modeled using the standard matching alleles model [6]. For this, we define two host and two parasite types, H_1 and H_2 for the host and P_1 and P_2 for the parasite. This is equivalent to a haploid system with two antagonists, each of which possesses two alleles at a single locus. The interaction according to the matching alleles model is described with the following six reactions,



In the matching alleles model, the interactions between alternate hosts and parasites (H_1, P_2 and H_2, P_1) are without consequence and thus do not appear here. While the absence of these interactions is the standard assumption in the matching alleles model, allowing a small amount of these interactions does not change our results qualitatively (see Appendix). In the limit of infinite population

size [42], we obtain a set of four coupled nonlinear differential equations,

$$\begin{aligned} \dot{h}_1 &= h_1(a - bp_1) \\ \dot{h}_2 &= h_2(a - bp_2) \\ \dot{p}_1 &= p_1(bh_1 - c) \\ \dot{p}_2 &= p_2(bh_2 - c), \end{aligned} \quad (4)$$

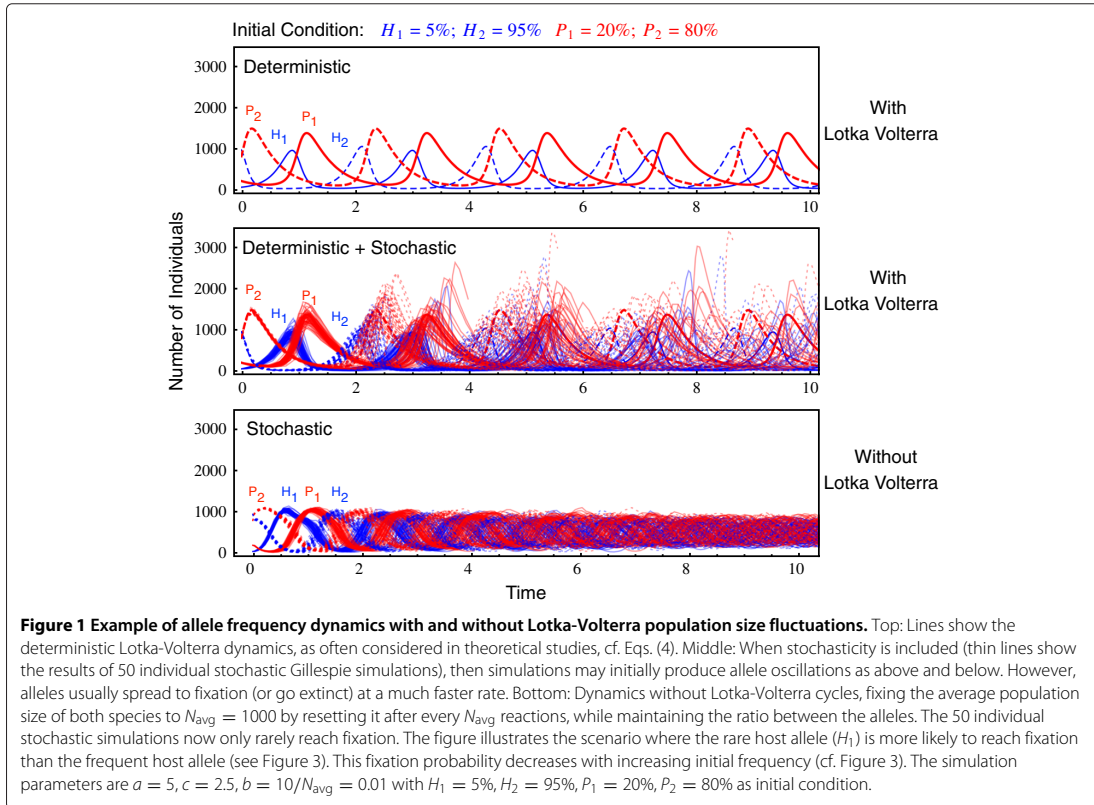
where the frequencies of H_i and P_i are given by h_i and p_i . The above equations consider interdependence of host and parasite demographics, allowing population sizes to vary in response to the interaction with the antagonist, consistent with the Lotka-Volterra model. The precise nature of the resulting oscillations in population size is determined by the parameters, most importantly by b .

As we are interested in the effects of population size variation induced by the Lotka-Volterra equations, we have to compare this to a scenario in which the population size is constant. Such constant population size models are common, e.g. the Wright-Fisher model or the Moran process. However, microscopically these models are distinct from the Lotka-Volterra equations considered above. Therefore, we used the above approach and enforced constant population size by resetting host and parasite population sizes to their initial values after every generation (N_{avg} transition events, see Appendix), while relative allele frequencies were maintained. The dynamics were subsequently assessed for different average population sizes. To ensure comparability of allele frequency fluctuations across population sizes and evolutionary models, we rescaled the interaction parameters with N_{avg} for the deterministic analogues of the considered stochastic scenarios (Appendix).

Results

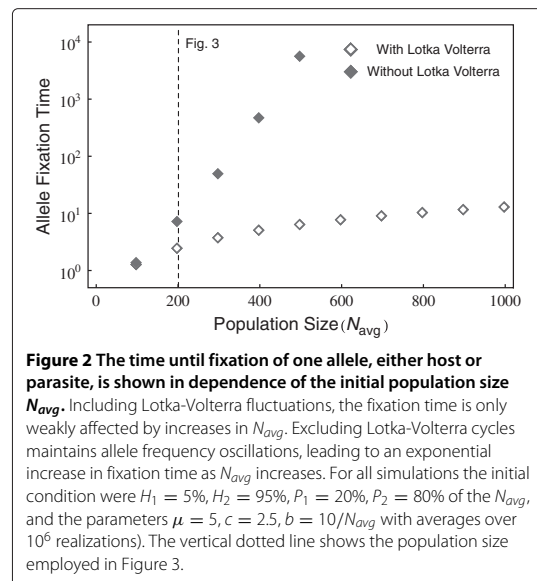
Host-parasite coevolutionary dynamics are analyzed in the presence and absence of Lotka-Volterra dynamics. Figure 1 illustrates an exemplary result. All models initially produce oscillatory allele frequency changes, but only with Lotka-Volterra dynamics are these accompanied by changes of population size. As a consequence, changes in allele numbers are also more pronounced (top versus bottom in Figure 1). As the deterministic model allows for arbitrary small frequencies of each type, it formally never leads to allele fixation and thus produces continuous oscillations. In contrast, the corresponding stochastic models have absorbing states, making fixation possible. Interestingly, allele fixation appears to be substantially faster in the stochastic model that includes Lotka-Volterra fluctuations (top versus bottom panels, Figure 1). As such, it seems that these conditions favor rapid termination of the Red Queen oscillations.

We next analyze the impact of the average population size on this pattern. In the following, we focus on the time



until one of the alleles from either of the antagonists has reached fixation in order to compare evolutionary rates across population sizes and models. In general, Lotka-Volterra dynamics cause a substantial increase in allele fixation rate (Figure 2). Interestingly, in this case, allele fixation rates depend only weakly on average population size. Figure 1 suggests that this is because allele frequencies can become very small during the Lotka-Volterra demographic fluctuations. In contrast, average population size has a much stronger effect when it is artificially kept constant. Here, the time until allele fixation increases exponentially with increasing population size (Figure 2).

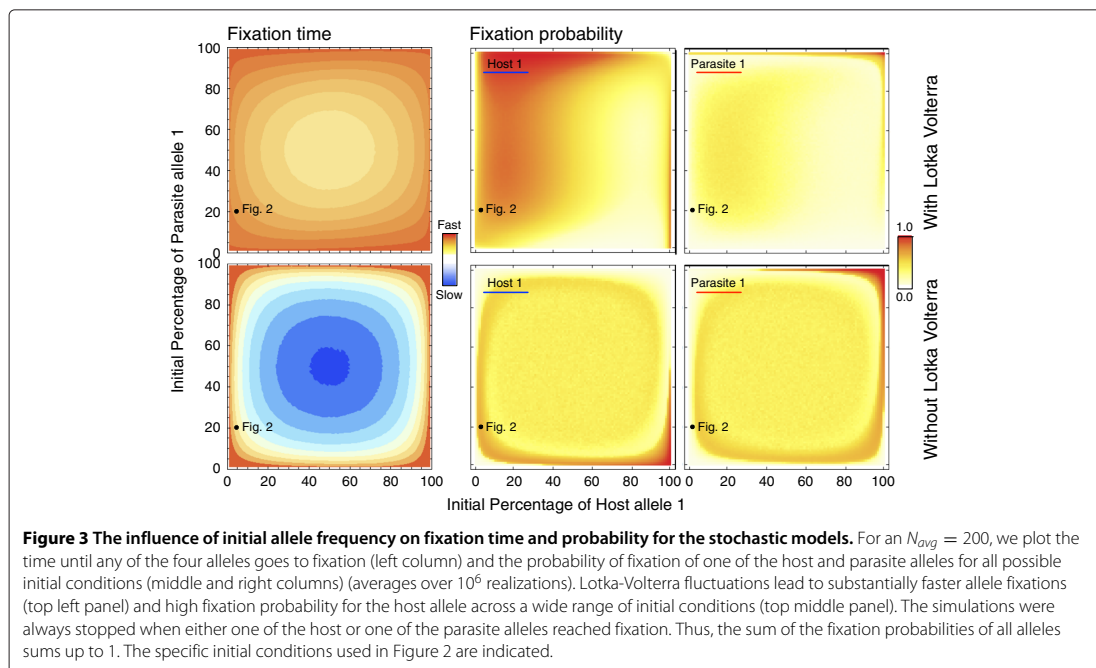
Figure 2 explores the time to fixation of any of the alleles in either the host or the parasite using a specific combination of initial allele frequencies (i.e., the rare host allele is present at 5%, the common at 95%, whereas the parasite alleles are at 20% and 80% respectively). How does this depend on the initial allele frequencies in both antagonists? For instance, the selective advantage of a rare allele is not only the result of its own frequency, but also determined by the abundance of the corresponding allele in the antagonist. Allele fixation rates were thus explored as a function of initial allele frequencies in the

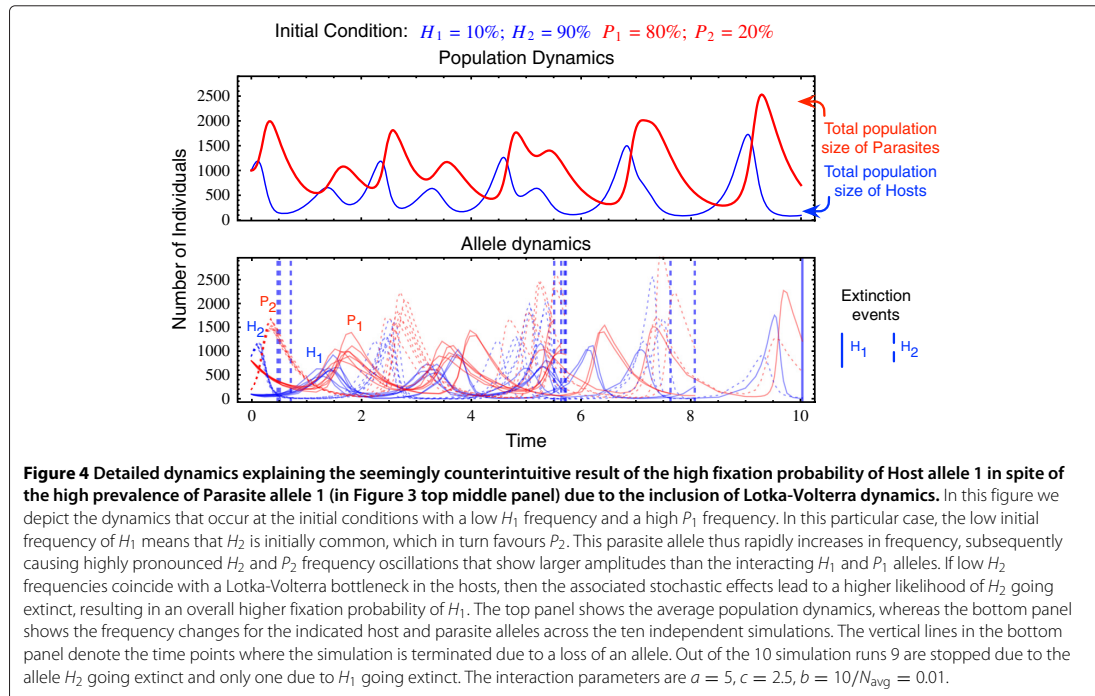


two antagonists. Most impressively, Lotka-Volterra fluctuations cause much faster allele fixation under almost all initial conditions (Figure 3, left column, top versus bottom panel). The detailed analysis then suggests that, in case of Lotka-Volterra fluctuations, host alleles can have a high fixation probability even if initially rare (Figure 3, middle panel in top row). This is true across a relatively wide distribution of initial frequencies for the corresponding parasite allele. Interestingly, it even applies when the corresponding parasite allele has high initial frequencies (Figure 3, top left corner in top middle panel). This counterintuitive result can be explained by consideration of the dynamics that ensue from these initial conditions. In this particular case, the low initial frequency of host allele 1 means that host allele 2 is initially common, whereas the high initial frequency of parasite allele 1 means that parasite allele 2 is rare. High host allele 2 abundance then specifically favors parasite allele 2, which rapidly increases in frequency. The unexpected consequence of these starting conditions is that these two interacting alleles subsequently engage in highly pronounced frequency oscillations that show larger amplitudes than those observed for host and parasite alleles 1 (Figure 4). If during these oscillations low allele 2 frequencies coincide with a Lotka-Volterra bottleneck and associated stochastic effects, then host allele 2 has a very high likelihood of going extinct, resulting in fixation of host allele 1 (see Figure 4).

The results also highlight that the dynamics are usually determined by fixation of one of the host alleles (red colour is mainly found in middle rather than right panel of the top row of Figure 3). Note that the simulations are stopped as soon as either one of the host or one of the parasite alleles reaches fixation and, thus, the fixation probabilities of both host as well as both parasite alleles sum up to one. In our case, fixation of the host allele is more likely than fixation of the parasite allele because for our parameter combination and initial condition, it is usually the host that first experiences a Lotka-Volterra bottleneck and consequentially a drop in the frequency of one of the alleles (see also Figure 4). Nevertheless, if both the parasite and corresponding host allele are common, then it is the parasite allele that has a high probability of fixation (Figure 3, top right).

The overall pattern looks different in the absence of Lotka-Volterra fluctuations (Figure 3, bottom row). Host allele fixation probability increases with its own high initial frequency and, at the same time, low initial abundance of the corresponding parasite allele (Figure 3 middle panel in bottom row). Parasite allele fixation is enhanced when both parasite and corresponding host alleles are initially common (Figure 3 bottom right). Under these conditions, fixation probabilities of both host and parasite alleles are almost identical at initially intermediate frequencies, most likely due to negative frequency dependent selection, as illustrated in Figure 1.





Discussion

Population size fluctuations represent an inherent property of host-parasite interactions. Unequivocal evidence for such interaction-dependent demographic variations was obtained from controlled host-parasite mesocosm experiments, for example with *E. coli* and its phage [10,30], *Hydra* hosts and its *Hydramoeba* parasite [43], house fly and its parasitic wasps [44,45], or azuki bean weevil *Callosobruchus chinensis* and its parasitoid *Heteropilus prosopidis* [46]. Similar observations were made under field conditions, for example for rabbits and their myxoma viruses [7], or red grouse and its nematode parasite [47]. Additional examples are summarized by [28] and [29]. As population size fluctuations produce regular bottlenecks, random genetic drift is likely to influence allele frequencies. Previous theoretical models, developed in a different context, strongly suggest that even large populations are influenced by such stochastic processes [48,49]. More generally, under natural conditions in a finite population, it is difficult to imagine that changes in population size do not affect evolutionary dynamics. Consequently, an in-depth understanding of the evolution of host-parasite interactions should take account of the associated ecological processes based on Lotka-Volterra fluctuations.

Very few previous theoretical models on host-parasite interactions have considered Lotka-Volterra fluctuations

[33-37]. These studies usually used a deterministic approach and thus excluded stochastic effects, which are most prominent during bottlenecks. Similarly, only few theoretical studies considered stochastic effects in this context [38,39], yet under constant population size, but not in combination with Lotka-Volterra dynamics. We are aware of only one study that looked at host-parasite coevolution in consideration of Lotka-Volterra interactions and stochasticity [40]. However, this study had a different focus, and thus, it did not include a systematic comparison to models without Lotka-Volterra cycles or without stochasticity. Consequently, the interaction of these two aspects for host-parasite coevolution is so far unexplored. At the same time, their relevance was demonstrated for evolution of only one of the antagonists, namely the parasite. For example, the probability of fixation of a beneficial mutation in a bacterial population was shown to be enhanced by periodical bottlenecks [50-52]. Similar results were obtained in a model that explored the effect of bottlenecks during pathogen transmission [53]. Our study explicitly evaluates the influence of both Lotka-Volterra fluctuations and stochastic effects on the dynamics of host-parasite interactions using a comparison to a model with constant population size and/or absence of stochasticity. As the demographic variations are an inherent property of such antagonistic interactions, their influence should apply across a wide range of environmental

conditions and thus be of general relevance for our understanding of host-parasite coevolution.

Based on our approach, we obtained evidence that both Lotka-Volterra fluctuations and associated stochastic effects significantly affect the course and pace of coevolutionary adaptations. In particular, both factors facilitate selective sweeps (i.e., the spread and fixation of an allele). Most impressively, this effect appears to be independent of average population size (Figure 2) and occur at a substantially faster rate (Figure 3, left column). Moreover, allele frequency changes are not exclusively due to drift, which should favor fixation of initially frequent alleles and loss of initially rare alleles. In contrast, our results indicate that initially rare host alleles can spread to fixation across a relatively wide range of conditions (Figure 3, top middle panel). Rare parasite alleles may not necessarily go extinct, but have a certain likelihood of spreading contingent on the frequency of the corresponding host allele (Figure 3, top right panel). Based on these results we propose that selective sweeps rather than oscillatory negative frequency-dependent selection may represent the main driving force during host-parasite coevolution.

Recurrent selective sweeps have been repeatedly suggested to determine coevolutionary dynamics for parasite or host systems with large population sizes such as bacterial hosts or microbial parasites, where novel mutations are frequent and often directly exposed to selection because of a haploid genetic system. If these selective dynamics also apply to multicellular host and parasite systems, then two contrasting effects may be expected on the coevolutionary process. On the one hand, these systems usually have much smaller population sizes, facilitating spread of alleles in spite of the often diploid genetic system. On the other hand, continuous coevolution may become difficult because it is usually assumed that small population size results in a reduced likelihood of the occurrence of advantageous novel mutations [6]. However, the latter assumption may not always be true. It is possible that new alleles become available for example by frequent immigration or a high rate of gene duplication. These processes may further favor the formation of novel genotypes if they act in combination with recombination and/or mutation. Interestingly, the possible impact of gene duplications is usually not addressed in theoretical work on host-parasite coevolution, even though such duplications are known to be common in almost all organisms [54-56] and often affect genes of relevance for the interaction such as virulence genes in parasites [57,58] or immunity genes in animal hosts [54,59,60].

Several additional factors may favor ongoing coevolution. One of these is founded on a more complex genetic architecture underlying host-parasite co-adaptation that

consists of several interacting loci across the genome (e.g., [61-64]). In this case, allele fixation at one locus may still permit maintenance of variation at other loci, which could then mediate evolutionary responses to the antagonist. Yet another possibility may depend on metapopulation structure, consisting of coevolutionary hot and cold spots and migration among demes, as evidenced for flax and its parasitic rust fungus [65] or the above mentioned snail-trematode interaction [17]. Such an interconnected network could then maintain allelic diversity across the entire metapopulation, even if alleles become temporarily fixed within single demes. Moreover, environmental gradients or perturbations are known to influence host-parasite coevolutionary dynamics [66]. They could similarly prevent loss of alleles, even if the coevolutionary interaction itself would specifically favour only one of the alleles. Obviously, the above processes act in combination with each other in natural systems. Therefore, it is indeed conceivable that recurrent selective sweeps shape long-lasting coevolutionary dynamics even in multicellular host systems.

Conclusion

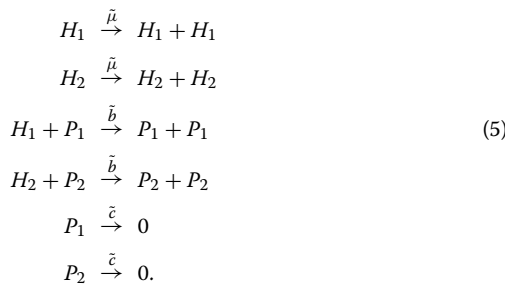
In conclusion, decades of empirical efforts have tried to demonstrate the presence of Red Queen dynamics during host-parasite coevolution. This has led to most ingenious experiments which repeatedly and independently confirmed negative frequency dependence as a driving force [8,9,26,67,68] and such a trend continues to date [21,69]. These studies yielded impressive evidence that parasite abundance typically increases first and, once the host evolves a defense mechanism, it decreases again. However, sustained allele frequency oscillations of a particular allele, as predicted by numerous theoretical models assuming constant population size in the absence of any stochastic effects, have not been reported. We here propose that Lotka-Volterra population size fluctuations and the associated stochastic effects represent an inherent property of host-parasite interactions that can lead to rapid fixation of alleles, even those initially rare, thus preventing sustained oscillations. Consequently, Lotka-Volterra population size fluctuations have the potential to stop the Red Queen - unless novel variants are introduced into the population and/or additional selective constraints maintain allelic diversity. In retrospect, our findings may not be entirely unexpected. However, to date, they have not yet been directly demonstrated using a systematic analysis approach, as implemented here. More importantly, they are generally neglected in the numerous current empirical studies on the topic, in spite of their potential importance. They clearly deserve specific attention in future theoretical and empirical work aimed at an improved understanding of host-parasite coevolutionary dynamics.

Appendix

Relating stochastic and deterministic dynamics

Stochastic models are often developed starting from deterministic formulations [42]. Since the same deterministic formulation can be the limiting case of many individual based models, this procedure may be problematic. Instead, beginning from a stochastic, individual based description and then calculating the deterministic analogue will provide only a single direct link between the two approaches and allows for their direct comparison.

We consider a haploid system involving two antagonistic pairs, two alleles in hosts and parasites each. Firstly, all possible changes are written in the form of simple chemical reactions. In our particular case we have eight such possible reactions. We denote the two hosts and the two parasites by H_1 and H_2 and P_1 and P_2 respectively. Thus we have,



For instance, a parasite 2 individual dies with the rate \tilde{c} . From these rate reactions, we obtain the transition rates of the system. Depending on the number of individuals of the different types namely $\mathbf{n} = \{n_{H_1}, n_{H_2}, n_{P_1}, n_{P_2}\}$, we write the rates as,

$$\begin{aligned}
 T(n_{H_1} + 1, n_{H_2}, n_{P_1}, n_{P_2} | \mathbf{n}) &= \tilde{\mu} \frac{n_{H_1}}{N_{\text{avg}}} \\
 T(n_{H_1}, n_{H_2} + 1, n_{P_1}, n_{P_2} | \mathbf{n}) &= \tilde{\mu} \frac{n_{H_2}}{N_{\text{avg}}} \\
 T(n_{H_1} - 1, n_{H_2}, n_{P_1} + 1, n_{P_2} | \mathbf{n}) &= 2\tilde{b} \frac{n_{H_1}}{N_{\text{avg}}} \frac{n_{P_1}}{N_{\text{avg}}} \\
 T(n_{H_1}, n_{H_2} - 1, n_{P_1}, n_{P_2} + 1 | \mathbf{n}) &= 2\tilde{b} \frac{n_{H_2}}{N_{\text{avg}}} \frac{n_{P_2}}{N_{\text{avg}}} \\
 T(n_{H_1}, n_{H_2}, n_{P_1} - 1, n_{P_2} | \mathbf{n}) &= \tilde{c} \frac{n_{P_1}}{N_{\text{avg}}} \\
 T(n_{H_1}, n_{H_2}, n_{P_1}, n_{P_2} - 1 | \mathbf{n}) &= \tilde{c} \frac{n_{P_2}}{N_{\text{avg}}}
 \end{aligned} \tag{6}$$

where the reaction rates, have been corrected by each reactions combinatorial possibility [70,71] and N_{avg} is the average population size which we consider to be the same for the hosts as well as the parasites (the difference in the average population size can be interpreted as the ratio between the growth rate of hosts and the death rate of

parasites). Using these rates, we can write down deterministic differential equations for the change in the average number of a certain type, e.g.

$$\frac{d\langle n_{H_1} \rangle}{dt} = \tilde{\mu} \frac{n_{H_1}}{N_{\text{avg}}} - 2\tilde{b} \frac{n_{H_1}}{N_{\text{avg}}} \frac{n_{P_1}}{N_{\text{avg}}}. \tag{7}$$

Introducing rescaled reaction rates, $\mu = \frac{\tilde{\mu}}{N_{\text{avg}}}$, $b = 2\frac{\tilde{b}}{N_{\text{avg}}}$ and $c = \frac{\tilde{c}}{N_{\text{avg}}}$, we obtain

$$\frac{d\langle n_{H_1} \rangle}{dt N_{\text{avg}}} = \mu \left\langle \frac{n_{H_1}}{N_{\text{avg}}} \right\rangle - b \left\langle \frac{n_{H_1}}{N_{\text{avg}}} \frac{n_{P_1}}{N_{\text{avg}}} \right\rangle. \tag{8}$$

In the limit of a large population size we recover the mean field approximation or the population level model [71],

$$\dot{h}_1 = h_1(\mu - b p_1) \tag{9}$$

where $\dot{h}_1 = \frac{d\langle n_{H_1} \rangle}{dt N_{\text{avg}}}$ and the frequencies of H_i and P_i are given by h_i and p_i . In the same way, we can derive deterministic differential equations for the frequencies of the other types,

$$\dot{h}_1 = h_1(\mu - b p_1) \tag{10}$$

$$\dot{h}_2 = h_2(\mu - b p_2) \tag{11}$$

$$\dot{p}_1 = p_1(b h_1 - c) \tag{12}$$

$$\dot{p}_2 = p_2(b h_2 - c) \tag{13}$$

Stochastic simulations

The Gillespie algorithm gives an exact numerical solution of the Master equation of the system [41,70,71]. Our stochastic simulations are implementations of this

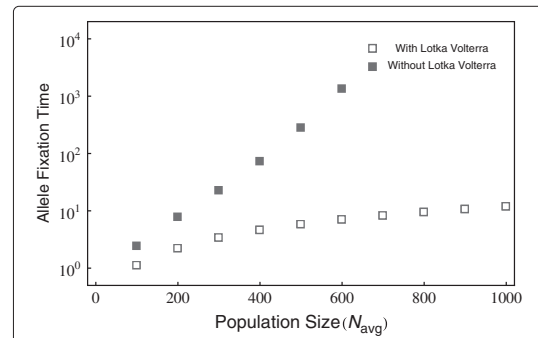


Figure 5 Allele fixation/extinction times for any of the interacting types when we do include a slight interaction between the otherwise independent Lotka-Volterra cycles. As compared to Figure 2 the fixation times in the case without Lotka-Volterra oscillations reduce with slight interaction between independent cycles. However for the case with Lotka-Volterra oscillations the fixation times are practically unchanged. For all simulations the initial condition were $H_1 = H_2 = N_{\text{avg}}/2$, $P_1 = 90N_{\text{avg}}/100$, $P_2 = 10N_{\text{avg}}/100$, and the parameters $\mu = 5$, $c = 2.5$, $b = 10/N_{\text{avg}}$ and $\epsilon = 0.1b$ with averages over 10^6 realizations).

algorithm with the transition rates as defined in Eqs. 6. Since the population size is not constrained, this simulation method includes a stochastic analogue of the Lotka-Volterra cycles.

We computationally remove the Lotka-Volterra cycles by culling the population of each species after N_{avg} transitions have taken place. During the N_{avg} transitions the types within a species can evolve to different frequencies. But in the end they are reset to sum up to N_{avg} while maintaining the relative abundances. The Gillespie method is discrete in the number of individuals but continuous in time. The unit of time is the same as in the deterministic system.

Alternatively we can consider a small amount ε of interactions between the otherwise independent Lotka-Volterra interactions. This is then represented by the following set of differential equations,

$$\dot{h}_1 = h_1(\mu - bp_1 - \varepsilon p_2) \quad (14)$$

$$\dot{h}_2 = h_2(\mu - bp_2 - \varepsilon p_1) \quad (15)$$

$$\dot{p}_1 = p_1(bh_1 + \varepsilon h_2 - c) \quad (16)$$

$$\dot{p}_2 = p_2(\varepsilon h_1 + bh_2 - c). \quad (17)$$

Even for this case, including Lotka-Volterra interactions causes a faster extinction of the Red Queen cycles involving all four types. As an example we provide simulation results where in addition to similar parameters as in Figure 2 we add a $\varepsilon = 0.1b$ (Figure 5). Although the fixation time is elevated as compared to the case with no interactions (Figure 2), they are still not comparable to the extremely high fixation times observed when Lotka-Volterra dynamics is excluded.

Competing interests

The authors declare that they have no competing interests.

Authors' contributions

HS and AP conceived the project. CSG and AT developed the model and performed simulations. All authors analysed the results and wrote the manuscript. All authors read and approved the final manuscript.

Acknowledgements

CSG and AT acknowledge financial support from the Emmy-Noether program of the Deutsche Forschungsgemeinschaft and the Max Planck Society; AP and HS from the Deutsche Forschungsgemeinschaft within the priority programme SPP1399 on host-parasite coevolution (grant SCHU 1415/8). We thank Christian Hilbe for helpful discussions.

Received: 8 August 2013 Accepted: 13 November 2013

Published: 19 November 2013

References

1. Carroll L: *Through the Looking-glass, and what Alice Found there*. London: Macmillan; 1871. Reprinted: Bloomsbury, London, 2001.
2. Ridley M: *Evolution*, 3rd edn. Oxford: Wiley-Blackwell; 2003.
3. Barton NH, Briggs DEG, Eisen JA, Goldstein DB, Patel NH: *Evolution*, 1st edn. NY: Cold Spring Harbor Laboratory Press; 2007.
4. van Valen L: **A new evolutionary law**. *Evol Theory* 1973, **1**:1–30.
5. Woolhouse MEJ, Webster JP, Domingo E, Charlesworth B, Levin BR: **Biological and biomedical implications of the co-evolution of pathogens and their hosts**. *Nat Genet* 2002, **32**(4):569–577.

6. Schmid-Hempel P: *Evolutionary Parasitology: The Integrated Study of Infections, Immunology, Ecology, and Genetics*. USA: Oxford Biology. Oxford University Press; 2011.
7. Fenner F, Fantini B: *Biological Control of Vertebrate pests. The History of Myxomatosis—an Experiment in Evolution*. Oxfordshire: CABI Publishing; 1999.
8. Jokela J, Dybdahl MF, Lively CM: **The maintenance of sex, clonal dynamics, and host-parasite coevolution in a mixed population of sexual and asexual snails**. *Am Nat* 2009, **174**(s1):43–53.
9. Decaestecker E, Gaba S, Raeymaekers JAM, R. Stoks LvK, Ebert D, Meester LD: **Host-parasite 'Red queen' dynamics archived in pond sediment**. *Nature* 2007, **450**:870–873.
10. Bohannan BJM, Lenski RE: **Linking genetic change to community evolution: insights from studies of bacteria and bacteriophage**. *Ecol Lett* 2000, **3**(4):362–377.
11. Buckling A, Rainey PB: **Antagonistic coevolution between a bacterium and a bacteriophage**. *Proc R Soc B* 2002, **269**:931–936.
12. Brockhurst MA, Morgan AD, Fenton A, Buckling A: **Experimental coevolution with bacteria and phage: The pseudomonas fluorescens-phi2 model system**. *Infect Genet Evol* 2007, **7**(4):547–552.
13. Schulte RD, Makus C, Hasert B, Michiels NK, Schulenburg H: **Multiple reciprocal adaptations and rapid genetic change upon experimental coevolution of an animal host and its microbial parasite**. *Proc Natl Acad Sci USA* 2010, **107**(16):7359–7364.
14. Morran LT, Schmidt OG, Gelarden IA, Parrish-II RC, Lively CM: **Running with the red queen: Host-parasite coevolution selects for biparental sex**. *Science* 2011, **333**:216–218.
15. Bérénos C, Schmid-Hempel P, Wegner KM: **Experimental coevolution leads to a decrease in parasite-induced host mortality**. *J Evol Biol* 2011, **24**(8):1777–1782.
16. Fischer O, Schmid-Hempel P: **Selection by parasites may increase host recombination frequency**. *Biol Lett* 2005, **1**(2):193–195.
17. King KC, Delph LF, Jokela J, Lively CM: **Coevolutionary hotspots and coldspots for host sex and parasite local adaptation in a snail-trematode interaction**. *Oikos* 2011, **120**(9):1335–1340.
18. Koskella B, Thompson JN, Preston GM, Buckling A: **Local biotic environment shapes the spatial scale of bacteriophage adaptation to bacteria**. *Am Nat* 2011, **177**(4):440–451.
19. Gandon S, Buckling A, Decaestecker E, Day T: **Host-parasite coevolution and patterns of adaptation across time and space**. *J Evol Biol* 2008, **21**:1861–1866.
20. Gaba S, Ebert D: **Time-shift experiments as a tool to study antagonistic coevolution**. *Trends Ecol Evol* 2009, **24**(4):226–232.
21. Brockhurst MA, Koskella B: **Experimental coevolution of species interactions**. *Trends Ecol Evol* 2013, **28**(6):367–375.
22. Lenski RE, Levin BR: **Constraints on the coevolution of bacteria and virulent phage: A model, some experiments and predictions for natural communities**. *Am Nat* 1985, **125**:585–602.
23. Scanlan PD, Hall AR, Lopez-Pascua LDC, Buckling A: **Genetic basis of infectivity evolution in a bacteriophage**. *Mol Ecol* 2011, **20**:981–989.
24. Meyer JR, Dobias DT, Weitz JS, Barrick JE, Quick RT, Lenski RE: **Repeatability and contingency in the evolution of a key innovation in phage lambda**. *Science* 2012, **335**:428–432.
25. Hall AR, Scanlan PD, Morgan AD, Buckling A: **Host-parasite coevolutionary arms races give way to fluctuating selection**. *Ecol Lett* 2011, **14**:635–642.
26. Lively CM, Dybdahl MF: **Parasite adaptation to locally common host genotypes**. *Nature* 2000, **405**:679–681.
27. Anderson RM, May RM: *Infectious Diseases of Humans: Dynamics and Control*. USA: Oxford University Press; 1992.
28. Dobson AP, Hudson PJ: **Microparasites: observed patterns in wild animal populations**. In *Ecology of Infectious Diseases in Natural Populations*. Edited by Grenfell BT, Dobson AP. Cambridge: Cambridge University Press; 1995:52–89.
29. Hudson PJ, Dobson AP: **Microparasites: observed patterns in naturally fluctuating animal populations**. In *Ecology of Infectious Diseases in Natural Populations*. Edited by Grenfell BT, Dobson AP. Cambridge: Cambridge University Press; 1995:144–176.
30. Bohannan BJM, Lenski RE: **Effect of prey heterogeneity on the response of a model food chain to resource enrichment**. *Am Nat* 1999, **153**:73–82.

31. Lotka AJ: **Analytical note on certain rhythmic relations in organic systems.** *Proc Nat Acad Sci USA* 1920, **6**:410–415.
32. Volterra V: **Variations and fluctuations of the number of individuals in animal species living together.** *J du conseil international pour l'exploration de la mer* 1928, **3**(1):3–51.
33. May RM, Anderson RM: **Epidemiology and genetics in the coevolution of parasites and hosts.** *Proc R Soc Lond B Biol Sci* 1983, **219**(1216):281–313.
34. Frank SA: **Ecological and genetic models of host-pathogen coevolution.** *Heredity* 1991, **67**:73–83.
35. Heesterbeek JAP, Roberts MG: **Mathematical models for microparasites of wildlife.** In *Ecology of Infectious Diseases in Natural Populations*, Edited by Grenfell BT, Dobson AP. Cambridge: Cambridge University Press; 1995:90–122.
36. Roberts MG, Smith G, Grenfell BT: **Mathematical models for macroparasites of wildlife.** In *Ecology of Infectious Diseases in Natural Populations*, Edited by Grenfell BT, Dobson AP. Cambridge: Cambridge University Press; 1995:177–208.
37. Gandon S, Nuismer SL: **Interactions between genetic drift, gene flow, and selection mosaics drive parasite local adaptation.** *Am Nat* 2009, **173**(2):212–224.
38. Kirby GC, Burdon JJ: **Effects of mutation and random drift on Leonard's gene-for-gene coevolution model.** *Phytopathology* 1997, **87**(5):488–493.
39. Salathé M, Scherer A, Bonhoeffer S: **Neutral drift and polymorphism in gene-for-gene systems.** *Ecol Lett* 2005, **8**:925–932.
40. Quigley BJZ, López DG, Buckling A, McKane AJ, Brown SP: **The mode of host-parasite interactions shapes coevolutionary dynamics and the fate of host cooperation.** *Proc R Soc B* 2012, **279**(1743):3742–3748.
41. Gillespie DT: **Exact stochastic simulation of coupled chemical reactions.** *J Phys Chem* 1977, **81**(25):2340–2361.
42. Black AJ, McKane AJ: **Stochastic formulation of ecological models and their applications.** *Trends Ecol Evol* 2012, **27**:337–345.
43. Stiven AE: **Experimental studies on the epidemiology of the host parasite system, hydra and hydramoeba hydroxena (Entz). II. the components of a simple epidemic.** *Ecol Monogr* 1964, **34**(2):119–142.
44. Bach PD, Smith HS: **Are population oscillations inherent in the host-parasite relation?** *Ecology* 1941, **22**(4):363–369.
45. Pimentel D: **Population regulation and genetic feedback evolution provides foundation for control of herbivore, parasite, and predator numbers in nature.** *Science* 1968, **159**(3822):1432–1437.
46. Utida S: **Cyclic fluctuations of population density intrinsic to the host-parasite system.** *Ecology* 1957, **38**(3):442–449.
47. Hudson PJ, Dobson AP, Newborn D: **Prevention of population cycles by parasite removal.** *Science* 1998, **282**(5397):2256–2258.
48. Gillespie JH: **Genetic drift in an infinite population: the pseudohitchhiking model.** *Genetics* 2000, **155**(2):909–919.
49. Lenormand T, Roze D, Rousset F: **Stochasticity in evolution.** *Trends Ecol Evol* 2009, **24**(3):157–165.
50. Campos PRA, Wahl LM: **The effects of population bottlenecks on clonal interference, and the adaptation effective population size.** *Evolution* 2009, **63**(4):950–958.
51. Wahl LM, Krakauer DC: **Models of experimental evolution: the role of genetic chance and selective necessity.** *Genetics* 2000, **156**(3):1437–1448.
52. Wahl LM, Gerrish PJ: **The probability that beneficial mutations are lost in populations with periodic bottlenecks.** *Evolution* 2001, **55**(12):2606–2610.
53. Handel A, Bennett MR: **Surviving the bottleneck: transmission mutants and the evolution of microbial populations.** *Genetics* 2008, **180**(4):2193–2200.
54. Ponting CP: **The functional repertoires of metazoan genomes.** *Nat Rev Genet* 2008, **9**:689–698.
55. Levasseur A, Pontarotti P: **The role of duplications in the evolution of genomes highlights the need for evolutionary-based approaches in comparative genomics.** *Biol Direct* 2011, **6**(11):1–12.
56. Andersson DI, Hughes D: **Gene amplification and adaptive evolution in bacteria.** *Ann Rev Genet* 2009, **43**:167–195.
57. Moran GP, Coleman DC, Sullivan DJ: **Comparative genomics and the evolution of pathogenicity in human pathogenic fungi.** *Eukaryotic Cell* 2011, **10**(1):34–42.
58. Merhej V, Raoult D: **Rickettsial evolution in the light of comparative genomics.** *Biol Rev* 2011, **86**:379–405.
59. Iskow RC, Gokcumen O, Lee C: **Exploring the role of copy number variants in human adaptation.** *Trends Genet* 2012, **28**(6):245–257.
60. Korbel JO, Kim PM, Chen X, Urban AE, Weissman S, Snyder M, Gerstein MB: **The current excitement about copy-number variation: how it relates to gene duplications and protein families.** *Curr Opin Struct Biol* 2008, **18**:366–374.
61. Lively CM, Apanius V: **Genetic diversity in host-parasite interactions.** In *Ecology of Infectious Diseases in Natural Populations*, Edited by Grenfell BT, Dobson AP. Cambridge: Cambridge University Press; 1995:421–449.
62. Frank SA: **Specific and non-specific defense against parasitic attack.** *J Theor Biol* 2000, **202**(4):283–304.
63. Agrawal AF, Lively CM: **Modelling infection as a two-step process combining gene-for-gene and matching-allele genetics.** *Proc R Soc B: Biol Sci* 2003, **270**(1512):323–334.
64. Fenton A, Antonovics J, Brockhurst MA: **Two-step infection processes can lead to coevolution between functionally independent infection and resistance pathways.** *Evolution* 2012, **66**(7):2030–2041.
65. Thrall PH, Laine A-L, Ravensdale M, Nemri A, Dodds PN, Barrett LG, Burdon JJ: **Rapid genetic change underpins antagonistic coevolution in a natural host-pathogen metapopulation.** *Ecol Lett* 2012, **15**(5):425–435.
66. Wolinska J, King KC: **Environment can alter selection in host-parasite interactions.** *Trends Parasitol* 2009, **25**(5):236–244.
67. Dybdahl MF, Lively CM: **Host-parasite coevolution: evidence for rare advantage and time-lagged selection in a natural population.** *Evolution* 1998, **52**(4):1057–1066.
68. Eizaguirre C, Lenz TL, Kalbe M, Milinski M: **Rapid and adaptive evolution of MHC genes under parasite selection in experimental vertebrate populations.** *Nat Commun* 2012, **3**(621):1–6.
69. Luijckx P, Fienberg H, Duneau D, Ebert D: **A matching-allele model explains host resistance to parasites.** *Curr Biol* 2013, **23**(12):1085–1088.
70. Gillespie D: **A general method for numerically simulating the stochastic time evolution of coupled chemical reactions.** *J Comput Phys* 1976, **22**:403–434.
71. McKane AJ, Newman TJ: **Stochastic models in population biology and their deterministic analogs.** *Phys Rev E* 2004, **70**:19.

doi:10.1186/1471-2148-13-254

Cite this article as: Gokhale et al.: Lotka-Volterra dynamics kills the Red Queen: population size fluctuations and associated stochasticity dramatically change host-parasite coevolution. *BMC Evolutionary Biology* 2013 **13**:254.

Submit your next manuscript to BioMed Central and take full advantage of:

- Convenient online submission
- Thorough peer review
- No space constraints or color figure charges
- Immediate publication on acceptance
- Inclusion in PubMed, CAS, Scopus and Google Scholar
- Research which is freely available for redistribution

Submit your manuscript at
www.biomedcentral.com/submit



Part III.

Population size influences the evolutionary trajectories of host-parasite interactions

Andrei Papkou, Rebecca Schalkowski, Mike-Christoph Barg, Ines Braker, Hinrich Schulenburg

Introduction

Host-parasite coevolution is generally viewed as an extremely fast and dynamic process[1]. Strong selection pressure draws antagonists into cycles of continuous adaptations and counter-adaptations. As a result, changes in the relevant traits, like parasite virulence and host resistance, manifest at short time scale making it possible to study coevolution in real-time[2]. However, the enormous complexity of natural systems limits the potential of field studies for causal inferences and motivates many scientists to bring host-parasite coevolution into a controlled laboratory context. Multigenerational passaging of interacting host and parasite lines, referred to as experimental coevolution, has become a powerful tool for precise tracking of antagonistic adaptations[3, 4, 10]. Within the last two decades, considerable progress has been made in establishing different experimental host-parasite systems ranging from bacterium-phage to snail-trematode interaction models, greatly enhancing our understanding of coevolution[5, 6, 7, 8, 9].

One of the first challenges in all evolutionary analyses consists of disentangling inherited adaptive changes from random variation and phenotypic plasticity. This is usually achieved by propagating and measuring many replicate host-parasite populations in a strictly controlled experimental set-up. Then, found temporal patterns in host and parasite traits are contrasted, and the causal relationships during antagonistic changes can be deduced. Ultimately, identification of the involved genetic regions, their associated trait functions, and also their temporal changes allow us to establish the exact mechanism of coevolutionary adaptation in the experiment. Such a comprehensive understanding of the coevolutionary dynamics at both phenotypic and genetic level represents a central objective for current research efforts on the topic that has not yet been achieved in a single study[12, 11]. The largest progress in experimental demonstration of coevolution and underlying genetic changes has been made in bacteria-phage systems[5, 14, 13], while similar studies involving eukaryotic hosts and, thus, more complex interaction types are usually lagging behind due to additional difficulties in manipulating and rearing these organisms. Moreover, many studies focus only on either host or parasite potentially missing important information from coevolving antagonist[11]. Thus, there is particular current interest in understanding coevolution for more complex host systems, using a defined experimental approach.

The strength of such experimental evolution approaches is that they allow us to test specific theoretical predictions on the consequences of coevolution, for instance, increased genetic diversity[16], rare advantage[7, 15], or local adaptation[17, 5, 18]. In this context, time-shift experiments represent a promising study approach, because they allow us to test alternative predictions on the underlying selection dynamics[19, 20]. In particular, evolved populations are confronted with antagonists from the past, present and future, and then their performance is compared. The selection dynamics determined by recurrent selective sweeps (often termed arms race dynamics) could then be indicated by the predicted pattern of ever-increasing fitness over time[1]. This pattern is a consequence of the accumulation of adaptive mutations, as previously shown for a bacteria-phage system[17]. The alternative dynamics based on negative frequency-dependent selection (NFDS, often referred to as Red Queen dynamics) would produce a

non-linear pattern in a time-shift experiment. In this case, the fitness of a particular genotype varies depending on the composition of the antagonist population, whereby rare genotypes are assumed to possess a fitness advantage since they represent a rare resource (i.e., rare host genotypes) or rare threat (i.e., rare parasite genotypes) that is usually less likely to favour adaptation in the antagonist. As a result, host and parasite genotypes oscillate in frequency over time with contemporaneous combinations predicted to differ in their type of interaction from the non-contemporaneous combinations[1]. To date, such NFDS dynamics could only once be directly demonstrated with the help of a time-shift experiment, in this case based on recovery and subsequent analysis of both the host *Daphnia magna* and its bacterial microparasite from different layers and, thus, time points of pond sediment[21, 19]. The most likely explanation for a lack of further examples is that for most eukaryotic host model organisms it is impossible to preserve genotypes from across evolution for subsequently performed time-shift experiments.

Analysis of the underlying selection dynamics must take into account the involved population genetic parameters. For example, contrary to arms race selection, NFDS dynamics does not necessarily require a continuous supply of new beneficial mutations and can operate on standing genetic variation. This is why it is considered as potentially a main mechanism of coevolution among eukaryotic hosts and their parasites[1, 22]. Eukaryotes have longer generation time and smaller population sizes, thus availability of standing genetic diversity is of primary importance. Many important biological aspects connected to production and maintenance of genetic variation, such as sexual reproduction[8, 23, 24], recombination[6] and migration[5], have been frequently addressed in relation to host-parasite coevolution. Yet, one essential factor, population size, is largely neglected in theoretical and empirical studies. Population size via modulating genetic drift and selection can strongly affect genetic diversity, and ultimately the coevolutionary process[25, 26, 27]. Though natural host-parasite interaction is most likely associated with high variations in population size, it is usually kept constant during experimental coevolution.

In this study, we aim to test (i) predictions on the patterns of reciprocal adaptation during experimental host-parasite coevolution and (ii) the particular role of population size for the adaptive process. Based on the previously established *Caenorhabditis elegans*-*Bacillus thuringiensis* interaction model[9, 18, 24], although using a novel high-throughput protocol, we simultaneously evolved a total of 176 populations under different demographic regimes. After 23 host generations of coevolution we carried out large-scale phenotypic characterizations, including a time-shift experiment for the host and parasite, and found adaptation patterns predicted by negative frequency-dependent selection. Additionally, we demonstrated that coevolutionary dynamics can be strongly influenced by population size.

Materials and Methods

Model organisms and the experimental system

We used the nematode *Caenorhabditis elegans* as a host model. A highly diverse androdioecious *C. elegans* population created by crossing 16 wild isolates (kindly

provided by H. Teotonio [34]) served as the starting host population. As a parasite, we used the Gram-positive spore-forming bacterium *Bacillus thuringiensis*, which produces nematocidal Cry toxins and infects its host infection upon oral uptake. In contrast to the previous experiments based on the same host-parasite system [9, 24], the starting parasite population was composed of a single clone of the *B. thuringiensis* laboratory strain MYBT18247. To facilitate analysis of this bacterium, MYBT18247 was transformed with the plasmid pHT315-pAphA'-rfp to express red fluorescent protein. This plasmid, kindly provided by C. Nielsen-LeRoux, is known to have stable low-copy replication [37, 38].

In order to take advantage of microtiter plates, we developed a novel viscous medium for nematode maintenance. S-medium, widely used for *C. elegans* liquid culture [35, 36], serves as the basis and is modified by addition of 1.1% of hydroxypropylmethyl cellulose (#56340 Sigma-Aldrich). The new viscous medium allows nematodes to move freely, mate and reproduce at the rate comparable to *C. elegans* reproduction on standard agar plates, while offering a less structured environment where bacteria are present in "suspended" form. The medium can be easily distributed into microtiter plates with sufficiently high accuracy using a positive-displacement pipette. A suspension containing host larvae or parasite spores can be added without significantly changing the medium's viscosity, provided that the inoculation volume does not exceed 10-15% of the final volume. Each well in a microtiter plate represents an isolated three-dimensional microcosm where the host grows, reproduces and gets infected by the parasite. Experimental plates are sealed with a gas-permeable foil (#3911262, VWR) ensuring oxygen supply and preventing cross-contamination and nematode escape. After two-fold dilution, the medium can be readily recovered from microtiter plates and handled with common pipettes.

Basic procedures for *C. elegans* maintenance (bleach synchronization, cryopreservation) were modified to be used in a 96-well format. For all separation steps (e.g. separation of nematodes from viscous medium, surrounding bacteria, bleaching or cryoprotecting solution) we used a custom multiwell filtration method instead of a laborious procedure of repeated centrifuging-resuspending in single tubes. Common 1000 μ l pipette filter-tips, which are supplied prearranged in 8 \times 12 matrix format, served as custom columns. Their filters stop all *C. elegans* stages while letting liquids and bacteria pass through. As has been verified in a pilot study, three filtration steps are sufficient to almost completely remove the bacterial cells unless they reside inside the nematodes (data not shown).

To handle in parallel many samples, *B. thuringiensis* was cultured in 48 deep well plates (#43001-0062, Ritter) with 2 ml of liquid T3-medium per well [39]. Deep well-plates were sealed with a gas-permeable foil (#3911262, VWR) and incubated at 25°C with orbital shaking (1200 rpm, 3 mm orbit diameter). *Escherichia coli* OP50 served as a food source for the nematodes. Overnight cultures were always started from -80°C stocks established before the experiment. Overnight cultures were prepared in 1 l flasks containing 350 ml of LB-medium (20h, 37°C, 150 rpm). *E. coli* cells were washed, concentrated by centrifuging, and resuspended in viscous medium to a concentration of 1g of cell pellet per 22.2 ml of viscous medium ($\approx 5 \times 10^9$ - 1×10^{10} cells/ml), ensuring *ad libitum* food supply for *C. elegans*.

Experimental evolution

Experimental design. The evolution experiment included five interaction and three demographic treatments (Figure 1). The interaction treatments included coevolution, host adaptation, parasite adaptation, host control and parasite control. In the coevolution treatment both the host and the parasite were forced to co-adapt to each other. In the host adaptation and parasite adaptation treatments, only the host or only the parasite was allowed to adapt and the other antagonist was always taken from the stock. In the two control treatments (host control, parasite control) host and the parasite lines were passaged without being exposed to each other. In addition, all host treatments (coevolution, host adaptation, host control) were subdivided into three different demographic regimes, consisting of small population size (100 nematodes), large population size (3000 nematodes) and fluctuating population sizes. In the first two regimes, host population sizes were kept constant. The populations under the fluctuating regime were propagated at large population size (3000) for the first 4 host generations and subjected to a bottleneck (100 nematodes) during the 5th round of the experiment. After the bottleneck the populations were recovered, and then the same cycle was repeated every 5 host generations (bottlenecks at host generation 5, 10, 15, 20). The different demographic regimes were based on using different volumes per microcosm (100 μ l for the 100 and 3000 μ l for the 3000 individuals-containing populations, respectively), ensuring identical host densities (1 nematode/ μ l) among the treatment groups. 100 μ l and 3000 μ l populations were accommodated in 96-well and 6-well plates, respectively, and were chosen to have the same surface-to-volume ratio (the same oxygen availability). The latter two measures served to minimize a possible influence of host density or oxygen availability on the results, thus treatment variation is most likely caused by the differences in demographic regimes. 24-well plates with 600 μ l of viscous medium per well were used to provide an environment of intermediate population size for population recovery after bottlenecks. Overall, the experimental design resulted in a total of 11 treatment groups (Figure 1). Each of these was run in 16 replicates.

Each round of the evolution experiment lasted one week and corresponded to one host generation (Figure S1). For clarity, we describe selection protocols for the host and the parasite separately.

Host selection protocol. An experimental round was started with host populations represented exclusively by L1 larvae stages, which were synchronized overnight in M9-buffer. Three samples from every population were counted to estimate larvae concentrations, and then the respective volumes containing either 100 or 3000 larvae were transferred into microtiter plates already containing viscous medium. Host populations were grown for 4 days at 16 °C by which time point they all consisted of only 4th stage larvae (L4) or young adults. On day 5, *B. thuringiensis* premixed with *E. coli* was added to host populations. Host control populations received only *E. coli*. On day 7 nematodes were separated from the viscous medium and surrounding bacteria and bleached using a custom filtration protocol. Briefly, the viscous medium containing the nematodes and bacteria was transferred from well plates on filters, where the nematodes were washed with M9-buffer and exposed to a bleaching reagent (1% sodium hypochlorite) for 4 min. The bleaching reagent was neutralized by a stop reagent (8% sodium thio-

sulfate buffered by 0.1 M monosodium phosphate), and washed with M9-buffer. This procedure efficiently killed the bacteria, including *B. thuringiensis* and all stages of *C. elegans* except of their eggs. The eggs were subsequently transferred in M9-buffer to well-plates and incubated overnight at 16 °C with agitation. During overnight incubation, L1 larvae hatched from the eggs and were additionally synchronized, as they lacked food source for continuing development [36].

Parasite selection protocol. *B. thuringiensis* populations were recovered out of nematode corpses from a previous selection round. The recovery took place on day 2 of the weekly time schedule and was directly followed by pasteurization at 70 °C for 10 min to kill all *E. coli*. The pasteurized populations were transferred to liquid T3-medium and cultured at 25 °C for 3 days in 48-deep well plates as described above. On day 5 *B. thuringiensis* cultures, mostly consisting of spores, were washed by centrifuging in S-buffer, and their concentration was adjusted based on OD₆₀₀ readings. Parasite spores were mixed with *E. coli* and added to corresponding host populations. Final parasite concentration in viscous medium was 0.15 OD (approx. 2×10^8 spore/ml), except that every 5th host generation the concentration was decreased in all treatment groups to 1×10^8 spore/ml in order to ensure host recovery after a bottleneck in the fluctuating host population size regime. On day 7 (approximately 40 h after spore inoculation) a sample of 15–20 host individuals (dead and alive) was taken from every host population prior to a bleaching procedure. These samples were washed 3 times with M9-buffer on custom columns to minimize bacterial presence on the outer surface of the nematode corpses, followed by transfer of each sample into wells of a 96-well plate containing 150 µl of T3-medium. *B. thuringiensis* was subsequently incubated at 25 °C for 40 h (until day 2 of the next round) in order to finalize sporulation.

Cryopreservation. Host and parasite populations from every round of the experiment were cryopreserved at -80 °C. On day 1 of the weekly time schedule, after starting experimental host populations, we initiated in parallel an identical set of host populations, which were allowed to reproduce for one generation without being exposed to the pathogen. After 9–11 days, when the nematodes had starved, host populations were mixed with dimethyl sulfoxide (up to the final concentration of 20% v/v), distributed into rack tubes (#781562, Brand), and then transferred to -80 °C. As for *B. thuringiensis*, the spores, which were left after inoculation on day 5, were mixed with glycerol (final concentration 15%) and distributed across sterile PCR plates. The plates were sealed with an aluminium foil and stored in a -80 °C freezer. 4 replicate samples were cryo-preserved for all host and parasite populations every round, and 8 replicates were prepared after the last generation.

Phenotypic assays

For phenotypic tests we used evolved and ancestral host and parasite populations. To recover host populations from -80 °C stock, they were grown for one generation, and then F1 offspring were used to measure the relevant traits. Similarly, *B. thuringiensis* populations were first grown overnight after thawing, and then the overnight cultures were used to initiate new cultures for phenotypic assessment. This strategy served to minimize any potential effect of cryopreservation on the measured phenotypes.

For all phenotypic assays one round of the evolution experiment was replayed in 96-well plates, following the above described selection protocol, in order to ensure measurement of trait variation under the relevant experimental conditions. Thus, infection was initiated by addition of parasite spores to host populations on day 5 and stopped after 40 h on day 7. Two general types of analyses were performed, for which (i) evolved populations were exposed to ancestral populations of the respective antagonist (general assessment of evolutionary change), and (ii) populations from the coevolution treatments were confronted with co-adapted antagonists from different time points, in each case derived from the same replicate population (time shift experiment for coevolved populations).

General assessment of evolutionary change. General changes were evaluated for host fecundity (or analogously the parasite’s effect on host fecundity), host male ratio, and host resistance (or analogously parasite virulence).

Host fecundity upon parasite exposure. The average number of eggs per hermaphrodite was used as a measure of host fecundity. The measurement was taken exactly at the time point, when transfer to the next selection round took place during the evolution experiment, following exactly the same protocol for preparation of the transferred material. Thus, host fecundity at this time point is most likely the most relevant trait under selection during experimental evolution. For this assay, evolved host populations were exposed to ancestral parasite at the same concentration as during experimental evolution (2×10^8 spore/ml). After 40 h we separated nematodes from the viscous medium and surrounding bacteria and fixed them in M9-buffer supplemented with 10 mM of sodium azide. The fixed samples were placed on microscopic slides and scanned using Leica dissecting microscope M205-FA with a motorized stage. Individual pictures were stitched with the help of ImageJ and plug-in “Stitching”, producing one mosaic image for an entire host population [40]. Eggs within hermaphrodites were manually counted using ImageJ plug-in “Cell Counter” and custom scripts. We scored up to 30 hermaphrodites per population which were randomly chosen on the mosaic picture following a predefined grid. The same procedure was used for evolved *B. thuringiensis* exposed to ancestral host populations, in order to assess any evolved parasite effect on host fecundity, which we here consider as a proxy for virulence *sensu lato*.

Host male ratio. For estimating male ratio we used mosaic pictures acquired for measuring host fecundity (see above). We recorded the number of males per group of 30-40 individuals, randomly chosen on the mosaic picture following a predefined grid.

Host resistance/Parasite virulence. As a proxy for host resistance *sensu lato* and parasite virulence *sensu stricto*, we determined the proportion of dead hermaphrodites upon exposure to *B. thuringiensis*. In the assay the host was confronted with the parasite following the selection protocol for coevolution. One exception was that a lower *B. thuringiensis* concentration (3.3×10^7 spore/ml) was used in order to ensure a higher level of variation among replicate populations (and thus higher sensitivity for detecting treatment differences) than during experimental evolution, where high parasite concentrations caused host mortality rates close to 85%. After 40 h of parasite exposure the nematodes were transferred onto custom filters, washed and resuspended in M9-buffer. Around 30–40 hermaphrodites per pop-

ulation were inspected under a dissecting microscope, and immobile nematodes under these conditions were considered as dead.

Time shift-experiment for coevolved populations. In the time-shift experiment we cross-infected the coevolved hosts from three different time-points (1, 10, 23 host generations) with the coevolved parasites from exactly the same time points. All possible combinations among the chosen time-points were considered. Generation 1 is represented by the ancestral host and parasite populations, which were subsequently subjected to one round of the evolution protocol during phenotypic analysis. We always combined hosts and parasites, which coevolved with each within the same replicate population. After replay of one round of experimental coevolution, two phenotypes were measured: (i) the proportion of dead hosts, and (ii) host fecundity, using in both cases the same methods as above.

Statistical analysis

To test whether host fecundity changed during experimental coevolution, we used a linear-mixed model with an average number of eggs per hermaphrodite as a response variable. Treatment and demographic regime were considered fully-crossed fixed factors, host generation a covariate and population identity a random factor. Based on the fitted model, we carried out post-hoc pairwise comparisons among different treatments and demographic regimes adjusting p values for multiple testing using the single-step method suggested by Hothorn et al. (similar to Tukey method but taking into account correlations among model coefficients[44]).

To examine host mortality changes during coevolution, we fitted a linear mixed-effect model. The power-transformed proportions of dead hermaphrodites were used as a response variable, treatment, demographic regime and their interactions as fixed factors. Population identity (biological replicate) with three nested technical replicates was included as a random effect.

The change in a male ratio during the experiment was analyzed with the help of a generalized linear-model. An average frequency of males summarized over replicate populations within each treatment group per time point was considered as response variable with an error following a Gaussian distribution. Treatment, demographic regime and their interactions were considered as fixed factors, and host generation as a covariate.

To evaluate the changes in parasite virulence, we started with a linear mixed-effect model which treated non-transformed proportion of dead hermaphrodites as a response variable assuming homogeneity of error variance. The only fixed factor in the model was a combination of treatments and demographic regimes with five levels (parasite control, parasite adaptation, coevolution in small populations, coevolution in large populations and coevolution in fluctuating populations). Host generation was taken as a covariate and biological replicate as a random factor. Because the assumption of homoscedasticity was clearly violated in the fitted model, it was refined by incorporating a variance function which takes into account temporal change in error variance depending on the treatment.

To compare the host and parasite fitness in the contemporaneous versus shifted combinations in the time-shift experiment, we fitted a linear-mixed effect model with the power-transformed values of average numbers of eggs per hermaphrodite as a response variable. Demographic regime, a combination of time-points and

interaction between them were considered as fixed effect and a biological replicate was considered as a random effect. In post-hoc comparisons, we tested one-sided hypothesis whether host reproduction in the contemporaneous combinations is reduced compared to the shifted combination. Temporal patterns obtained in the time-shift experiment for individual host and parasite populations were analyzed as follows. First, we classified all individual patterns into three possible outcomes, and then we examine employing exact multinomial test whether the observed frequencies in the data can be explained by a chance alone. After the test p values were adjusted by Holm method controlling for the family-wise error rate.

To compare host and parasite fitness in the contemporaneous versus shifted combinations in the time-shift experiment, we fitted a linear-mixed effect model with the power-transformed values of average numbers of eggs per hermaphrodite as a response variable. Demographic regime, the combination of time-points and interaction between them were considered as fixed effects and biological replicate was considered as a random effect. In post-hoc comparisons, we tested the one-sided hypothesis that host reproduction in the contemporaneous combinations is reduced compared to the shifted combination. Temporal patterns obtained in the time-shift experiment for individual host and parasite populations were analyzed with a frequency test as follows. First, we classified all individual patterns into three possible outcomes, and then the resulting counts were compared using an exact multinomial test. After the test p values were adjusted by Holm method controlling for the family-wise error rate.

All statistical analysis performed with R[42] using specific packages for fitting mixed-effect models (`nlme` [41]), performing post-hoc multiple comparisons (packages `lsmeans`[43] and `multcomp`[44]) and exact multinomial test (`EMT`[45]).

Results

In order to study coevolution dynamics, we performed an evolution experiment for 23 host generations using a variety of treatments relevant for our main research questions (Figure 1). In particular, we included control evolution treatments to assess how host and parasite may adapt to the experiment protocol. We then included and compared an adaptation treatment (where only one species is evolving and the other is always taken from a stock) and coevolution to test to what extent one evolving antagonist affects the evolution of the other. In addition, three different demographic regimes were imposed on evolving hosts in a fully factorial manner with the idea to measure the effect of population size on the adaption process. We used a 30 times difference in census size, thus allowing us to compare evolution under conditions of increased randomness in small populations with rather “deterministic” adaptation in the large populations. The experimental lines with fluctuating population size were included to simulate a scenario of extreme, environmentally induced variation in population size, which is likely common for natural populations (because of predation, food shortage or seasonal changes). After each transfer during the experiment, we archived almost every host and parasite population at -80°C , permitting us to reconstruct coevolution from different angles. First, we recovered either host or parasite from 5 different time-points and exposed them to the unchanged ancestral antagonist. The second approach is essentially a time-shift experiment, where host and para-

site from different generations (1, 10 and 23) were confronted in all combinations. In the latter case, we included all host and parasite lines exclusively from the coevolution treatment. Throughout phenotypic assays, we mostly focused on two traits, host fecundity and host mortality upon infection.

Evolving host versus ancestral parasite

As a proxy for host fitness we chose fecundity, which was measured as an average number of eggs within a hermaphrodite after 40 h of infection. This is justified by the fact that at the end of each coevolution transfer we bleach-synchronized the host (see Methods), and, during this procedure host eggs which were inside hermaphrodites had far better chances to survive compared to already laid eggs and hatched larvae. When comparing host fecundity across treatments we found a dramatic increase across time for the coevolution and adaptation treatments but not for the control treatment suggesting that this is a general response to selection from the pathogen during evolution (Figure 2; Table 1 - $p < 0.0001$, $F = 35.429$ for Treatment effect; and $p < 0.0001$, $F = 13.026$ for interaction Treatment \times Generation). Post-hoc comparisons confirmed that the largest difference is in between the control populations and the populations adapting/coevolving to parasite (Table 2). In addition, the regression analysis showed that a demographic regime significantly influences the temporal changes in host fecundity (Table 1 - $p < 0.0008$ ($F = 7.338$) for interaction Demography \times Generation). Interestingly, the interaction between treatments and demographic regimes was not significant, meaning that different population sizes affected coevolution and adaptation in a similar way (Table 1). At the same time, the temporal trends (fitted slopes in the model) appear to differ for small versus large population size for the coevolution treatment (Table 3, $p < 0.0076$, $z = -3.695$), confirming that increased stochasticity in the small populations influenced adaptation to the antagonist. The host lines evolved under the fluctuating demographic regime have reached comparable values in host fecundity as the small and large populations (Figure 2, Table 2 and Table 3). However, these lines seem to diverge more rapidly from each other, as can be seen in Figure S2 showing variance among population means within the same treatment combination.

We next measured host mortality upon 40 h of infection. The results in host mortality generally follow the patterns observed for host fecundity, as host populations in all treatments except the control treatment showed directional response. Interestingly, adaptation or coevolution with the parasite always led to increased mortality compared to the control (Figure 3, Table 4, Table 5). Although this may sound contradictory, the two phenotypes are not strictly dependent on each other in our set-up, because host embryos which have begun their development prior to hermaphrodite death, can develop normally and contribute to the next generation. Thus, two genotypes may considerably differ in mortality but not in fecundity (Figure S3). Taking this into account, our results may suggest that selection for increased fecundity was stronger than that for increased survival. Alternatively, the two traits may be controlled by linked loci that are negatively correlated. For host mortality, we found neither an effect of the demographic regime (Table 4, Table 5) nor higher population divergence for fluctuating population size (Figure 3).

We also assessed in how the proportion of males in the host populations change during the experiment. As *C. elegans* hermaphrodites are able to reproduce by outcrossing with males and by selfing, male proportion may vary considerably, depending on male fitness in the presence of parasites and also male-hermaphrodite outcrossing rates. As shown in Figure 4, male ratio in all populations facing the parasite rapidly dropped to approximately 5%, where it stayed more or less unchanged until the last generation (Table 6 - effect of Treatment $p < 0.0001$, deviance=0.22684; interaction term Treatment \times Generation $p < 0.0003$, deviance=0.03389).

Evolving parasite versus ancestral host

To analyze parasite virulence evolution, we challenged ancestral host with evolved parasite lines from 5 different time-points (Figure 5). No significant difference in virulence was found among treatments and demographic regimes (Table 7). Instead, we observe almost complete loss of virulence for some individual lines independent of the treatment (thin gray lines on Figure 5). This result is unlikely be due to measurement errors, as a strong reduction in virulence was reproduced for many of these populations, when we repeated the same assay (not shown). Thus, we hypothesized that different selection regimes may influence the extent of heterogeneity among individual lines. Indeed, our regression analysis revealed a distinct variance distribution for different treatments (Figure S4, likelihood ratio test, LR=28.61, $p < 0.0001$), suggesting that at least some of the extreme changes in virulence result from reciprocal adaptation.

Selection pattern in time-shift experiment

In the time-shift experiment we focused exclusively on the coevolution treatment, but we looked at both coevolving parties. Host populations were always matched exactly to the parasites populations they coevolved with. This single large-scale experiment includes all 16 individual host and parasite populations for each demographic regime and all possible combinations of 3 time-points (1, 10 and 23). To characterize host-parasite interactions, we scored a proportion of dead hermaphrodites and a number of eggs within hermaphrodites after 40 h of infection. The first phenotype is a proxy for host resistance and for parasite virulence, while the second one is an estimate of host fecundity and parasite harm to host reproduction.

Using the same phenotypes to simultaneously measure host and parasite evolution allows us to compare them on the same scale. Such a comparison turns out to be very informative for dissecting observed coevolution trajectories into individual responses of the host and parasite and their combined effect (Figure 6). The first observation is that the host, on average, experienced changes of higher magnitudes compared to the parasite (dotted line with open circles versus dashed lines with closed triangles on Figure 6). Second, the combined effect of reciprocal adaptation (red solid lines) can be well predicted by individual responses in relation to host resistance/parasite virulence, but not for host fecundity/parasite harm (top panel versus bottom panel on Figure 6). In the former case, the trajectories of combined effect (red lines) follow more closely the host response (dotted

lines), suggesting that host mortality in coevolution was largely determined by the host. In addition, there is an indication that responses in parasite virulence and parasite harm to host reproduction are correlated, as their trajectories "mirror" each other when compared within the same demographic regime (compare the dashed lines of the top panels to the corresponding lines from the bottom panels). The evolution of host fecundity and host survival may be connected in a complex, non-linear manner as has been discussed above. Third and most interestingly, the patterns of host fecundity/parasite harm (the bottom panels) are strongly influenced by population size. For small population size the combined effect still can be well predicted based on individual responses (the red line positioned between the two black ones, the bottom left panel, Figure 6). However, measurements of the combined effect for large population size strongly deviate from what can be expected based on the host and parasite responses (the bottom middle panel in Figure 6, but see also Figure S5). Despite the fact that the host population from generation 10 shows an increase in fecundity on the original parasite, and the co-evolved parasite exert less harm on ancestral host reproduction, their combination does not lead to an increase for host fecundity. Similar patterns although with smaller amplitudes can be observed for fluctuating population size. This finding suggests that evolved fitness of one antagonist depends on the adaptation history of the other, i. e. there is likely reciprocal selection dynamics.

The Red Queen hypothesis predicts that the faster adapting species (usually parasite) should be temporally adapted to contemporary antagonist. To test whether such temporal patterns in adaptation can be confirmed, we considered all time-point combinations from the time-shift experiment (Figure S6). If the parasite is temporally adapted, then host reproduction should be reduced in the contemporaneous combinations corresponding to diagonal squares on Figure 12 (1×1 , 10×10 , 23×23). For large population size, regression analysis revealed lower host performance for contemporaneous combinations compared to all others combinations (off-diagonal squares) (Table 8 and Table 9, $z=1.916$, $p=0.0277$). This was not the case for small and fluctuating population size (Table 9). Thus, adaptation dynamics are consistent with the Red Queen hypothesis and, moreover, they were influenced by demographic regime.

The analysis above does not take into account the individual trajectories in the detected selection dynamics. To address this question, we compared fitness of individual host lines from generation 10 on contemporaneous parasite (generation 10) versus their fitness on past or future parasites (generation 1 and 23, accordingly, Figure 7, the top panels). The reciprocal design was applied to individual parasite populations from generation 10 (Figure 7, the bottom panels). Then, we classified all host and parasite trajectories into three categories ignoring the magnitude of change: the fitness is higher on contemporaneous antagonist than on antagonist from past or future ("−+−"), the fitness is lower on contemporaneous antagonist than on antagonist from past or future ("+-+"), and fitness on contemporaneous antagonist has intermediate values ("−++", "+--"). Most of the host populations evolved under large population size showed "+-+" pattern (Table 10, goodness-of-fit test, $p=0.0048$). This result was reflected in the parasite which produced the "−+−" pattern in 10 out of 16 parasite lines (Table 10, goodness-of-fit test, $p=0.0065$). Thus, the results provide strong support for the

action of negative frequency-dependent selection during our experiment, where parasite is adapted to the most common contemporaneous host genotype. 10 out of 15 measured host lines evolving under fluctuating demographic regime also showed reduced fecundity on concurrent parasites (“+−+” Table 10, goodness-of-fit test, $p=0.0080$), but patterns produced by corresponding parasite populations could be explained by chance alone (Table 10, $p=0.00651$).

Discussion

Experimental evolution can be used for a direct test of key theoretical hypotheses on host-parasite coevolution[4, 10]. Of particular value are model systems for which the interacting species can be cryopreserved or conveniently propagated in large replicate numbers, allowing simultaneous analysis of material from different time points and also comparison of independently evolved lines, respectively. Here, we developed a novel protocol based on viscous medium allowing us to employ multiwell plates and thus large replicate numbers for the experiment. Importantly, the novel protocol enabled us to simulate diverse demographic scenarios and, at the same time, control parasite and host density. As a result, we evolved a total of 176 individual experimental lines for 23 generation and, afterwards, performed large-scale phenotypic evaluations. Comprehensively archived samples permitted the simultaneous analysis of evolved hosts and parasites from different generations. We found a directional response in host fecundity and mortality when assayed on the ancestral parasite. In contrast, the analysis of parasite traits on the ancestral host did not reveal any directional pattern, instead we observed the accumulation of heterogeneity among replicated populations. Most importantly, the time-shift experiment provided direct evidence of negative-frequency dependent selection with largely synchronous and consistent patterns for the host and parasite populations coevolved at large population size.

To our knowledge, this paper reports the first laboratory time-shift experiment that captured for both antagonists the pattern predicted by NFDS during host-parasite coevolution. It has been almost 7 years since publication of the seminal study on reconstruction of NFDS dynamics for the pathogen in pond sediment[21]. The importance of the previous study is that the results were based on a natural system, consisting of the waterflea *Daphnia magna* and its microparasite *Pasteuria ramosa*, while in our case, the material was generated in a laboratory-controlled evolution experiment. Our results shows that temporal adaptation patterns can arise for both antagonists (and not just for the parasite as in the above study) in as few as 10 host generations, confirming an extremely rapid rate of coevolution and requiring an explanation of the underlying genetic mechanisms. Most likely, standing genetic variation involved in NFDS played a major role in such fast host counter-adaptations, but the contribution of other processes like outcrossing and recombination needs additionally be considered. Moreover, it has been increasingly recognized that copy number variation can take part in short term species adaptation (including *C. elegans*)[28, 29, 30]. Thus, in order to elucidate underlying genetic mechanism of the NFDS dynamics found, a genomic analysis of the coevolved populations is necessary.

The comparison of evolved lines only by exposing them to ancestral host or ancestral parasite was not sensitive to detect NFDS dynamics, highlighting once

again the power of time-shift experiments. This could be expected, as changes in fitness are assumed to be “hidden” by reciprocal NFDS[1, 21]. The absence of clear directional response of parasite is consistent with this prediction, while, interestingly enough, the host populations showed an apparent increase in fecundity in the course of the experiment, suggesting general selection from the parasite in parallel to more contextual NFDS dynamics. Both, the directional adaptation pattern (typical for recurrent selective sweep dynamics) and NFDS dynamics are not mutually exclusive, because different parts of the genome can be exposed to different selection pressures[9]. In addition, partitioning combined coevolution trajectories into individual host and parasite responses (as in Figure 6) revealed their additive contribution in one case (host mortality) and reciprocal interaction in the second case (host fecundity), pointing to complex relation and potentially different evolutionary trajectories for the two phenotypes.

Population size is rarely considered in the context of host parasite coevolution. This partially stems from a widespread view that an accurately chosen constant population size (i. e. effective population size) is sufficient to imitate the properties of natural population with diverse demographic histories. As a result, most of the current theoretical models assume infinite or constant population size, and population size is usually kept constant in coevolution experiments. However, there are good reasons to question the generality of this view, taking into account few empirical and theoretical studies where a problem of population size in host-parasite coevolution has been addressed[32, 25, 31, 26, 27]. For example, a recent paper showed that conventional models of host-parasite coevolution require constant or infinite population size in order to reproduce NFDS dynamics[27]. In the current study, we tested a range of demographic scenarios during coevolution and found that they resulted in different selection dynamics. Dynamics consistent with NFDS was found in large but not small populations, suggesting that genetic drift interfered with selection. Alternatively, genetic variation necessary for selection was quickly lost in the small populations. Under fluctuating population size, the negative-frequency dependent dynamics was only partially confirmed, probably, due to disturbance of the allele frequencies involved in host-parasite interactions during bottlenecks. More specifically, under NFDS a parasite is adapted to the most common host genotype, however bottlenecks would shuffle genotype frequencies and, therefore maladapt the parasite. This result is especially interesting as the populations under fluctuating demographic regime experienced only four bottlenecks in the experiment with the smallest census size of 100 nematodes, which is apparently not the most severe scenario for highly structured and heterogeneous natural environments. Thus, dynamic demographic histories have the potential to explain the previously observed absence of local adaptation in a variety of field studies[33].

In the current study, we have adopted a previously established *C. elegans* - *B. thuringiensis* host-parasite model[24, 9, 18], but, contrary to the previous studies, we used a viscous medium instead of a solid agar medium. Despite such different physical environments, we obtained a very consistent pattern for changes in male ratio during coevolution: the proportion of males in the host populations confronted with the pathogen quickly dropped in the first few selection rounds, but then the males did not go extinct by the end of the experiment. In the previous

studies, the same pattern obtained for the two independent evolution experiments was explained by joint effect of poor male performance on the pathogen and a long-term adaptive advantage of outcrossing[24]. Our results additionally support this explanation, as changes in male ratio following the same pattern independent of different experimental conditions and demographic regimes cannot be introduced by the experiemntal protocol.

To conclude, in this study we reported reciprocal adaptations of the nematode *C. elegans* and its microparasite *B. thuringiensis* during experimental coevolution. By exposing evolved populations either to the ancestral antagonist or to the coevolved antagonist from different time points, we directly tested for coevolution dynamics. Our result provides the first demonstration of negative-frequency dependent selection dynamics simultaneously for the two antagonist. Additionally, we examined the consequences of different demographic scenarios for coevolution, including the conditions of small population size and externally induced bottlenecks, which are common in natural populations but usually avoided in evolution experiments. We found that negative-frequency dependent selection dynamics was significantly altered or even prevented if the population size was not constant and not large enough. This recalls a potential relevance of population size in host-parasite coevolution and suggests that better understanding of natural host-parasite relationship can be achieved by incorporating more realistic assumptions about population size into theoretical and experimental models.

References

- [1] Mark E. J. Woolhouse, Joanne P. Webster, Esteban Domingo, Brian Charlesworth, and Bruce R. Levin. Biological and biomedical implications of the co-evolution of pathogens and their hosts. *Nature Genetics*, 32(4):569–577, December 2002.
- [2] Frank Fenner and Bernardino Fantini. *Biological Control of Vertebrate Pests: The History of Myxomatosis - an Experiment in Evolution*. CABI, New York, NY, USA, first edition, December 1999.
- [3] D Ebert. Experimental evolution of parasites. *Science (New York, N.Y.)*, 282(5393):1432–1435, November 1998.
- [4] Tadeusz J. Kawecki, Richard E. Lenski, Dieter Ebert, Brian Hollis, Isabelle Olivieri, and Michael C. Whitlock. Experimental evolution. *Trends in Ecology & Evolution*, 27(10):547–560, October 2012.
- [5] Michael A Brockhurst, Andrew D Morgan, Andrew Fenton, and Angus Buckling. Experimental coevolution with bacteria and phage. the pseudomonas fluorescens–phi2 model system. *Infection, Genetics and Evolution: Journal of Molecular Epidemiology and Evolutionary Genetics in Infectious Diseases*, 7(4):547–552, July 2007.
- [6] O Fischer and P Schmid-Hempel. Selection by parasites may increase host recombination frequency. *Biology Letters*, 1(2):193–195, June 2005.
- [7] Britt Koskella and Curtis M Lively. Advice of the rose: experimental coevolution of a trematode parasite and its snail host. *Evolution; International Journal of Organic Evolution*, 61(1):152–159, January 2007.
- [8] Levi T. Morran, Olivia G. Schmidt, Ian A. Gelarden, Raymond C. Parrish, and Curtis M. Lively. Running with the red queen: Host-parasite coevolution selects for biparental sex. *Science*, 333(6039):216–218, July 2011.
- [9] Rebecca D. Schulte, Carsten Makus, Barbara Hasert, Nico K. Michiels, and Hinrich Schulenburg. Multiple reciprocal adaptations and rapid genetic change upon experimental coevolution of an animal host and its microbial parasite. *Proceedings of the National Academy of Sciences*, 107(16):7359–7364, April 2010.
- [10] Michael A. Brockhurst and Britt Koskella. Experimental coevolution of species interactions. *Trends in Ecology & Evolution*, 28(6):367–375, June 2013.
- [11] Nelson E. Martins, Vítor G. Faria, Viola Nolte, Christian Schlötterer, Luis Teixeira, Élio Sucena, and Sara Magalhães. Host adaptation to viruses relies on few genes with different cross-resistance properties. *Proceedings of the National Academy of Sciences*, page 201400378, April 2014.
- [12] Justin R. Meyer, Devin T. Dobias, Joshua S. Weitz, Jeffrey E. Barrick, Ryan T. Quick, and Richard E. Lenski. Repeatability and contingency in

- the evolution of a key innovation in phage lambda. *Science*, 335(6067):428–432, January 2012. PMID: PMC3306806.
- [13] Britt Koskella and Michael A. Brockhurst. Bacteria–phage coevolution as a driver of ecological and evolutionary processes in microbial communities. *FEMS Microbiology Reviews*, pages n/a–n/a, March 2014.
- [14] Bruce R. Levin, Sylvain Moineau, Mary Bushman, and Rodolphe Barrangou. The population and evolutionary dynamics of phage and bacteria with CRISPR–Mediated immunity. *PLoS Genet*, 9(3):e1003312, March 2013.
- [15] Britt Koskella and Curtis M Lively. Evidence for negative frequency-dependent selection during experimental coevolution of a freshwater snail and a sterilizing trematode. *Evolution; International Journal of Organic Evolution*, 63(9):2213–2221, September 2009.
- [16] C. M. Lively and V. Apanius. Genetic diversity in host–parasite interactions. In *Ecology of infectious diseases in natural populations*, volume 7, page 421. 1995.
- [17] A. Buckling and P. B. Rainey. Antagonistic coevolution between a bacterium and a bacteriophage. *Proceedings of the Royal Society of London. Series B: Biological Sciences*, 269(1494):931–936, May 2002.
- [18] Rebecca D. Schulte, Carsten Makus, Barbara Hasert, Nico K. Michiels, and Hinrich Schulenburg. Host–parasite local adaptation after experimental coevolution of *Caenorhabditis elegans* and its microparasite *Bacillus thuringiensis*. *Proceedings of the Royal Society B: Biological Sciences*, 278(1719):2832–2839, September 2011.
- [19] Sabrina Gaba and Dieter Ebert. Time-shift experiments as a tool to study antagonistic coevolution. *Trends in Ecology & Evolution*, 24(4):226–232, April 2009.
- [20] François Blanquart and Sylvain Gandon. Time-shift experiments and patterns of adaptation across time and space. *Ecology Letters*, 16(1):31–38, 2013.
- [21] Ellen Decaestecker, Sabrina Gaba, Joost A. M. Raeymaekers, Robby Stoks, Liesbeth Van Kerckhoven, Dieter Ebert, and Luc De Meester. Host–parasite ‘Red Queen’ dynamics archived in pond sediment. *Nature*, 450(7171):870–873, November 2007.
- [22] Dieter Ebert. Host–parasite coevolution: Insights from the daphnia–parasite model system. *Current Opinion in Microbiology*, 11(3):290–301, June 2008.
- [23] Kayla C King, Lynda F Delph, Jukka Jokela, and Curtis M Lively. The geographic mosaic of sex and the red queen. *Current Biology: CB*, 19(17):1438–1441, September 2009.

- [24] Leila Masri, Rebecca D. Schulte, Nadine Timmermeyer, Stefanie Thanisch, Lena Luise Crummenerl, Gunther Jansen, Nico K. Michiels, and Hinrich Schulenburg. Sex differences in host defence interfere with parasite-mediated selection for outcrossing during host–parasite coevolution. *Ecology Letters*, 16(4):461–468, April 2013.
- [25] Steven A. Frank. Coevolutionary genetics of plants and pathogens. *Evolutionary Ecology*, 7(1):45–75, 1993.
- [26] S. Gandon and Y. Michalakis. Local adaptation, evolutionary potential and host–parasite coevolution: interactions between migration, mutation, population size and generation time. *Journal of Evolutionary Biology*, 15(3):451–462, May 2002.
- [27] Chaitanya S Gokhale, Andrei Papkou, Arne Traulsen, and Hinrich Schulenburg. Lotka-volterra dynamics kills the red queen: population size fluctuations and associated stochasticity dramatically change host-parasite coevolution. *BMC evolutionary biology*, 13:254, 2013.
- [28] Dan I. Andersson and Diarmaid Hughes. Gene amplification and adaptive evolution in bacteria. *Annual Review of Genetics*, 43(1):167–195, 2009.
- [29] Jason S Maydan, Adam Lorch, Mark L Edgley, Stephane Flibotte, and Donald G Moerman. Copy number variation in the genomes of twelve natural isolates of *caenorhabditis elegans*. *BMC genomics*, 11:62, 2010.
- [30] Ismael A Vergara, Maja Tarailo-Graovac, Christian Frech, Jun Wang, Zhaozhao Qin, Ting Zhang, Rong She, Jeffrey S C Chu, Ke Wang, and Nansheng Chen. Genome-wide variations in a natural isolate of the nematode *caenorhabditis elegans*. *BMC genomics*, 15(1):255, 2014.
- [31] Sylvain Gandon, Yvan Capowiez, Yvain Dubois, Yannis Michalakis, and Isabelle Olivieri. Local adaptation and gene-for-gene coevolution in a metapopulation model. *Proceedings of the Royal Society of London. Series B: Biological Sciences*, 263(1373):1003–1009, August 1996.
- [32] R. M. May and R. M. Anderson. Epidemiology and genetics in the coevolution of parasites and hosts. *Proceedings of the Royal Society B: Biological Sciences*, 219(1216):281–313, October 1983.
- [33] Megan A. Greischar and Britt Koskella. A synthesis of experimental work on parasite local adaptation. *Ecology Letters*, 10(5):418–434, May 2007.
- [34] Henrique Teotonio, Sara Carvalho, Diogo Manoel, Miguel Roque, and Ivo M. Chelo. Evolution of outcrossing in experimental populations of *caenorhabditis elegans*. *PLoS ONE*, 7(4):e35811, April 2012.
- [35] J E Sulston and S Brenner. The DNA of *caenorhabditis elegans*. *Genetics*, 77(1):95–104, May 1974.
- [36] Theresa Stiernagle. Maintenance of *c. elegans*. *WormBook*, 2006.

- [37] O Arantes and D Lereclus. Construction of cloning vectors for bacillus thuringiensis. *Gene*, 108(1):115–119, December 1991.
- [38] Nadine Daou, Christophe Buisson, Michel Gohar, Jasmina Vidic, H el ene Bierne, Mireille Kallassy, Didier Lereclus, and Christina Nielsen-LeRoux. IIsA, a unique surface protein of bacillus cereus required for iron acquisition from heme, hemoglobin and ferritin. *PLoS Pathogens*, 5(11):e1000675, November 2009.
- [39] Russell S. Travers, Phyllis A. W. Martin, and Charles F. Reichelderfer. Selective process for efficient isolation of soil bacillus spp. *Applied and Environmental Microbiology*, 53(6):1263–1266, June 1987.
- [40] Stephan Preibisch, Stephan Saalfeld, and Pavel Tomancak. Globally optimal stitching of tiled 3D microscopic image acquisitions. *Bioinformatics*, 25(11):1463–1465, June 2009.
Cell counter.
- [41] Jose Pinheiro, Douglas Bates, Saikat DebRoy, Deepayan Sarkar, and R. Core Team. *nlme: Linear and Nonlinear Mixed Effects Models*. 2014. R package version 3.1-117.
- [42] R.Core-Team. *R: A Language and Environment for Statistical Computing*. R Foundation for Statistical Computing, Vienna, Austria, 2014.
- [43] Russell V. Lenth. *lsmeans: Least-Squares Means*. 2014. R package version 2.00-5.
- [44] Torsten Hothorn, Frank Bretz, and Peter Westfall. Simultaneous inference in general parametric models. *Biometrical Journal*, 50(3):346–363, 2008.
- [45] Uwe Menzel. *EMT: Exact Multinomial Test: Goodness-of-Fit Test for Discrete Multivariate data*. 2013. R package version 1.1.

Figures

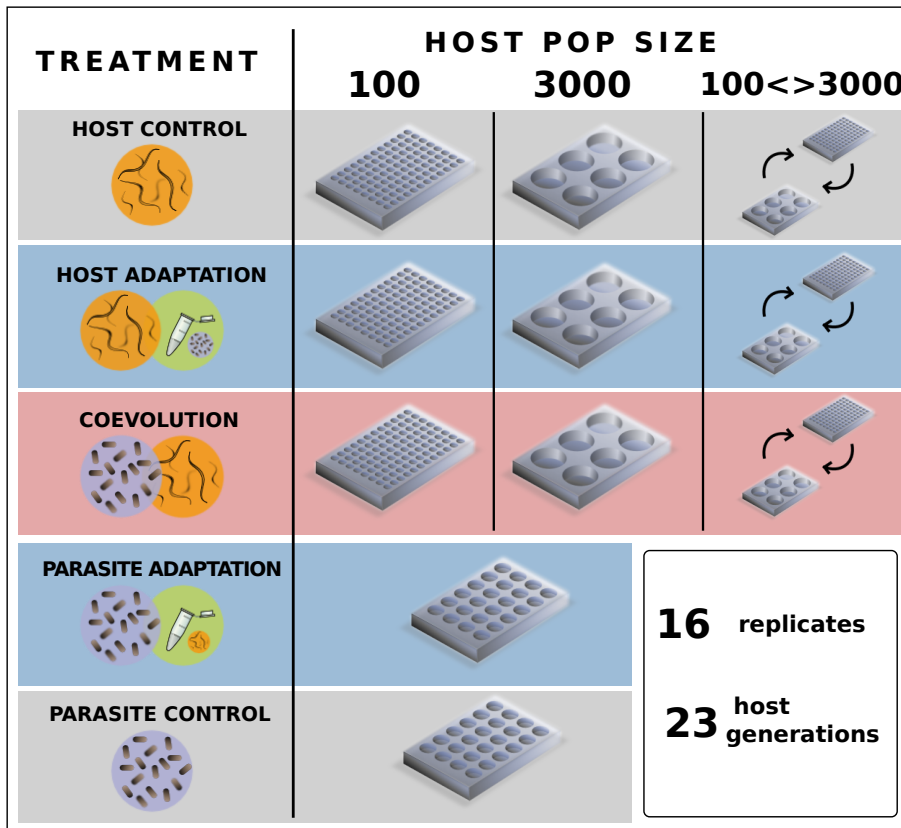


Figure 1: Experimental design

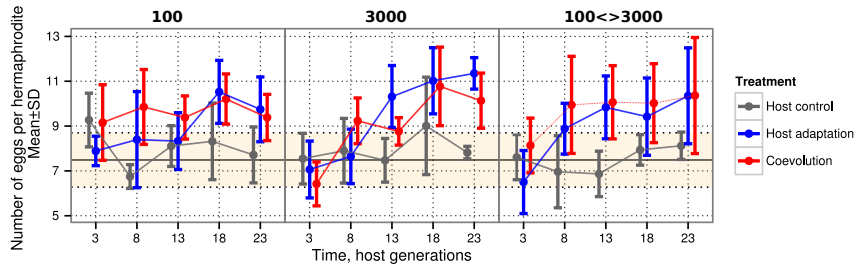


Figure 2: Change in fecundity during coevolution. The figure compares populations evolved under different treatments (in colours) and demographic regimes (different panels), which were recovered from host generations 3, 8, 13, 18, 23 (x -axis). Host fecundity was evaluated as an average number of eggs per 30 hermaphrodites upon exposure to the ancestral pathogen. Each point shows a mean value for 8 populations within each treatment combination per time point and error bars shows ± 1 SD. Treatments are shown in different colours: host control is in grey, host adaptation in blue and coevolution in red. Left, middle and right column correspond to small, large and fluctuating population size, respectively.

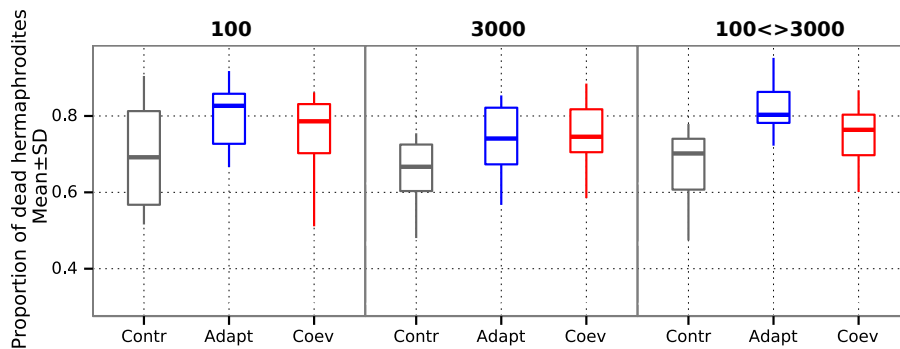


Figure 3: Increase in mortality of the host during coevolution. Each boxplot is based on estimates for 16 replicate populations from the last generation of the experiment. Mortality was measured as proportion of dead hermaphrodites in population ($n \approx 30$) exposed to ancestral parasite for 40 h. Each biological replicate was measured in triplicate.

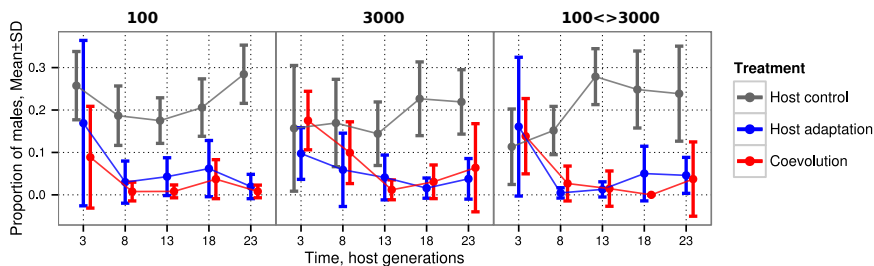


Figure 4: Change in male proportion. Proportions of males were estimated in a sample of 30–40 individuals per population. The graph shows ± 1 SD of 8 replicate populations for each treatment combination per time point. Treatments are shown in different colours, as explained in the legend. Left, middle and right column correspond to small, large and fluctuating population size during evolution.

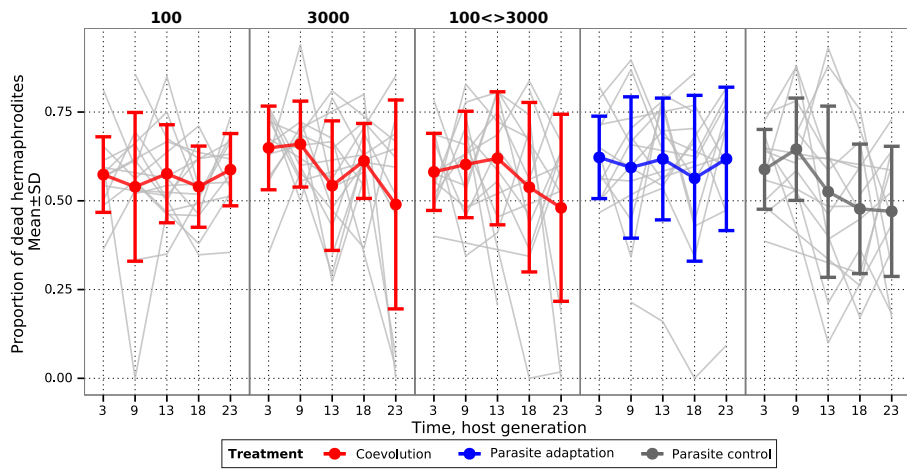


Figure 5: Change in parasite virulence during coevolution. The figure compares populations evolved under different treatments (shown in different colours) and demographic regimes for coevolution treatment (first three panels from the left). The fourth and fifth panels show the parasite adaptation and parasite control treatments, correspondingly. Each point shows a mean value for 12 replicate pathogen populations per time point (out of 16 used in the experiment) and error bars show ± 1 SD. Parasite populations were recovered from host generations 3, 9, 13, 18, 23 (x -axis) and confronted with the ancestral host. The proportion of dead host hermaphrodite ($n \approx 30$) after 40 h of infection is used as a proxy for parasite virulence. Thin grey lines show individual population trajectories to emphasise high variability within treatments.

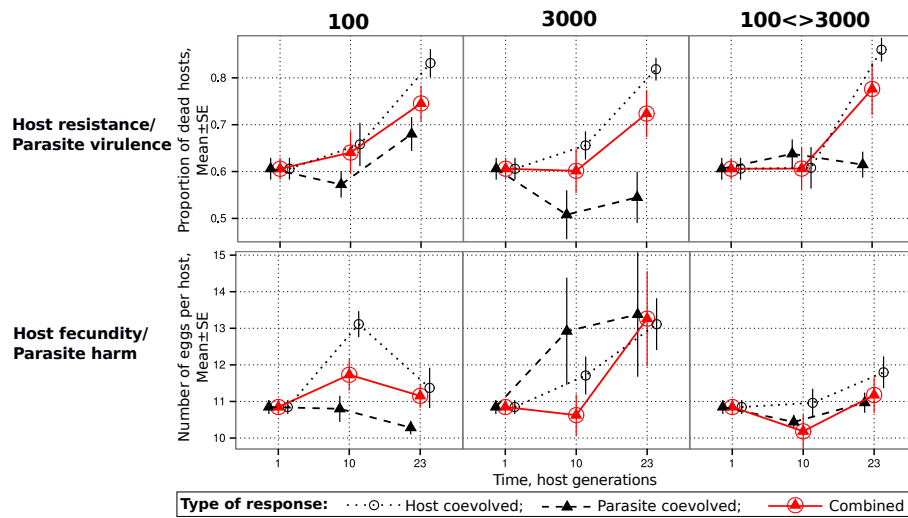


Figure 6: Partitioning coevolution trajectories into host and parasite parts. Host response to coevolution was measured by exposing host populations to ancestral parasite (dotted lines with open circles), parasite response by infecting ancestral host with evolved parasites (dashed line with filled triangles), and their combined effect (coevolution trajectories) by confronting contemporaneous antagonists (red solid line with triangles bounded by circles). Results are presented for two phenotypes (top and bottom panels), three demographic regimes (left, middle and right panels) and three time-points (x -axis). The errorbars show ± 1 standard error of 16 population means. For the first time-point, we evaluated performance of 16 replicate ancestral host populations on ancestral parasite, and this data is repeated on all panels. Large error bars for large populations size (middle panels) are mostly influenced by two parasite populations which almost completely lost virulence. For that reason we also produced a similar plot by excluding these samples, without any major difference in the overall pattern produced (Figure S5).

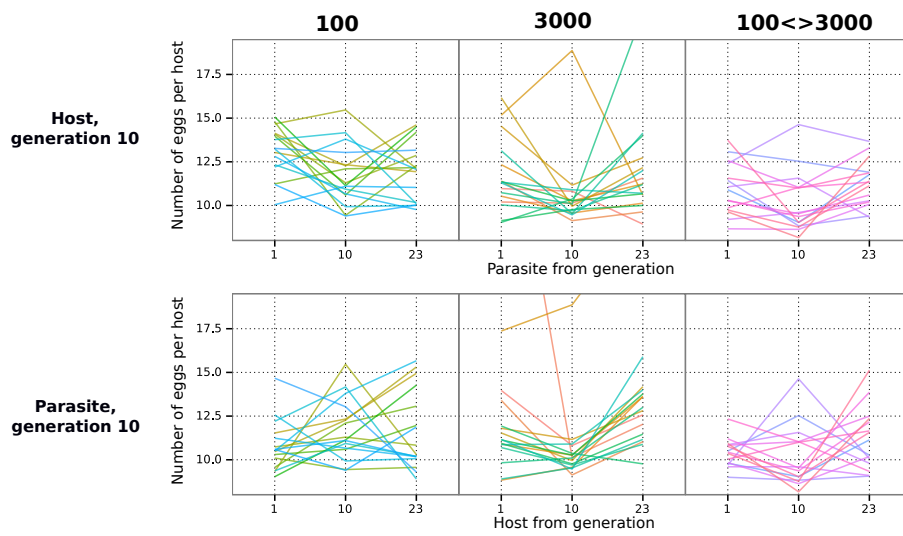


Figure 7: Temporal coevolution patterns obtained for individual host and parasite lines in the time-shift experiment by measuring host fecundity. Data is shown for three different demographic regimes (three columns). Host (top panels) and parasite (bottom panels) from host generation 10 were cross-infected with antagonists from generation 1, 10 and 23 (x -axis). Individual lines are shown in different colours indicating an average number of eggs per hermaphrodite ($n \approx 30$). Note that the host fitness rises as host fecundity increases and the parasite fitness is assumed to increase as host reproduction decreases.

Tables

Table 1. ANOVA results for the linear mixed-effect model of the change in host fecundity during coevolution experiment^a

	<i>d.f.</i> ^b	den <i>d.f.</i> ^c	<i>F</i> -value	<i>p</i> -value	
(Intercept)	1	195	9946.639	<0.0001	***
Treatment	2	122	35.429	<0.0001	***
Demography	2	122	0.054	0.9475	
Generation	1	195	70.921	<0.0001	***
Treatment×Demography	4	122	1.43	0.2282	
Treatment×Generation	2	195	13.026	<0.0001	***
Demography×Generation	2	195	7.338	0.0008	***
Treatment×Demography×Generation	4	195	1.396	0.2369	

^aIn the model, we used a population average of egg number per hermaphrodite ($n=30$) as response variable. Treatment (control vs. adaptation vs. coevolution) and demography (small vs. large vs. fluctuating population size) and their interactions were considered as fixed effects and generation was supplied as a covariate. In the assay, we chose randomly 8 out of 16 replicate populations for each treatment combination per time point, but we still accounted for their dependence by including population identity as a random factor (which was marginally significant with $p=0.0493$ (LR=3.866) in the likelihood ratio test.

^bdegrees of freedom

^cdenominator degree of freedom used to estimate *p*-value from *F*-distribution (see Gałecki A., Burzykowski T. Linear Mixed-Effects Models Using R. 2013 p.297-299).

Table 2. Post-hoc pairwise comparisons of treatments and demographic regimes averaged over time covariate (generations) based on the linear mixed-effect model of the change in host fecundity

Factor	Comparison	Estimate	Std. Error	z value	Pr(> z) ^a	
Treatment	Control vs. Adaptation	-1.44989	0.22349	-6.487	<0.0001	***
	Control vs. Coevolution	-1.67345	0.21785	-7.682	<0.0001	***
	Adaptation vs. Coevolution	-0.22356	0.21833	-1.024	0.808	
Demography	Small vs. Large	-0.08551	0.22071	-0.387	0.994	
	Small vs. Fluctuating	0.02648	0.22174	0.119	1	
	Large vs. Fluctuating	0.11199	0.21724	0.516	0.981	

^a*p*-values based on simultaneous inference procedure and adjusted to control the family-wise error rate. See [44]

Table 3. Post-hoc pairwise comparisons of temporal trends for different treatments and demographic regimes based on the linear mixed-effect model of the change in host fecundity^a

Grouping level	Comparison	Estimate	Std. Error	z value	Pr(> z) ^b	
<i>Comparisons of treatment trends within different demographic regimes</i>						
Small	Control vs. Adaptation	-0.12451	0.05557	-2.24	0.4791	
	Control vs. Coevolution	-0.01061	0.05096	-0.208	1.0000	
	Adaptation vs. Coevolution	0.1139	0.05222	2.181	0.5265	
Large	Control vs. Adaptation	-0.20084	0.04591	-4.374	0.0004	***
	Control vs. Coevolution	-0.14935	0.04581	-3.26	0.0347	*
	Adaptation vs. Coevolution	0.05148	0.04628	1.112	0.9976	
Fluctuating	Control vs. Adaptation	-0.09692	0.04821	-2.01	0.6661	
	Control vs. Coevolution	-0.05023	0.04543	-1.106	0.9978	
	Adaptation vs. Coevolution	0.04669	0.04939	0.945	0.9997	
<i>Comparisons of demographic regime trends within different treatments</i>						
Control	Small vs. Large	-0.03395	0.05012	-0.677	1.0000	
	Small vs. Fluctuating	-0.04415	0.04954	-0.891	0.9998	
	Large vs. Fluctuating	-0.0102	0.0448	-0.228	1.0000	
Adaptation	Small vs. Large	-0.11028	0.05181	-2.129	0.5695	
	Small vs. Fluctuating	-0.01657	0.05439	-0.305	1.0000	
	Large vs. Fluctuating	0.09372	0.04924	1.903	0.7490	
Coevolution	Small vs. Large	-0.1727	0.04673	-3.695	0.0076	**
	Small vs. Fluctuating	-0.08378	0.04698	-1.783	0.8291	
	Large vs. Fluctuating	0.08892	0.04643	1.915	0.7396	

^aIn the test we compare slopes of fitted lines among different levels of fixed factors.

^b*p*-values based on simultaneous inference procedure and adjusted to control the family-wise error rate. See [44]

Table 4. ANOVA results for the linear mixed-effect model of host mortality after coevolution^a

	<i>d.f.</i> ^b	den <i>d.f.</i> ^c	<i>F</i> -value	<i>p</i> -value	
(Intercept)	1	279	2409.7107	<0.0001	***
Treatment	2	131	13.6753	<0.0001	***
Demography	2	131	2.4785	0.0878	
Treatment × Demography	4	131	0.7602	0.553	

^aIn the model, the response variable is a proportion of dead hermaphrodies ($n \approx 30$) in a population after 40h of infection by ancestral parasite. The treatments (control vs. adaptation vs. coevolution) and demographic regimes (small vs. large vs. fluctuating population size) and their interactions are considered as fixed effects. Each treatment combination (Treatment × Demography) includes 16 biological replicates and each biological replicate has 3 technical replicates. This model considers a biological replicate with nested technical replicates as a random factor. The random factor was highly significant in the likelihood ratio test ($p < 0.0001$, LR=46.318).

^bdegrees of freedom

^cdenominator degree of freedom used to estimate *p*-value from *F*-distribution (see Gájecki A., Burzykowski T. Linear Mixed-Effects Models Using R. 2013 p.297-299).

Table 5. Post-hoc pairwise comparisons among treatments and demographic regimes based on the linear mixed-effect model of host mortality

Fixed effect	Comparison	Estimate	Std. Error	z value	Pr(> z) ^a	
Treatment	Control vs. Adaptation	-0.14191	0.02763	-5.137	<0.0001	***
	Control vs. Coevolution	-0.09717	0.02798	-3.473	0.00296	**
	Adaptation vs. Coevolution	0.04474	0.02815	1.59	0.43751	
Demography	Small vs. Large	0.05924	0.02812	2.106	0.16911	
	Small vs. Fluctuating	0.01643	0.02815	0.584	0.97069	
	Large vs. Fluctuating	-0.04282	0.02747	-1.558	0.45802	

^a*p*-values based on simultaneous inference procedure and adjusted to control the family-wise error rate. See [44]

Table 6. Regression analysis of change of male frequencies in host populations during experimental coevolution^a

	<i>d.f.</i>	Deviance ^b	Residual <i>d.f.</i>	Residual deviance	<i>p</i> -value ^c	
Null deviance			44	0.33855		
Treatment	2	0.22684	42	0.11171	<0.00001	***
Demography	2	0.000123	40	0.11159	0.9713078	
Generation	1	0.004903	39	0.10668	0.1282772	
Treatment × Demography	4	0.009871	35	0.09681	0.3242929	
Treatment × Generation	2	0.033892	33	0.06292	0.0003369	***
Demography × Generation	2	0.001255	31	0.06167	0.7436533	
Treatment × Demography × Generation	4	0.004444	27	0.05722	0.7179609	

^aIn this model, the response variable is an average frequency of males summarized over replicate populations in each treatment combination (Treatment × Demography per time point). The treatments (control vs. adaptation vs. coevolution) and demographic regimes (small vs. large vs. fluctuating population size) and their interactions are considered as fixed effects. Time measured in host generations is considered as a covariate.

^bThe model is a generalized linear model, so the analysis of deviance table is used

^c*p*-value in χ^2 -test for significance of model terms

Table 7. ANOVA table for the linear mixed-effect model of change in parasite virulence during coevolution ^a

	<i>d.f.</i> ^b	den <i>d.f.</i> ^c	<i>F</i> -value	<i>p</i> -value	
(Intercept)	1	214	1335.8786	<0.0001	***
Treatment	4	75	0.8333	0.5083	
Generation	1	214	4.9894	0.0265	*
Treatment×Generation	4	214	1.7886	0.1322	

^aIn the model, the response variable is a proportion of dead hermaphrodites ($n \approx 30$) in an ancestral host population after 40h of infection by evolved parasite. Treatment was the only fixed factor. As a treatment we considered parasite control, parasite adaptation and three coevolution treatments (coevolution small population size, coevolution large population size, coevolution fluctating population size). Within each treatment we measured virulence in 12 out of 16 biological replicates for every time point. The model considers a biological replicate as a random factor. The random factor was significant in the likelihood ratio test ($p=0.0044$, LR=8.1149).

^bdegrees of freedom

^cdenominator degree of freedom used to estimate *p*-value from *F*-distribution (see Galecki A., Burzykowski T. Linear Mixed-Effects Models Using R. 2013 p.297-299).

Table 8. Regression analysis comparing mixed-effect model of host fecundity in the time-shift experiment ^a

	<i>d.f.</i> ^b	den <i>d.f.</i> ^c	<i>F</i> -value	<i>p</i> -value	
(Intercept)	1	311	2626.5475	<0.0001	***
Combination	7	311	3.5688	0.001	**
Demography	2	45	4.1907	0.0214	*
Demography×Combination	14	311	2.9671	0.0003	**

^aIn the model, the response variable is an average number of eggs per hermaphrodite ($n \approx 30$), power-transformed to meet the criterion of normality. Demographic regime and a time-point combination and their interaction were considered as fixed factors. Different time-point combinations were nested within the individual lines, making it analogous to repeated measures ANOVA. 1×1 combination was excluded from analysis to avoid pseudoreplication. The model considers an individual line as a random factor, which was significant in the likelihood ratio test ($p=0.0001$, LR=19.327).

^bdegrees of freedom

^cdenominator degree of freedom used to estimate *p*-value from *F*-distribution (see Galecki A., Burzykowski T. Linear Mixed-Effects Models Using R. 2013 p.297-299).

Table 9. Post-hoc comparisons of the effect of contemporaneous versus shifted combinations on host fecundity performed separately for each demographic regime

Demography	Comparison	Estimate	Std. Error	z value	$\Pr(> z)^a$
Small	Contemp. vs. Shifted	0.012500	0.003076	-4.064	1
Large	Contemp. vs. Shifted	0.006739	0.003518	1.916	0.0277 *
Fluctuating	Contemp. vs. Shifted	0.004460	0.002994	1.489	0.0682

^a p -value for the one-sided test based on simultaneous inference procedure and adjusted to control the family-wise error rate. See [44]

Table 10. Comparison of temporal patterns for host fecundity found in the time-shift experiment

Focal antagonist ^a	Demographic regime	Temporal pattern of fitness			Exact multinomial test ^b	adjusted p-values ^c
		“-+-”	“+-+”	“-++” or “+--”		
Host	Small populations	4	8	4	0.1232	
	Large populations	1	11	4	0.0048	**
	Fluctuating	2	10	3	0.0080	**
Parasite	Small populations	3	5	8	0.8508	
	Large populations	10	0	6	0.0065	**
	Fluctuating	8	3	3	0.0651	

^aFocal populations from generation 10 of either host or parasite were exposed to the corresponding antagonist from host generation 1, 10 and 23

^bExact multinomial test was based on the probability of encountering observed pattern by chance alone. The null probability distribution for all possible outcomes was assumed to be (0.25,0.25,0.50)

^cp-values were corrected using Holm method to control for the family-wise error rate. Significant p-values are presented in bold text

Supplementary Figures

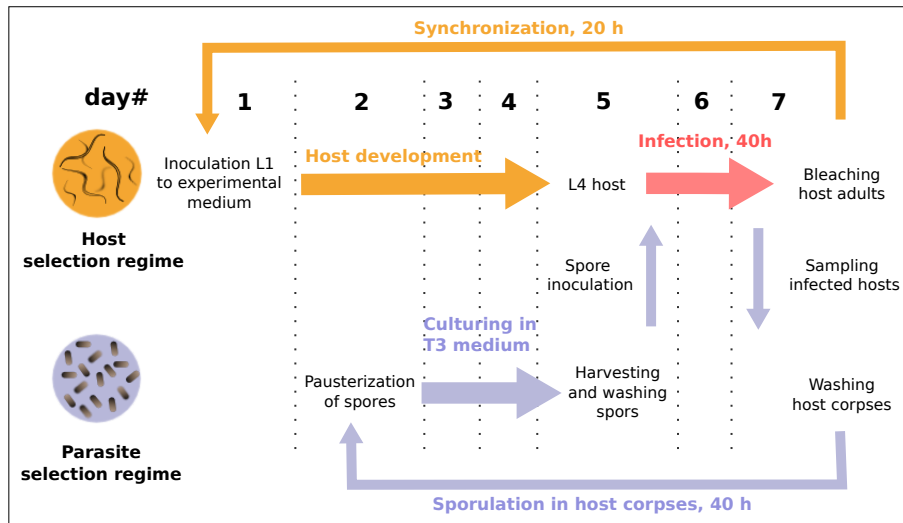


Figure S1: Selection protocol for host and parasite during coevolution

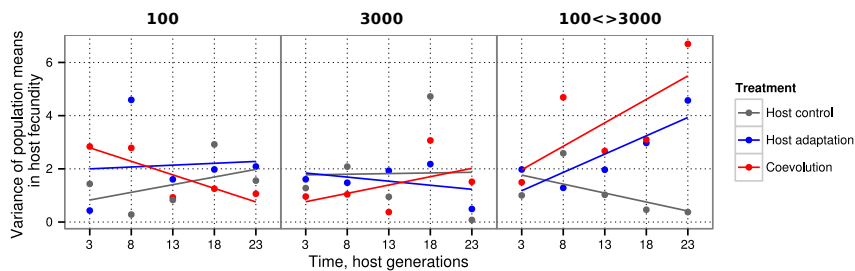


Figure S2: Increased divergence in trajectories during coevolution under fluctuating regime measured as variance of population means for host fecundity. Each point shows a variance value for 8 populations within each treatment combination. The solid lines represent linear regression lines.

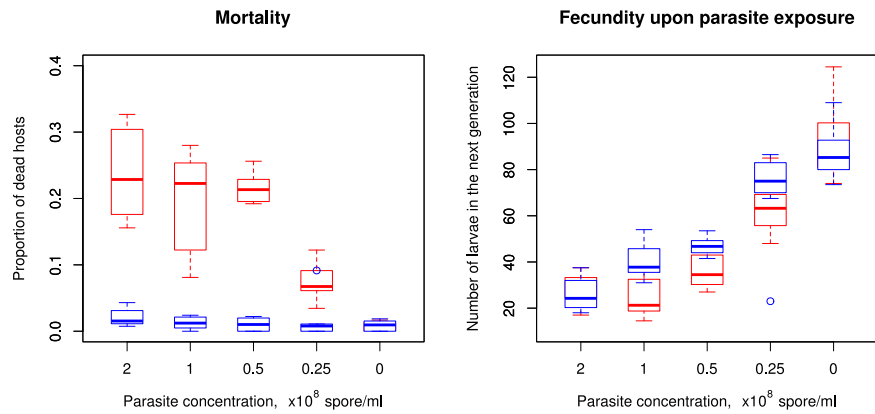


Figure S3: Mortality and fecundity of two standard laboratory host strains (N2 – in red, CB4856 – in blue) illustrating a weak relation of the two traits when exposed to a range of parasite concentrations. Each boxplot is based on 8 technical replicates.

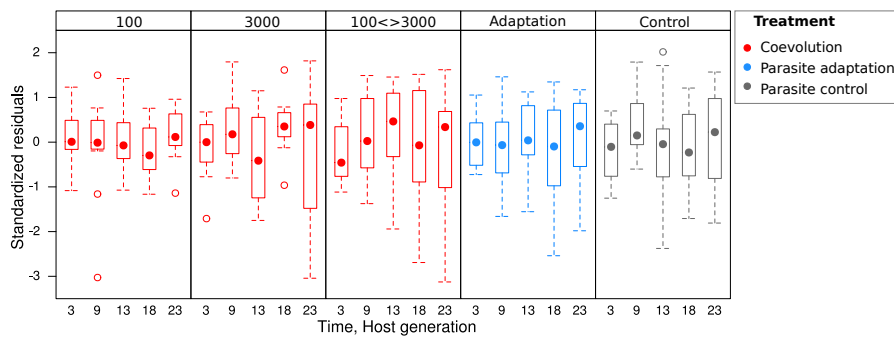


Figure S4: Residuals from the linear model of virulence change of parasite showing different variability pattern and potentially suggesting differences in evolutionary trajectories under different demographic regimes. This model assumes an equal variance across all treatments and demographic regimes. If a variance function is used to account for the differences in variance for different groups, it explains a significant proportion of variation (likelihood ratio test, LR=28.61, $p < 0.0001$).

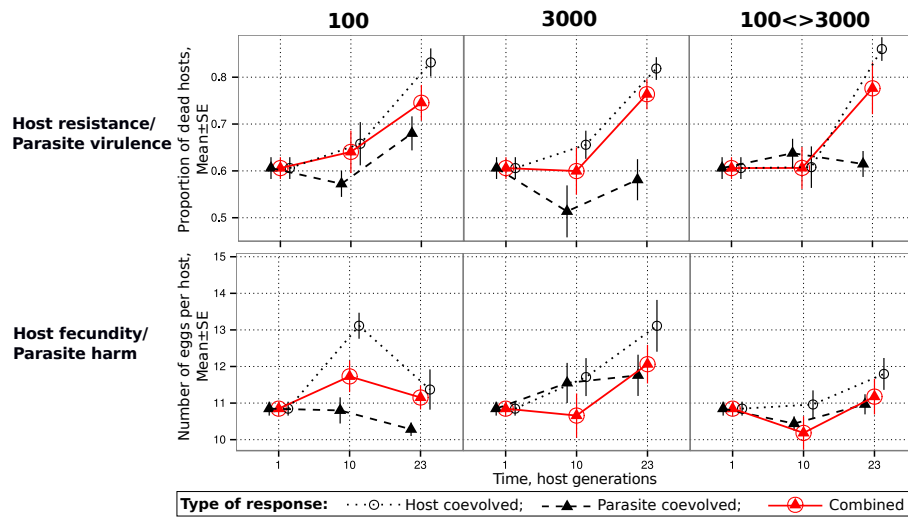


Figure S5: The same as Figure 6, but with 2 populations excluded from the middle panel (large population size). Excluding these replicates does not remove the interaction pattern.

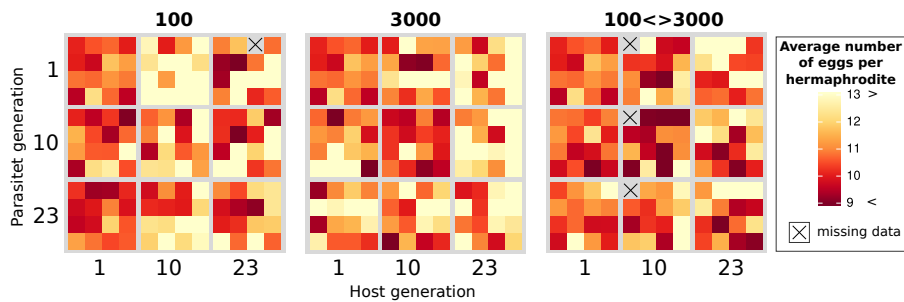


Figure S6: Temporal coevolution patterns obtained in time-shift experiment by measuring host fecundity. Data is shown for three different demographic regimes (three panels) and for host and parasite from host generation 1, 10 and 23 in all combinations (9 squares within each panel). Each combination includes 16 replicate populations illustrated as small squares with colour intensity indicating an average number of eggs per hermaphrodite ($n \approx 30$). Dark red colour would imply decreased host fecundity or larger parasite harm, while light yellow includes improved host fecundity or decrease in parasite virulence

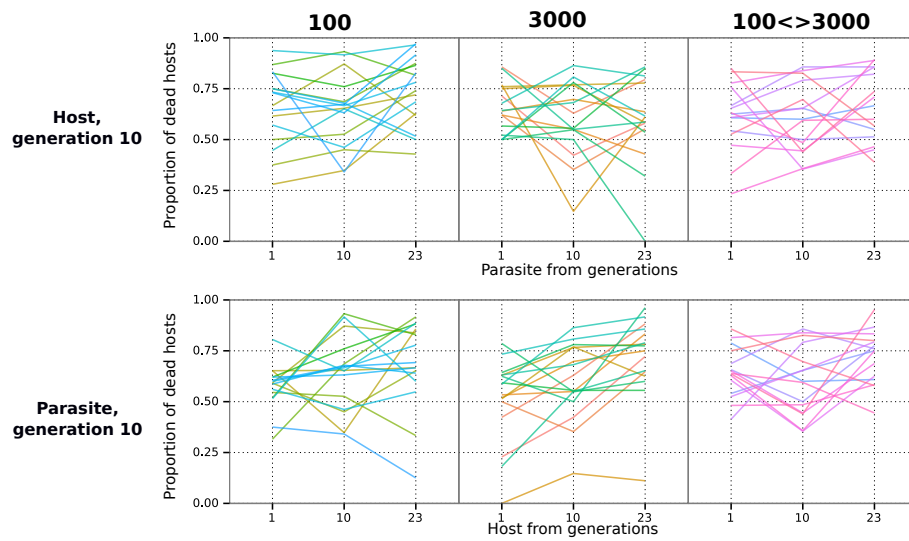


Figure S7: Temporal coevolution patterns obtained for individual host and parasite lines in the time-shift experiment by measuring host mortality. Data is shown for three different demographic regimes (three columns). Host (top panels) and parasite (bottom panels) from host generation 10 were cross-infected with antagonists from generation 1, 10 and 23 (x-axis). Individual lines are shown in different colours indicating a change in the proportion of dead hermaphrodite ($n \approx 30$).

Part IV.

The selective benefit of toxins
during pathogen coevolution
with a host

The selective benefit of toxins during pathogen coevolution with a host

Leila Masri^{1,2,3‡}, Antoine Branca^{4,5‡}, Anna E. Sheppard^{1,6‡}, Andrei Papkou¹, David Laehnemann^{1,2}, Patrick S. Günther², Swantje Prahl¹, Manja Saebelfeld¹, Philip R. Crain⁴, Jakob Strauß⁴, Jacqueline Hollensteiner⁷, Heiko Liesegang⁷, Elzbieta Brzuszkiewicz⁷, Rolf Daniel⁷, Nicolaas K. Michiels², Rebecca D. Schulte⁸, Joachim Kurtz⁴, Philip Rosenstiel⁹, Arndt Telschow⁴, Erich Bornberg-Bauer⁴, Hinrich Schulenburg^{1,2*}

¹Department of Evolutionary Ecology and Genetics, Zoological Institute, Christian-Albrechts-University of Kiel, Germany

²Department of Animal Evolutionary Ecology, Institute of Evolution and Ecology, University of Tuebingen, Germany

³Present address: Institute of Science and Technology Austria, Klosterneuburg, Austria

⁴Institute for Evolution and Biodiversity, University of Muenster, Muenster, Germany

⁵Present address: Laboratory Ecologie, Systématique et Evolution, CNRS-Université Paris-Sud, Orsay, France

⁶Present address: Nuffield Department of Medicine, University of Oxford, Oxford, UK

⁷Goettingen Genomics Laboratory, Institute of Microbiology and Genetics, Georg-August-University of Goettingen, Goettingen, Germany

⁸Department of Behavioural Biology, University of Osnabrueck, Osnabrueck, Germany

⁹Institute for Clinical Molecular Biology, Christian-Albrechts-University, Kiel, Germany

‡ These authors contributed equally to this work

* Corresponding author: Hinrich Schulenburg, hschulenburg@zoologie.uni-kiel.de

Reciprocal coevolution between host and pathogen is widely seen as a major driver of evolution and biological innovation^{1,2}, yet the exact genes and associated trait functions under selection are generally unknown³. We here combined experimental evolution of the bacterial biocontrol agent *Bacillus thuringiensis* and its nematode host *Caenorhabditis elegans*⁴ with large-scale phenotyping, mathematical modelling, genomic analysis, and functional genetics to demonstrate the selective benefit of pathogen toxins during the adaptation process. (i) High virulence was specifically favored during pathogen-host coevolution rather than pathogen one-sided adaptation to a non-changing host or an environment without host. (ii) The pathogen genotype MYBT18679 with known nematocidal toxins swept to fixation in the coevolving populations and to a lesser extent those subject to one-sided adaptation with host. (iii) High virulence in the MYBT18679-dominated populations correlated with elevated copy numbers of the nematocidal toxin genes. (iv) Loss of virulence in the MYBT18679 genotype was reconstituted by genetic reintroduction or external addition of the toxins. In conclusion, our study provides experimental evidence for the adaptive advantage of nematocidal toxins during pathogen-host coevolution. Unexpectedly, the maintenance of high pathogen virulence, as desired for pest control, appears to be contingent on the unwanted co-adaptation of the target host.

The Gram-positive bacterium *B. thuringiensis* is of economic importance as a pest control agent^{5,6} and infects insect or nematode hosts upon oral uptake via toxin-mediated destruction of intestinal cells and expression of additional virulence factors^{5,6}. The interaction between *B. thuringiensis* and its nematode host *C. elegans* was previously established as an experimental evolution model for studying the consequences of coevolution^{4,7-10}. Here, we used this interaction model for a new experimental design that consists of five distinct evolution conditions, during which genetically variable pathogen and host populations were forced over 28 transfers to either reciprocally co-adapt to each other, adapt to a non-changing antagonist, or adapt to environmental conditions without antagonist (Fig. 1a; further details in supplementary information, SI). This experimental design allowed us to ask how reciprocal coevolution differs from other types of related selective constraints and how the respective adaptations are achieved at the genetic level. Such information is central for our understanding of the postulated high impact of coevolution on the evolution of organisms and their trait functions³. We now present our findings on the evolved phenotypic changes across time,

which we combined with mathematical modelling, followed by results from population genomic analyses and a subsequent functional genetic assessment.

The imposed selection conditions of the experimental evolution protocol led to distinct phenotypic changes in both host and pathogen. For the host, survival in the presence of the pathogen significantly increased over time during coevolution but not other treatment conditions, suggesting evolution of resistance *sensu lato* in the presence of a co-adapting antagonist (Fig. 1b, Supplementary Tables 1 and 2). For the pathogen, one-sided adaptation caused extinction in more than half of the pathogen populations, which was not observed under coevolution or control conditions (Fig. 1c). The pathogen's ability to kill the host (i.e., virulence) was maintained during coevolution, but was lost during control evolution and decreased under one-sided adaptation (Fig. 1c, Extended Data Figs. 1a-b; Supplementary Tables 3 and 4). In contrast, pathogen infection load was highest during one-sided adaptation (Fig. 1c, Supplementary Tables 3 and 4), while the ability to form biofilms was favored under control evolution, yet lost under coevolution and, to a lesser extent, one-sided adaptation (Fig. 1c, Supplementary Table 5). Analysis of individual clones from the evolved populations consistently revealed that biofilm particle size was larger for control-evolved and avirulent bacteria (Extended Data Figs. 1c-e). Interestingly, the competitiveness of biofilm-producing clones was significantly higher on nutrient-poor medium, as used during experimental evolution, but significantly lower under nutrient-rich conditions (Extended Data Fig. 1f, Supplementary Table 6).

Our findings of distinct coevolutionary consequences on trait evolution extend the results from the few studies, all based on bacteria-phage interaction models, which previously contrasted coevolution with one-sided adaptation for the pathogen. For instance, phage $\Phi 2$ produced distinct changes in infection characteristics depending on whether it was experimentally evolved with a co-adapting or a non-changing host bacterium *Pseudomonas fluorescens*^{11,12}. Importantly, our new findings now suggest that the different selection conditions favored pathogen characteristics likely of relevance during different phases of its life cycle. (i) Prior to host infection, *B. thuringiensis* must ensure persistence in an unfavorable environment, for instance through biofilm formation¹³. This stage of the life cycle was under specific selection during control evolution without host (Fig. 1c). The ability to form biofilms coincided with a lack of pathogenicity (Fig. 1c), suggesting a life-history trade-off. (ii) After host entry, a central next step for *B. thuringiensis* is toxin-mediated tissue damage, which

weakens the host, easing access to nutritional resources^{5,6}. As toxins ultimately cause host death^{5,6}, selection on this step may lead to variation in host killing rate. Thus, the toxin effects appear of particular selective benefit during coevolution (Fig. 1c), possibly because of ongoing resistance evolution in the host (Fig. 1b). (iii) After host weakening, pathogens must achieve high infection load. This step seems under particular selection in the one-sided adaptation treatment (Fig. 1c), apparently at the cost of toxin-mediated virulence (Fig. 1c), again indicating a life-history trade-off. This trait combination may also result, at least initially, from the coexistence of toxin-producing, yet slowly replicating cells and non-toxin-producing but fast replicating cells in the population, as indicated by the previous finding that a combination of both maximizes overall fitness in insecticidal *B. thuringiensis*¹⁴. Using a simple mathematical model for our study system (SI), a mixture of both was indeed favored under intermediate host resistance (as representative for non-changing hosts in the one-sided adaptation treatment), while sustained predominance of toxin producers and thus high virulence requires high host resistance (as reflected under coevolution conditions by the counter-adapting hosts) (Upper lines in light grey in Fig. 1d; Extended Data Fig. 2). Low host resistance can also lead to loss of toxin producers (Lower lines in dark grey in Fig. 1d), thus precluding subsequent infection of new hosts, possibly explaining population extinctions under one-sided adaptation (Fig. 1c).

Genetic changes in the pathogen were subsequently explored through whole genome sequence analysis and a toxin gene screen of *B. thuringiensis* populations from three time points (transfers 0, 12, and 20). As a basis for our analysis, we first assembled reference genomes for five strains represented in the ancestral population and established an analysis pipeline that ensured reliable variant detection in genetically variable populations (Fig. 2a; SI, Extended Data Figs. 3-4; Supplementary Tables 8-9). We identified a dramatic change in strain composition from the ancestral (Fig. 2b) to the evolved populations, most of which were dominated by single *B. thuringiensis* strains (Fig. 2c; Supplementary Table 10), highlighting the importance of clonal interference during bacterial adaptation¹⁵. In contrast to the findings from a previous study that opposite to the current work included pathogen immigration^{4,9}, coevolution did not increase pathogen genetic diversity, supporting previous modelling results that diversity during coevolution can be enhanced by immigration^{16,17}. Almost all coevolved and many one-sided adapted populations showed high prevalence of the strain MYBT18679 (Fig. 2c), which is known to have stronger nematocidal effects compared to other *B. thuringiensis* strains^{4,18}. Consistent with this observation, known nematocidal toxin

genes were found during the evolution experiment to be almost exclusively restricted to the MYBT18679 genotype and thus enriched under coevolution and one-sided adaptation (Extended Data Fig. 5, Supplementary Tables 11-13). Interestingly, both virulent and avirulent *B. thuringiensis* strains were selected across the one-sided adapted populations (Fig. 2c), consistent with our above suggestion that the absence of a counter-adapting host may favor both phenotypes. In contrast, control evolution was ultimately dominated by only one strain, MYBT22 (Fig. 2c), with an apparent avirulent, biofilm-forming phenotype (Figs. 1c; Extended Data Figs. 1c-e).

We next assessed whether specific genetic changes were selectively favored within the MYBT18679-dominated populations under coevolution and one-sided adaptation conditions. We used two complementary analyses to identify candidate regions under selection based on either: (i) comparisons between coevolution and one-sided adaptation treatments, or (ii) correlations between genetic and associated phenotypic variations across all MYBT18679-dominated populations (SI, Fig. 3a, Extended Data Figs. 6-7, Supplementary Tables 14-20). Genetic changes were surveyed for single nucleotide polymorphisms (SNPs; measured through their frequency or effect on population genetic statistics like θ_w , π , and Tajima's D), structural variations including indels, sequence region copy number, and presence of horizontally transferred fragments (SI), resulting in identification of more than 100 regions from the treatment comparison and four regions from the correlational analysis (Supplementary Table 20). The relevance of these candidate regions is difficult to assess, because many only contain genes with unknown function. However, three of these regions harbor genes previously implicated in bacterial interactions with a host (See more detailed descriptions in SI). One of these refers to an approximately 65 kb region of a large plasmid, for which population genetic measures consistently indicate significantly higher variation under coevolution conditions and which contains putative host interacting genes encoding toxins, a membrane protein, germination proteins, and an acid phosphatase (Extended Data Fig. 6). Variation in the two remaining regions correlated significantly with killing ability. One of these regions encompasses a gene with unknown function that contains an mvIN domain previously linked to virulence in different pathogens¹⁹⁻²¹ and for which the frequency of a deletion correlates negatively with virulence (Fig. 3b, 3c). The second region refers to a plasmid with two known nematocidal toxin genes, *cry14Aa1* and *cry21Aa2*²², for which copy number positively correlates with virulence and which yielded one of the highest significance levels of the identified candidate regions (Fig. 3b, 3c), emphasizing its relevance for the

observed variation in killing ability. Indeed, we could confirm experimentally that the virulence of a toxin-plasmid-lacking MYBT18679 strain could be reconstituted by re-introduction of a plasmid with either of the two toxin genes or by addition of a high concentration of a Cry21Aa2-expressing *E. coli* (Fig. 3d; Supplementary Tables 21-23). These results strongly suggest that the two toxin genes and possibly their copy number account for the nematocidal effects.

In conclusion, our study provides the first experimental evolution study that uses a bacterial pathogen and its animal host to dissect the phenotypic and genomic consequences of coevolution rather than one-sided adaption, thus extending related previous experiments, which were all exclusively based on bacteria-phage interaction models^{11,23-25}. Our results highlight that coevolution favors distinct pathogen life-history traits, especially high virulence. Importantly, we characterized for the first time the genetic basis of coevolutionary adaptation for a bacterial pathogen and found that nematocidal toxin genes and their high copy number yield a selective advantage. Moreover, our findings also suggest that the high levels of virulence required for efficient pest eradication may only be maintained if the target host is able to co-adapt, which may compromise sustainable biocontrol strategies.

Methods Summary

Experimental evolution and phenotypic analysis

Genetically variable host and pathogen populations^{4,26} were evolved in ten replicates per five distinct evolution treatments (Fig. 1a) over 28 transfers. Trait changes were evaluated by exposing *C. elegans* and *B. thuringiensis* populations from transfers 0, 12, 20, and 28 to ancestral populations of the respective antagonist.

Mathematical model of pathogen evolution

Following our current understanding of *B. thuringiensis* life cycle^{5,6}, infection dynamics was modeled as a two-phase process: (i) pathogen invasion until host death, during which toxin-producing bacteria have a selective advantage due to increased access to resources; and (ii) the period after host death until resource depletion, when non-producers lacking toxin-production costs are favored.

Broad-scale genome sequence analysis

Using assembled genomes for five *B. thuringiensis* strains as reference, we inferred changes in strain composition through analysis of whole genome sequences of the ancestral population and ten populations per treatment for transfers 12 and 20. Variation in presence of five known nematocidal toxin genes²² was assessed by diagnostic PCR for *B. thuringiensis* clones from the same replicate populations.

Fine-scale genome sequence analysis of MYBT18679 populations

We focused on the MYBT18679-dominated populations to assess genetic differences among treatments or a correlation between genetic and phenotypic variation, taking into account variation in copy number, indels, SNPs, or genetic diversity measures (Watterson's θ_w , Tajima's π and D^{27}).

Functional genetic analysis of *Cry14Aa1* and *Cry21Aa2* toxin genes

We assessed the killing ability of a toxin-plasmid-lacking MYBT18679 variant, in which the *Cry14Aa1* and *Cry21Aa2* coding sequences were separately re-introduced or which was combined with a *Cry21Aa2*-expressing *E. coli*.

References

- 1 Woolhouse, M. E., Webster, J. P., Domingo, E., Charlesworth, B. & Levin, B. R. Biological and biomedical implications of the co-evolution of pathogens and their hosts. *Nature Genet***32**, 569-577, (2002).
- 2 Schmid-Hempel, P. *Evolutionary parasitology*. (Oxford University Press, 2011).
- 3 Brockhurst, M. A. & Koskella, B. Experimental coevolution of species interactions. *Trends Ecol Evol***28**, 367-375, (2013).
- 4 Schulte, R. D., Makus, C., Hasert, B., Michiels, N. K. & Schulenburg, H. Multiple reciprocal adaptations and rapid genetic change upon experimental coevolution of an animal host and its microbial parasite. *Proc Natl Acad Sci U S A***107**, 7359-7364, (2010).
- 5 Griffiths, J. S. & Aroian, R. V. Many roads to resistance: how invertebrates adapt to Bt toxins. *Bioessays***27**, 614-624, (2005).
- 6 Nielsen-LeRoux, C., Gaudriault, S., Ramarao, N., Lereclus, D. & Givaudan, A. How the insect pathogen bacteria *Bacillus thuringiensis* and *Xenorhabdus/Photorhabdus* occupy their hosts. *Curr Op Microbiol***15**, 220-231, (2012).
- 7 Schulte, R. D., Hasert, B., Makus, C., Michiels, N. K. & Schulenburg, H. Increased responsiveness in feeding behaviour of *Caenorhabditis elegans* after experimental coevolution with its microparasite *Bacillus thuringiensis*. *Biol Lett***8**, 234-236, (2012).
- 8 Schulte, R. D., Makus, C., Hasert, B., Michiels, N. K. & Schulenburg, H. Host-parasite local adaptation after experimental coevolution of *Caenorhabditis elegans* and its microparasite *Bacillus thuringiensis*. *Proc Biol Sci***278**, 2832-2839, (2011).
- 9 Schulte, R. D., Makus, C. & Schulenburg, H. Host-parasite coevolution favours parasite genetic diversity and horizontal gene transfer. *J Evol Biol***26**, 1836-1840, (2013).
- 10 Masri, L. *et al.* Sex differences in host defence interfere with parasite-mediated selection for outcrossing during host-parasite coevolution. *Ecol Lett***16**, 461-468, (2013).
- 11 Paterson, S. *et al.* Antagonistic coevolution accelerates molecular evolution. *Nature***464**, 275-278, (2010).
- 12 Poullain, V., Gandon, S., Brockhurst, M. A., Buckling, A. & Hochberg, M. E. The evolution of specificity in evolving and coevolving antagonistic interactions between a bacteria and its phage. *Evolution***62**, 1-11, (2008).
- 13 Lopez, D., Vlamakis, H. & Kolter, R. Biofilms. *Cold Spring Harbor Perspect Biol***2**, a000398, (2010).
- 14 Raymond, B., West, S. A., Griffin, A. S. & Bonsall, M. B. The dynamics of cooperative bacterial virulence in the field. *Science***337**, 85-88, (2012).
- 15 Sniegowski, P. D. & Gerrish, P. J. Beneficial mutations and the dynamics of adaptation in asexual populations. *Phil Trans R Soc London B***365**, 1255-1263, (2010).
- 16 Morgan, A. D., Gandon, S. & Buckling, A. The effect of migration on local adaptation in a coevolving host-parasite system. *Nature***437**, 253-256, (2005).
- 17 Tellier, A. & Brown, J. K. Spatial heterogeneity, frequency-dependent selection and polymorphism in host-parasite interactions. *BMC Evol Biol***11**, 319, (2011).
- 18 Wang, J., Nakad, R. & Schulenburg, H. Activation of the *Caenorhabditis elegans* FOXO family transcription factor DAF-16 by pathogenic *Bacillus thuringiensis*. *Dev Comp Immunol***37**, 193-201, (2012).
- 19 Carsiotis, M., Stocker, B. A., Weinstein, D. L. & O'Brien, A. D. A *Salmonella typhimurium* virulence gene linked to *flg*. *Infect Immunity***57**, 3276-3280, (1989).

-
- 20 Ling, J. M., Moore, R. A., Surette, M. G. & Woods, D. E. The *mviN* homolog in *Burkholderia pseudomallei* is essential for viability and virulence. *Canadian J Microbiol***52**, 831-842, (2006).
- 21 Ulland, T. K. *et al.* Cutting edge: mutation of *Francisella tularensis* *mviN* leads to increased macrophage apoptosis in melanoma 2 inflammasome activation and a loss of virulence. *J Immunol***185**, 2670-2674, (2010).
- 22 Wei, J. Z. *et al.* *Bacillus thuringiensis* crystal proteins that target nematodes. *Proc Natl Acad Sci U S A***100**, 2760-2765, (2003).
- 23 Kashiwagi, A. & Yomo, T. Ongoing phenotypic and genomic changes in experimental coevolution of RNA bacteriophage Qb and *Escherichia coli*. *PLoS Genet***7**, e1002188, (2011).
- 24 Scanlan, P. D., Hall, A. R., Lopez-Pascua, L. D. & Buckling, A. Genetic basis of infectivity evolution in a bacteriophage. *Mol Ecol***20**, 981-989, (2011).
- 25 Meyer, J. R. *et al.* Repeatability and contingency in the evolution of a key innovation in phage lambda. *Science***335**, 428-432, (2012).
- 26 Teotonio, H., Carvalho, S., Manoel, D., Roque, M. & Chelo, I. M. Evolution of outcrossing in experimental populations of *Caenorhabditis elegans*. *PLoS One***7**, e35811, (2012).
- 27 Begun, D. J. *et al.* Population genomics: whole-genome analysis of polymorphism and divergence in *Drosophila simulans*. *PLoS Biol***5**, e310, (2007).

Supplementary Information is linked to the online version of the paper.

Acknowledgements

We thank Sylvia Cremer, Dieter Ebert, Michel Gohar, Francis Jiggins, Christina Nielsen-LeRoux, Andrew Read, Thorsten Reusch, Vincent Sanchis, Paul Schmid-Hempel, Jacqui Shykoff, Arne Traulsen, Mathias Wegner, and the Michiels and Schulenburg labs for advice; Martina Hohloch, Nadine Timmermeyer, Susanne Weller, Rania Nakad, Karoline Fritzsche, Antje Thomas, and the Kiel ICMB sequencing team (especially Markus Schilhabel, Melanie Friskovec, Melanie Schlapkohl, Daniela Esser) for technical support. AP is an associate member of the International Max-Planck Research School for Evolutionary Biology at the University of Kiel. We are very grateful for funding from the German Science Foundation (DFG) to HS (SCHU 1415/8, SCHU 1415/9), PR (RO 2994/3), EBB (BO 2544/7), HL (LI 1690/2), AT (TE 976/2), RDS (SCHU 2522/1), JK (KU 1929/4), and also from the Kiel Excellence Cluster Inflammation at Interfaces to HS and PR.

Author contributions

LM conceived, performed, and analysed the evolution experiment, and drafted the manuscript. AB conceived and performed genomic analysis of evolved pathogens, and drafted the manuscript. AES conceived and performed pathogen toxin analysis, and drafted the manuscript. DL, PSG, SP supported performance and analysis of evolution experiment. MS supported pathogen toxin analysis. AP, JH performed functional analysis of pathogen toxins. PRC, JS, AT developed, implemented, and analysed the mathematical model. EB, HL, RD supported pathogen whole genome analysis. NKM, RDS, JK contributed to design and analysis of evolution experiment. PR, EBB contributed to genome data analysis. HS conceived and supervised the study, contributed to data analysis, and drafted the manuscript. All authors read and approved the final manuscript.

Author information

Genome sequence data has been deposited to the European Nucleotide Archive (ENA; <http://www.ebi.ac.uk/ena/>) with the study accession number PRJEB5931. The authors declare that they have no competing interests. Correspondence should be addressed to Hinrich Schulenburg (hschulenburg@zoologie.uni-kiel.de).

Figure legends

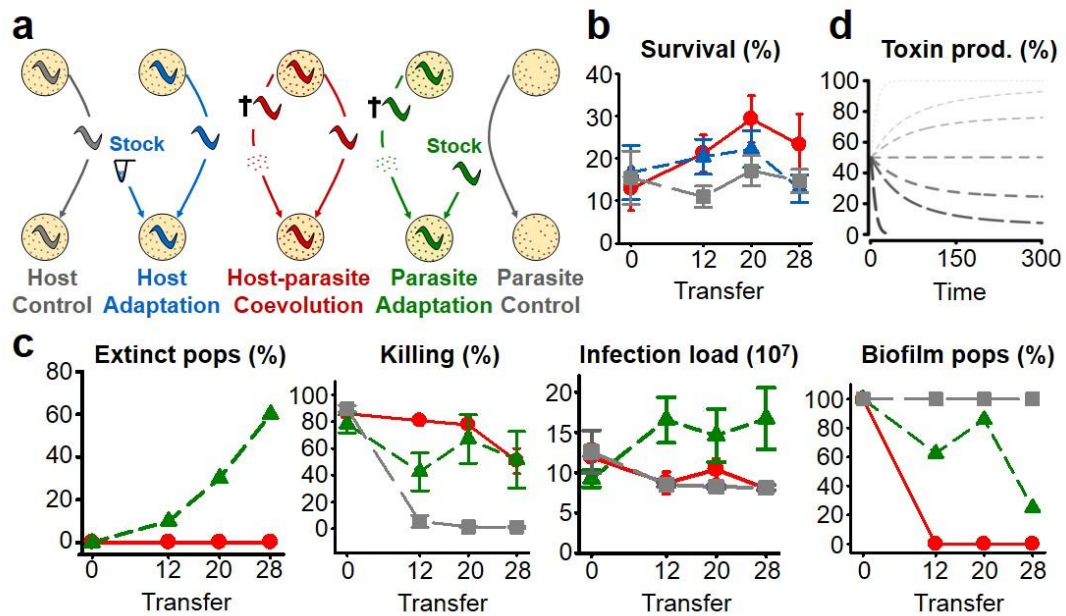


Figure 1. Experimental host-pathogen coevolution causes phenotypic changes in both antagonists. **a**, The five evolution treatments. **b**, Changes in host survival upon pathogen exposure. **c**, Changes in pathogen population extinctions, pathogen virulence (killing), pathogen infection load, and pathogen biofilm formation. Red circles and solid lines indicate coevolution, blue triangles and dotted lines one-sided host adaptation, green triangles and dotted lines one-sided pathogen adaptation, and grey squares and dashed lines control evolution. Bars denote standard errors. **d**, Model simulations show increased toxin producer frequencies (X axis) across time when host resistance levels increase (different lines, resistance levels increase from bottom to top).

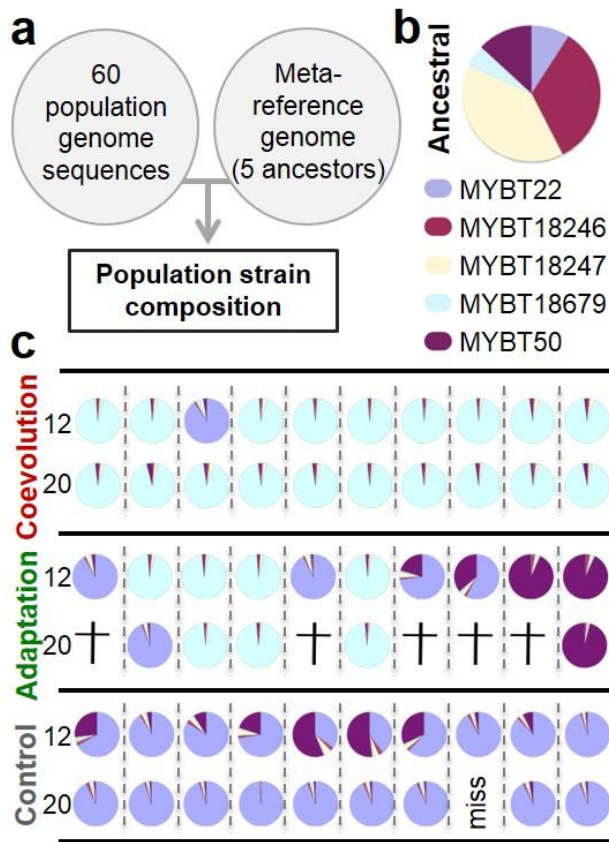


Figure 2. Broad-scale genomic analysis reveals clonal selection during experimental evolution. **a**, Genome analysis workflow: A meta-reference genome created from five genomes representative of the ancestral population was used for sequence read mapping and subsequent identification of strain composition for 60 evolved populations. **b-c**, Pie charts show pathogen strain composition of the ancestral and the evolved populations from ten replicates per treatment (horizontal axis) and two time points (transfer 12 and 20). Coloured slices indicate the relative abundance of the various *B. thuringiensis* strains. Crosses indicate extinction of replicates and "miss" that genetic material for the population was unavailable.

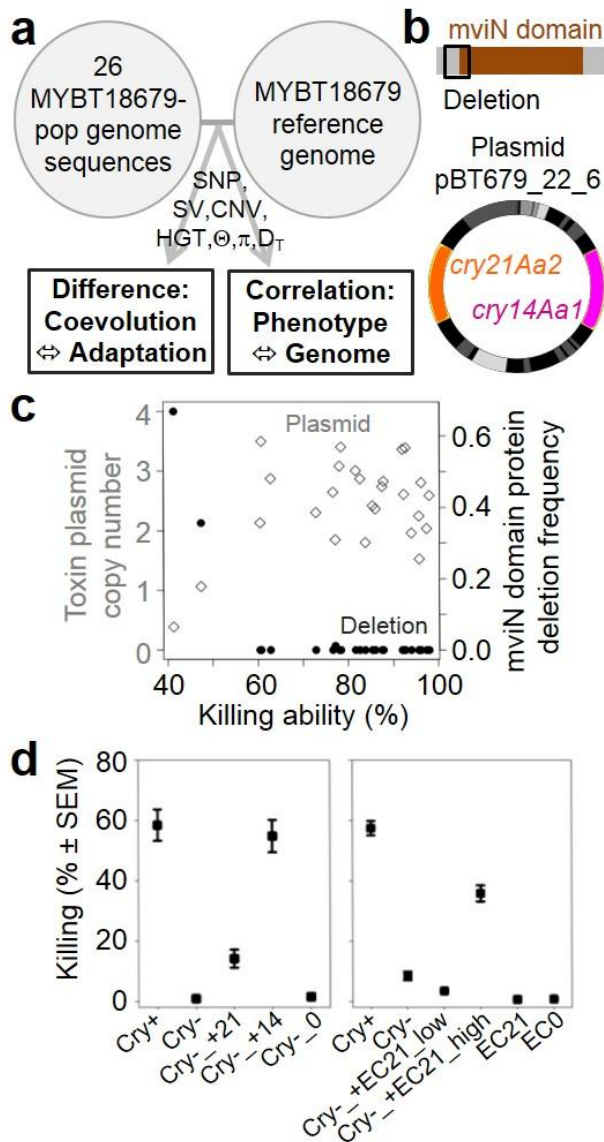
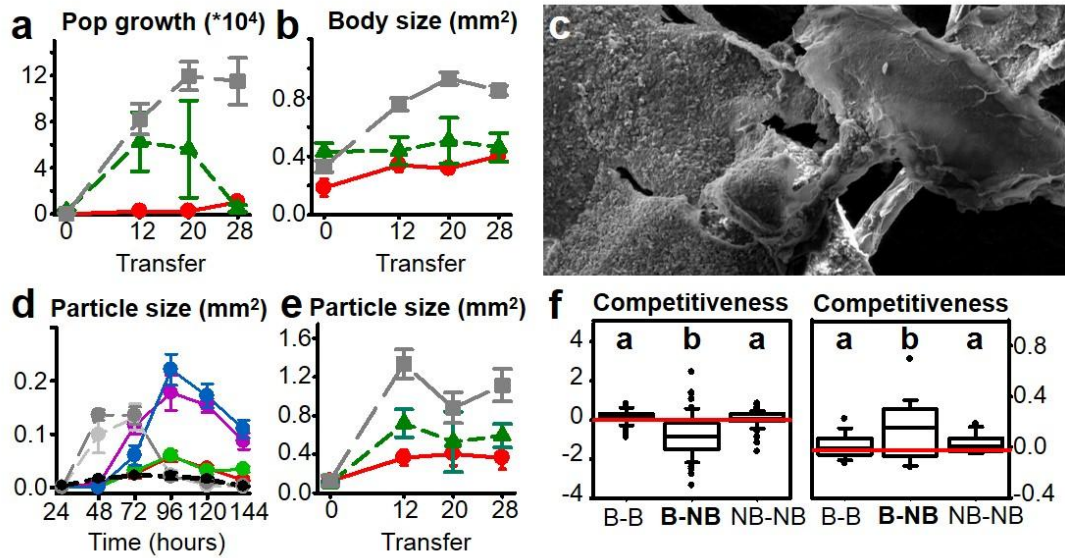
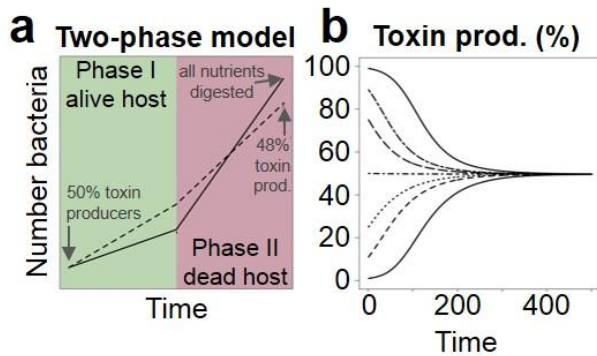


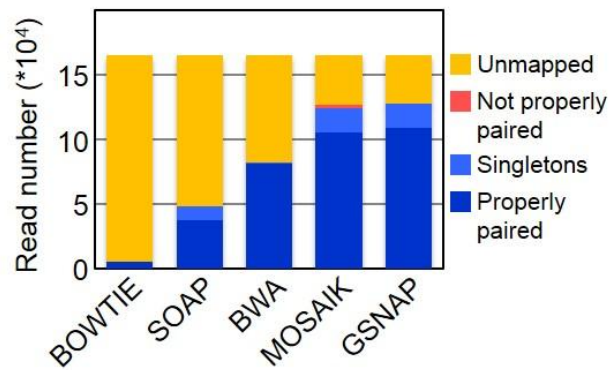
Figure 3. Fine-scale genomics and functional analysis demonstrate importance of nematocidal toxins during adaptation. **a**, Workflow: Genomic variation of MYBT18679 populations was contrasted between treatments or correlated with phenotypic variation. **b**, *mviN* gene deletion and plasmid with *Cry14Aa1* and *Cry21Aa2* toxins. **c**, Pathogen killing ability correlates negatively with *mviN* deletion frequency (left axis, filled circles) and positively with toxin plasmid copy number (right axis, open diamonds). **d**, Mean virulence of plasmid-lacking MYBT18679 (Cry-) with re-introduced *Cry14Aa1* (+14) or *Cry21Aa2* (+21; left panel) or two concentrations of *Cry21Aa2*-expressing *E. coli* (+EC21_low, +EC21_high; right panel). 0, empty vector control. Cry+, plasmid-bearing MYBT18679.



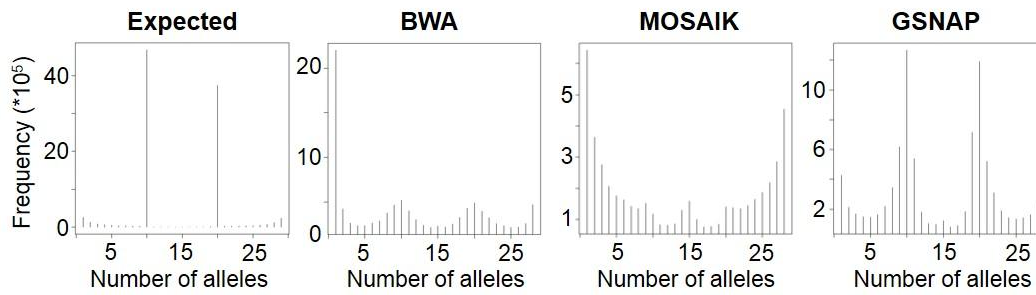
Extended Data Figure 1. Variation of evolved *B. thuringiensis* in their effect on the host and in biofilm formation. **a**, Effects on host population growth. **b**, Effects on host body size. Red circles and solid lines indicate coevolution, green triangles and dotted lines one-sided adaptation, and grey squares and dashed lines control evolution. [Supplementary Tables 3 and 4](#) show the results of the corresponding statistical analyses. **c**, Electron micrograph of a large biofilm particle produced by an evolved pathogen strain from the control evolution treatment. **d**, Temporal dynamics of biofilm formation, measured as mean particle size, for four evolved clones and three ancestral strains; grey shades indicate three ancestral strains (light grey: MYBT18247; dark grey: MYBT18246; black: MYBT18679); red a coevolved clone, green a one-sided adapted clone that is able to form biofilms, purple a one-sided adapted clone unable to form biofilms, and blue a non-biofilm-forming control-evolved clone. **e**, Mean biofilm particle size for the evolved populations across transfers from the evolution experiment. Red indicates coevolution, green one-sided adaptation, and grey control evolution. **f**, Competitive ability of biofilm-forming (B) versus non-biofilm-forming (NB) clones on nutrient-rich nematode growth medium (left) or nutrient-poor peptone-free medium (right). The value for the second listed phenotype was subtracted from the value for the first listed phenotype (B-NB, value for biofilm-producer minus value for non-biofilm-producer). The red horizontal line indicates a value of 0 (i.e., no difference). Different letters on top indicate significant variation. [Supplementary Tables 5 and 6](#) show the corresponding statistical results.



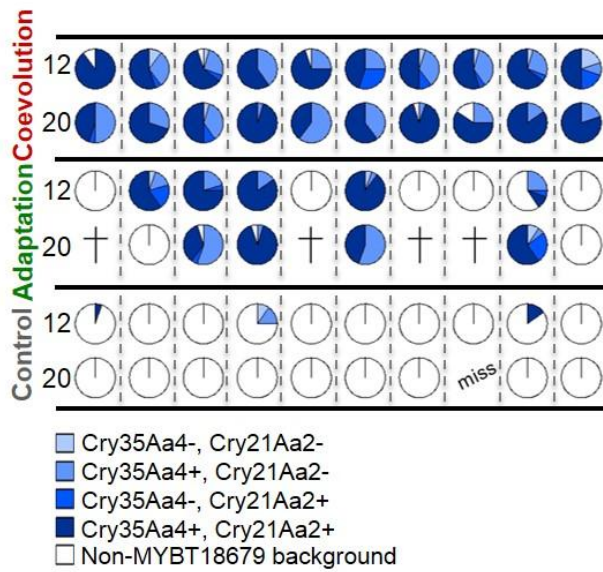
Extended Data Figure 2. Results of the mathematical model on *B. thuringiensis* infection dynamics. **a**, Illustration of the structure of the model as a two-phase process, where the first phase covers the period from beginning of infection until host death (toxin-producers have an advantage since toxins ease access to nutritional resources) and the second phase encompasses the period from host death until depletion of host resources (non-toxin producers have an advantage because they do not suffer from the cost of toxin production). Increases in host resistance are simulated by extending the first phase (increased period until host death). As shown in Fig. 1d of the main text, such an increase favours spread of toxin-producers, whereas the decrease in resistance (shortening of the first phase) leads to a lower proportion or even extinction of toxin producers. **b**, Evolutionary dynamics for varying initial frequencies of toxin producers (b_T). The frequency of toxin producers can increase or decrease depending on the starting condition, but reaches the same equilibrium. Note that low values of $b_T < 0.1$ are not considered here because this leads to scenarios where the amount of toxins is too small to kill the host. From top to bottom: $b_T = 0.99, 0.89, 0.75, 0.5, 0.25, 0.11, 0.1$. Other parameters are $r_{T1} = 1.2$; $r_{T2} = 1.5$; $r_{01} = 0.9$; $r_{02} = 1.9$; $d = 0.8015$; $c = 10$; $m = 0.001$; $g = 700$; $r = 500$; $n_u = 3500$.



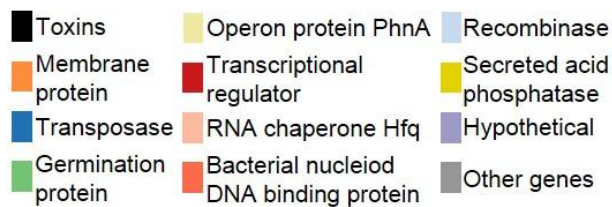
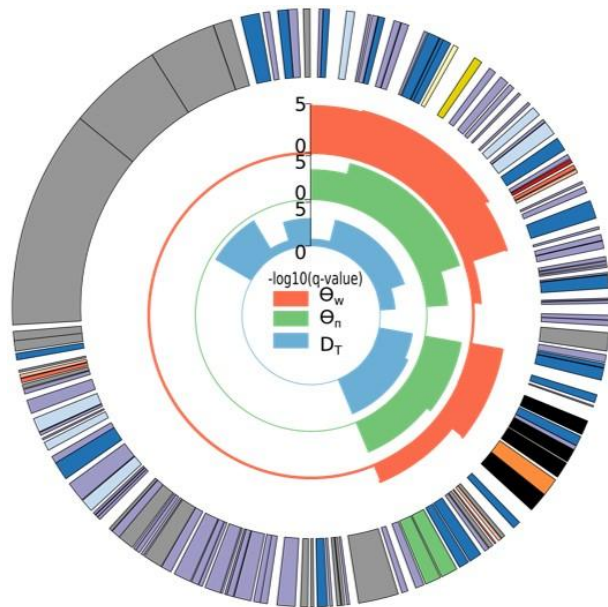
Extended Data Figure 3. Analysis of five mapping programs as to their ability to correctly align simulated reads from *B. thuringiensis* genomes. The five mapping softwares are given along the x-axis. The y-axis presents the total number of reads mapped, classified in 4 categories following the samtools flagstat function: (i) Reads unmapped (orange bar area); (ii) Not properly paired: both reads of a pair are mapped onto the reference genome but expected insert size and/or orientation is incorrect (red bar area); (iii) Singletons: only one read of the pair is mapped (light blue area); and (iv) Properly paired: both reads are mapped onto the reference genome with correct orientation and expected insert size (dark blue area).



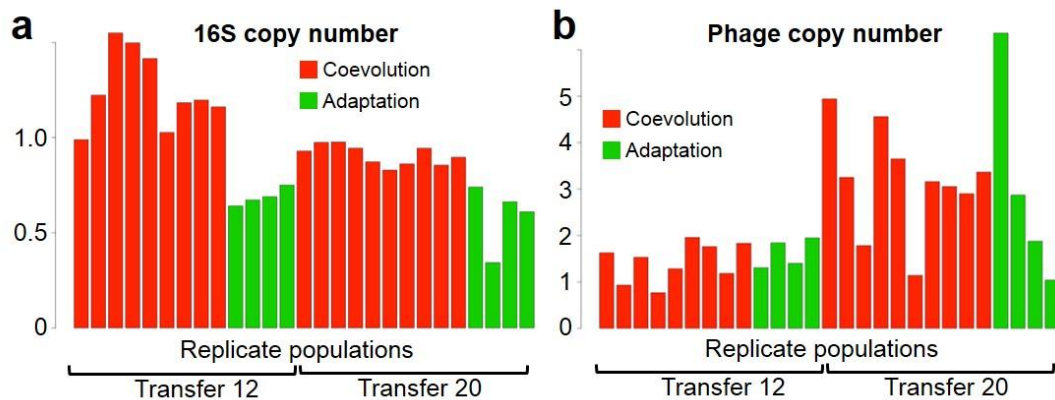
Extended Data Figure 4. Site frequency spectrum of 30 simulated *B. thuringiensis* genome sequences derived from three reference genomes. **a**, Original spectrum relative to the reference genome NC_014171.1 (expected results on far left), and the results obtained with the mapping software BWA, MOSAIK, and GSNAP.



Extended Data Figure 5. Frequency of MYBT18679 toxins Cry21Aa2 and Cry35Aa4 among the evolved replicate populations. . The different shades of blue indicate alternative combinations of toxin genes present, as indicated. The toxin genes were all restricted to evolved clones of the MYBT18679 background (i.e. horizontal transfer was not detected). The top two rows refer to the coevolved, the middle two rows to one-sided adapted, and the bottom two rows to the control evolved replicate populations. Replicate populations are given along the horizontal axis. Data is shown for both transfer 12 and 20. Crosses indicate the populations that went extinct by transfer 20 and "miss" denotes the replicate, for which DNA was not available.



Extended Data Figure 6. Significant variation in population genomic statistics for the plasmid Bti_GWDALJX04I0LJH_51-405_fm319.5. Approximately 65 kb of the plasmid yield significant ANOVA q-values, demonstrating significant variation among the evolution treatments. This region contains genes encoding for transposases, toxins with unknown effect, a membrane protein, a secreted acid phosphatase, and other proteins. The total size of the plasmid is about 126 kb.



Extended Data Figure 7. Exemplary cases of horizontal transfers with significant variation between treatments or transfers. a, Significant variation among treatments for a 16S rRNA gene, horizontally transferred from the MYBT50 ancestral strain to the MYBT18679 genotype. **b,** Horizontal transfer and spread of a phage from the non-nematocidal ancestral strain MYBT50 in the MYBT18679 coevolved and one-sided adapted populations across time. The different replicate populations are given along the X axis and phage frequency on the Y axis. Red indicates coevolution, green one-sided adaptation, light colours transfer 12, and dark colours transfer 20.

Supplementary Information

I Supplementary Methods

1 Evolution experiment and phenotyping

1.1 *C. elegans* and *B. thuringiensis* material

1.2 Experimental evolution

1.3 Phenotypic analysis

2 Mathematical Model of *B. thuringiensis* infection dynamics

2.1 Intra-host dynamics

2.1.1 First phase: Host alive

2.1.2 Second phase: Host dead

2.2 Evolutionary dynamics

3 Genome sequence analysis

3.1 Sequencing

3.1.1 Reference strains

3.1.1 Evolved populations

3.2 Broad-scale genome analysis

3.2.1 Comparison of mapping software

3.2.2 Strain composition of evolved populations

3.3 Fine-scale genome analysis of MYBT18679-dominated populations

3.3.1 Variant detection

3.3.2 Copy number variation and horizontal gene transfer

3.3.3 Population genetic analysis

3.3.4 Statistical analyses

3.3.5 Overview of identified genome regions

4 Toxin gene screen

5 Functional analysis of toxin genes

II Supplementary Tables

III References

1. Evolution experiment and phenotyping

1.1 *C. elegans* and *B. thuringiensis* material

The starting *Caenorhabditis elegans* host population was previously generated through consecutive crosses among 16 natural isolates (PB306, AB1, CB4858, CB4855, N2, JU400, MY16, JU319, PX174, MY1, PX179, JU345, CB4856, CB45507, RC301 and CB4852)¹. These isolates cover the known worldwide genotype diversity for *C. elegans*. We adapted this genetically diverse population to our experimental conditions by maintaining it for 10 generations at 19 °C in 40 replicates in the presence of a non-pathogenic *Bacillus thuringiensis* (DSM-350). This adaptation step served to minimize potential artifacts in the results of the main evolution experiment caused by predominance of environmental selection unrelated to the host-parasite interaction. These laboratory adapted populations were mixed and cryo-preserved in glycerol at -80 °C in 200 aliquots (containing each an average of approximately 5000 worms) for later use in the main evolution experiment. Note that *C. elegans* larvae survive cryo-preservation, thus allowing storage of worm populations for subsequent applications². For all phenotypic experiments, hermaphroditic fourth instar larvae (L4) were used.

The starting pathogen population was similar to that used in our previous experiment³ and consisted of a mixture of genotypes of the Gram-positive *Bacillus thuringiensis*, including as dominant genotypes the strains MYBT18246 and MYBT18247 (both at an abundance of more than 10%) and also MYBT18679, MYBT22, and MYBT50 (less than 10% and more than 1%; see also Fig. 2b of the main text). The host control treatment (see below) contained the non-nematocidal *B. thuringiensis* strain DSM-350. Prior to the evolution experiment, large quantities of *B. thuringiensis* cultures were prepared, aliquotted and conserved at -20 °C for later use³. In all experiments, *B. thuringiensis* was added at a concentration of 1.2×10^9 particles/ml and always mixed at a 1:10 ratio with the standard *C. elegans* food source *Escherichia coli* OP50 (concentration of 2×10^9 cells/ml).

1.2 Experimental evolution

The evolution experiment consisted of five treatments (Fig. 1a of the main text): (i) host control, during which the host adapted to general laboratory conditions in the absence of pathogenic *B. thuringiensis*; (ii) host one-sided adaptation, where the host was allowed to adapt to a non-evolving pathogenic *B. thuringiensis* taken from a frozen stock culture at each transfer step; (iii) host-pathogen coevolution, in which both antagonists were continuously forced to coevolve with each other; (iv) pathogen one-sided adaptation, where the parasite was allowed to adapt to a non-evolving *C. elegans* population taken from a frozen culture at each transfer step; and (v) pathogen control, during which the pathogen adapted to general laboratory conditions in the absence of the nematode host.

The evolution experiments was run at a temperature of 19 °C and included transfers to fresh media twice per week. Each treatment was run in ten replicates for a total of 28 transfers

(equivalent to 14 weeks). Host population size was set to 500 individuals at each transfer step. 5 % of the original hosts (but not of the pathogen) population were added at every second transfer to simulate immigration to reduce drift effects. All treatments were maintained in worm balls, which we established as environments for *C. elegans*-*B. thuringiensis* coevolution experiments³. These consist of two halves of a transparent plastic ball, which are filled with a thin layer of the respective medium, followed by addition of bacteria and worms, and subsequent closure of the halves³. The evolving host populations were purified and synchronized at every second transfer step with alkaline hypochlorite:NaOH, which is only survived by nematode eggs², thus eliminating any bacteria present³. The resulting eggs were raised to L4 larvae on NGM plates with *E. coli* and then a total of 500 worms (475 evolved worms and 25 from the ancestral stock culture as immigrants) were transferred to the next round of the evolution experiment. Nematodes for the pathogen one-sided adaptation treatment were thawed at each transfer step from frozen aliquots and then raised as above before addition to the wormballs. In case of *B. thuringiensis*, the host-adapting populations were always isolated from dead worms, which were specifically collected at each transfer step and maintained for two additional days in phosphate buffered saline (PBS), followed by pasteurization at 80 °C for 10 min to eliminate bacterial contaminants³, subsequent culturing on NGM plates for 3-5 days, mixing with *E. coli* food at 1:10 ratio and transfer to the next selection round. *B. thuringiensis* for the host one-sided adaptation treatment were always taken from frozen stock cultures and those from the pathogen control treatment were directly washed off the worm balls, followed by pasteurization and all subsequent steps listed above. Random samples from all replicate populations were cryo-preserved at transfers 12, 20 and 28. The general experimental protocol is similar to that used for our previous evolution experiments³, and the exact methods for most of the host side of the experiment were recently published in Masri *et al.*⁴.

1.3 Phenotypic analysis

Phenotypic changes across time and treatments were studied for the frozen host and parasite samples from transfer steps 0, 12, 20, and 28, using the same general environmental conditions as in the evolution experiment. All treatment samples from the various transfer steps were also studied simultaneously and in random order to avoid artifacts due to observer bias and/or random environmental or temporal fluctuations. Both nematodes and bacteria were raised and purified prior to the experiments (alkaline hypochlorite:NaOH treatment for worms², pasteurization for bacteria). The hermaphroditic worms were used once they reached the L4 stage and the final *B. thuringiensis* concentration was adjusted to 1.2×10^8 particles/ml. The following phenotypic traits were evaluated.

Changes in host resistance (i.e., the ability of the host to survive pathogen exposure) and pathogen virulence (i.e., the ability of the pathogen to kill the host) were assessed by respectively measuring nematode survival and *B. thuringiensis* killing ability in the presence of the respective ancestral antagonist³. For this measure, 50 worms were exposed to *B. thuringiensis* and the proportion of surviving hosts was counted after 48 h. As additional indirect measures of host resistance and pathogen virulence we also examined the bacterium's

effect on worm body size and population growth³. For both traits, 35 L4 *C. elegans* were exposed to *B. thuringiensis*. After 48 hours, body size was measured as whole worm area for four to six nematodes using differential interference contrast (DIC) microscopy (DM5000B microscope; Leica) and the program ImageJ 1.36b (<http://rsb.info.nih.gov/ij/>), followed by calculation of the average body size per replicate population for later statistical analysis. After five days of exposure, population growth was determined by washing off all worms from the wormballs with 2 ml PBS, counting of animals in three 10 μ l subsamples, and subsequent calculation of the total number of worms per replicate population.

Infection load was quantified with a new protocol to characterize the ability of *B. thuringiensis* to ensure high abundance inside the host as well as the corresponding host immune competence to influence this trait. For this assay, 35 worms were exposed to *B. thuringiensis* – *E. coli* mixtures (final concentrations respectively of 1.2×10^8 particles/ml and 1.8×10^9 cells/ml) on PFM plates. After 48 hours, three to six live worms per replicate were transferred onto a 12-well microscopic slide, followed by body size measurements using ImageJ 1.36b. To remove bacteria adhering to the cuticle, the worms were carefully washed with approximately 20 μ l sterile H₂O under a dissecting microscope, followed by their transfer into 1.5 ml tubes containing 100 μ l H₂O. The number of externally associated bacteria, which could not be removed, was estimated by counting cells in the surrounding solution using standard Thoma counting chambers (0.1 mm depth). For each replicate, bacteria were subsequently extracted by sonicating the worms for 10 sec, 6 cycles at 60 Hz, followed by addition of four 1 mm Zirconia beads and vortexing for 3 sec. The number of extracted bacteria was quantified using Thoma chambers. The infection load was then calculated as the number of extracted bacteria minus the number of bacteria in the surrounding solution, adjusted for worm size and averaged per replicate population.

The characteristics of biofilm formation were studied for all of the evolved replicate populations, and, additionally, a selection of replicate populations, and also isolated clones from these populations. All evolved replicate populations from transfers 0, 12, 20, and 28 were characterized with two assays. (i) As a rough qualitative proxy of biofilm formation, we scored the proportion of replicate populations per treatment that produced clearly visible flakes ([Extended Data Fig. 1c](#)). (ii) Biofilm formation was quantified by measuring average particle size produced by each replicate population. 20 μ l per population were grown for 48 hours at 19 °C on NGM, washed off with 3 ml PBS, vortexed for five seconds in 15 ml tubes, followed by measuring particle area (in mm²) for the five largest particles within a random 20 μ l sample of the culture using DIC microscopy and ImageJ. Four random 20 μ l samples were assessed per replicate and averaged for subsequent statistical analysis.

A more detailed analysis of biofilm formation was performed for four representative populations from transfer 20, which were either highly virulent but did not form a biofilm (one population each from the coevolution and the one-sided adaptation treatments) or were avirulent yet biofilm-forming (one population each from the one-sided adaptation and the control treatments). These four populations were characterized using the following two approaches. (i) Bacterial colony size and colony density were assessed on NGM plates after

96 hours growth at 19 °C, using contrast microscopy and ImageJ to measure colony diameter (in mm²) and density (absorbance). We used the average of 20 colonies per considered population for statistical comparisons. (ii) Bacterial competitive ability was studied under either low nutrient conditions on PFM or high nutrient conditions on NGM. Biofilm forming and non-biofilm forming bacteria (concentration of 1.2*10⁹ particle/ml) from the selected evolved populations were streaked out along thin lines in parallel to each other at a distance of 5 mm and grown at 19 °C for 96 hours on NGM and 21 days on PFM (due to the absence of nutrition, growth was substantially reduced under these conditions). Thereafter, the growth expansion of one population in the direction of the other population was measured as the distance from the original streak to the farthest area of the grown culture. An analogous measurement was taken for the competing bacterium. A competitiveness index was subsequently calculated for a particular population by taking its growth expansion measurement and subtracting from it the respective measurement of the competitor. Thus, a competitiveness index of 0 indicates equality, whereas a positive index suggests higher competitiveness for the focal population (Extended Data Fig. 1f).

An additional analysis of the dynamics of biofilm formation was performed for four individual clones, isolated from transfer 20 from above selected populations. We confirmed that the isolated clones showed the same general characteristics as their source populations (i.e., one highly virulent, non-biofilm-forming clone from the coevolution treatment; one highly virulent, non-biofilm-forming clone from the one-sided adaptation treatment; one low virulent, biofilm-forming clone from the one-sided adaptation treatment; and one low virulent, biofilm-forming clone from the control). The dynamics of biofilm production was characterized by growing the selected four clones and also three of the ancestral strains (MYBT18246, MYBT18247, and MYBT18679) on 9 cm NGM plates in several replicates. Every 24 h, an entire plate was washed off for particle size measurements as described above. The entire analysis was performed for a total of 144 h (Extended Data Fig. 1d).

Statistical analysis of phenotypic data was based on JMP[®] 9 (SAS). Variations between the treatments in all traits except competitiveness were evaluated with a general linear model including transfer and treatment as fixed factors, and replicate nested within treatment as a random factor. A likelihood ratio test was used to assess the relative influence of factors in the model. Variation in competitiveness was compared with the Mann-Whitney U test (MWU). Graphs were generated with SigmaPlot version 11.0 (Systat Software Inc.). The results of the statistical analysis of the phenotypic data are shown in [Supplementary Tables 1-6](#).

2 Mathematical Model of *B. thuringiensis* infection dynamics

A mathematical model was designed that reflects the basic structure of the experimental set-up. It consists of two parts: (i) the intra-host infection dynamics of two bacterial genotypes, and (ii) the evolutionary dynamics including bacterial transmission between hosts. The parameters of the mathematical model are given in [Supplementary Table 7](#).

2.1 Intra-host dynamics

A discrete time step model describes the intra-host infection dynamics in two separate phases. The model considers four variables: the number of toxin-producing bacteria (B_T), the number of non-toxin producing bacteria (B_0), the amount of undigestible nutrient (N_u), and the amount of digestible nutrient (N_d). The variables of subsequent time steps are indicated by “ t ” and “ $t+1$ ”. Within each time step, the following events occur in order: (i) nutrient toxin-interaction, (ii) nutrient uptake and bacterial growth, and (iii) bacterial mortality. Intermediate values of the variables are indicated by superscript “+” (after first step) and “++” (after second step).

At the beginning of an infection, the host is exposed to a certain number of bacteria (b). Initially, there are $B_T(0)=b_T$ toxin producers, and $B_0(0)=b_0$ non-toxin-producers ($b_T+b_0=b$). The initial amount of toxin (T) is purely determined by the number of toxin producing bacteria at the onset of infection, i.e. $T=B_T(0)=b_T$. The amount of toxin does not change during infection (i.e., the amount of toxin cannot increase or decrease after a host is initially infected). Finally, the host begins with $N_u(0)=n_u$ units of undigestible nutrients and $N_d(0)=0$ units of digestible nutrients.

The model consists of two separate phases that differ with respect to the bacterial growth rates. The first phase starts with the bacterial infection of the host and lasts either until host death or until a maximal number of time steps g is reached. Host death occurs when the fraction d of the undigestible nutrient n_u has been converted into digestible nutrient. Note that no more than dn_u nutrient is used in the first phase. The second phase starts with host death and ends after g time steps. There is no second phase if the host doesn't die in phase one.

2.1.1 First phase: host alive

(i) *Nutrient-toxin interaction.* Each unit of toxin converts one unit of undigestible nutrient into one unit of digestible nutrient. If the amount of undigestible nutrient exceeds the amount of toxin or is equal to it ($N_u(t) \geq T$) then it holds that

$$(1) \quad N_u^+(t) = N_u(t) - T,$$
$$(2) \quad N_d^+(t) = N_d(t) + T.$$

If $N_u(t) < T$ then it holds that

$$(3) \quad N_u^+(t) = 0,$$
$$(4) \quad N_d^+(t) = N_d(t) + N_u(t).$$

The number of bacteria doesn't change during this step, i.e. $B_T^+(t) = B_T(t)$ and $B_0^+(t) = B_0(t)$.

(ii) *Nutrient uptake and bacterial growth.* The growth rates of toxin producers and non-toxin producers are denoted by r_{T1} and r_{01} , respectively. Two cases need to be distinguished. First,

there is no food limitation inside the body if $N_d^+(t) \geq c(r_{T1}B_T^+(t) + r_{01}B_0^+(t))$. Then, bacterial numbers and nutrient change to

$$\begin{aligned} (5) \quad & B_T^{++}(t) = (1 + r_{T1})B_T^+(t), \\ (6) \quad & B_0^{++}(t) = (1 + r_{01})B_0^+(t), \\ (7) \quad & N_d^{++}(t) = N_d^+(t) - c(r_{T1}B_T^+(t) + r_{01}B_0^+(t)). \end{aligned}$$

Here, c is the conversion rate from digestible nutrient into bacteria. Second, food limitation occurs if $N_d^+(t) < c(r_{T1}B_T^+(t) + r_{01}B_0^+(t))$. Then, digestible nutrient and bacterial numbers after consumption and growth compute to

$$\begin{aligned} (8) \quad & B_T^{++}(t) = \left(1 + \frac{r_{T1}N_d^+(t)}{c(r_{T1}B_T^+(t) + r_{01}B_0^+(t))}\right) B_T^+(t), \\ (9) \quad & B_0^{++}(t) = \left(1 + \frac{r_{01}N_d^+(t)}{c(r_{T1}B_T^+(t) + r_{01}B_0^+(t))}\right) B_0^+(t), \\ (10) \quad & N_d^{++}(t) = 0. \end{aligned}$$

Undigestible nutrient doesn't change during this step, i.e. $N_u^{++}(t) = N_u^+(t)$.

(iii) *Bacterial mortality.* A fraction m of each type of bacteria dies. This step completes the time step. It holds that

$$\begin{aligned} (11) \quad & B_T(t+1) = (1 - m)B_T^{++}(t), \\ (12) \quad & B_0(t+1) = (1 - m)B_0^{++}(t), \\ (13) \quad & N_d(t+1) = N_d^{++}(t), \\ (14) \quad & N_u(t+1) = N_u^{++}(t). \end{aligned}$$

2.1.2 Second phase: dead host

The second phase starts with host death, i.e. when dn_u units of undigestible nutrient have been converted into digestible nutrient. The infection dynamics are described by equations (1)-(14), but with the modification that bacterial growth rates change from r_{T1} to r_{T2} and from r_{01} to r_{02} . Note that we consider only cases with $r_{01} < r_{T1} = r_{T2} < r_{02}$ for the analysis. An important aspect of phase 2 is that all nutrients are digestible. Therefore, the nutrient variables are set to $N_u = 0$ and $N_d = \tilde{N}_d + (1 - d)n_u$, where \tilde{N}_d denotes the amount of digestible nutrient at the end of phase 1.

2.2 Evolutionary dynamics

The evolutionary model describes how bacterial frequencies change between two subsequently infected hosts. It is assumed that the two hosts are characterized by the same parameter values (including n_u and n_d), and that the infection dynamics in both hosts follow model (1)-(14). We assume that the first host is infected by $B_T(0) = b_T$ toxin producers and $B_0(0) = b_0$ non-toxin-producers ($b_T + b_0 = b$). After g time steps, the bacterial numbers have changed to $B_T(g)$ and $B_0(g)$, respectively. Inter-host transmission occurs when the second host

is infected by b bacteria. These b bacteria consist of $\frac{B_T(g)}{B_T(g)+B_0(g)}b$ toxin producers and $\frac{B_0(g)}{B_T(g)+B_0(g)}b$ non-toxin producers. The number of bacteria infesting a new host is kept constant at b in the model, but the bacterial frequencies can vary. For the analysis, we iterated this process r times, and plotted the frequency of toxin producers as a function of r and for different parameter constellations.

The dynamics of toxin producer frequencies is related to different levels of host resistance (as modeled by d) in Fig. 1c of the main text. For this figure, seven different values for d were used ($d=0.6, 0.34, 0.32, 0.296, 0.272, 0.252, 0.1$). Other settings were initially $b_T=b_0=50$, and also: $r_{T1}=1.2; r_{T2}=1.5; r_{01}=1; r_{02}=2; c=10; m=0.001; g=30; r=300; n_u=5450$. The dynamics of toxin producer frequencies was also evaluated in dependence of alternative starting values, always resulting in similar equilibrium frequencies, as shown in [Extended Data Fig. 2](#).

3 Genome sequence analysis

3.1 Sequencing

Draft genome sequences for five *B. thuringiensis* strains from the starting population (MYBT246, MYBT247, MYBT679, MYBT22 and MYBT50) were used as references for mapping of the population genomic data. For each of these strains, genomic DNA was isolated using a DNeasy Blood and Tissue Kit (Qiagen). Whole genome sequencing was performed using the Roche 454 Genome Sequencer FLX platform. The resulting reads were assembled using GS *De Novo* Assembler (Roche). For MYBT18679, a partially closed reference was generated through targeted PCR and Sanger sequencing, consisting of 31 scaffolds, including more than ten plasmids. The final meta-reference was submitted to the European Nucleotide Archive database under study accession number PRJEB5931 (ENA; www.ebi.ac.uk/ena/), and a summary of the data and assemblies for each strain is shown in [Supplementary Table 8](#).

For pooled samples of the ancestral population and each of the evolved replicate populations from transfer 12 and 20, genomic DNA was isolated following the Qiagen DNeasy[®] Blood and Tissue kit procedures for Gram-positive bacteria. Prior to DNA extraction, 10 μ l of the frozen bacterial populations were spread onto NGM and grown for 14-16 h at 25 °C. Bacteria were washed off NGM plates with 1 ml of autoclaved H₂O, followed by DNA extraction. For samples showing the biofilm phenotype, four replicates were extracted and pooled while three replicates were extracted for the other samples. DNA quantity, measured with Qubit[®] Fluorometric Quantitation, ranged between 9.13 ng/ μ L and 55.1 ng/ μ L. For Illumina sequencing, genomic paired-end libraries were prepared following standard methods⁵. Insert sizes (excluding adapters) ranged from 200-450 nucleotides. Libraries were sequenced using GAII or GAIIx Illumina sequencing instruments to yield paired 100mers. The Illumina image analysis pipeline with default parameters was used for image analysis, base-calling and read

filtering. Further filtering served to remove adapter and PhiX contamination based on blast alignment (pairs with ≥ 14 nt aligned at $\geq 98\%$ were removed). The reads were subsequently processed with SeqPrep (<https://github.com/jstjohn/SeqPrep>) software to remove adapter sequences and merge overlapping read pairs. The population genomic data is available from the ENA database (ENA; www.ebi.ac.uk/ena/) under study number PRJEB5931.

3.2 Broad-scale genome analysis

3.2.1 Comparison of mapping software

We assessed suitability of mapping software programs (Bowtie⁶; BWA⁷; MOSAIK⁸; SOAP⁹; and GSNAP¹⁰) to correctly align Illumina reads from pooled population samples (thus including nucleotide and structural variation) to our concatenated meta-reference. We first generated reads from three of the publicly available *B. thuringiensis* genome sequences (Genbank accession number NC_014171.1, NC_005957.1 and NC_008600.1) using the dwgsim tool from the dnaa 0.1.2 software suite (<http://sourceforge.net/projects/dnaa/>). A depth of coverage of 1x for each genome was generated corresponding to 55000 reads of 100 bp with a fragment size of 350 bp per genome and maximum quality. A meta-reference was generated by aligning the five genomes using progressiveMAUVE¹¹ and polymorphic sites were recorded following ambiguity IUPAC codes to avoid counting them as mismatches in the alignment. For GSNAP, a SNP file was created to account for variation. Indel positions were kept without gaps. Usage of SOAP and Bowtie led to low mapping efficiency ([Extended Data Fig. 3](#)), apparently because of imprecise alignment of polymorphic positions. MOSAIK and GSNAP performed equally well while BWA aligned substantially fewer reads to the meta-reference ([Extended Data Fig. 3](#)). Based on these results, SOAP and Bowtie were excluded from subsequent analyses.

A second set of simulated data was generated to test the influence of allele frequency biases, which are likely to be present in the evolved populations. Ten genomes of each of the three references were generated with SNP variation, resulting in a total of 30 different genome sequences that were simulated as 100 bp paired-end reads with 1000x read depth. These produced the site frequency spectrum shown in [Extended Data Fig. 4](#). The reads were mapped with the three programs, followed by detection of single nucleotide polymorphisms (SNPs) using SNVer¹² and allele frequency calculations based on the number of SNP reads divided by the total read depth. Based on this data set, which is likely to be representative of the sequence data from our evolved populations, we found GSNAP to produce a site frequency spectrum most similar to the original distribution ([Extended Data Figs. 4](#)). GSNAP was therefore used for the subsequent analyses.

3.2.2 Strain composition of evolved populations

Our strategy for estimating the frequency of the five ancestral strains in pooled population samples consisted of four steps ([Fig. 2a](#) of main text). We first generated a concatenated meta-reference based on the five ancestral strains. Secondly, the obtained reads of the considered

population samples were mapped onto the meta-reference using GSNAP, resulting in 90-97% mapping efficiency ([Supplementary Table 8](#)). Thirdly, we identified the polymorphic sites where only one of the five reference strains shows a substitution. For the population samples, we then determined the frequency of substitutions at each of these diagnostic polymorphic positions and took these as independent estimates of strain frequencies. Fourthly, as such frequency distributions are usually asymmetric (e.g., left-skewed), we calculated the mode of the distribution as the final frequency estimate, using the function `mlv` from package `modeest`¹³ in R¹⁴. The inferred values per strain are listed in [Supplementary Table 9](#), the results of the statistical comparison among the evolved populations are given in [Supplementary Table 10](#), and a graphical illustration of our findings is presented in [Fig. 2](#) of the main text.

3.3 Fine-scale genome analysis of MYBT18679-dominated populations

3.3.1 Variant detection

For the fine-scale genome analysis, we focused on the evolved populations dominated by the MYBT18679 strain. These populations still showed substantial variation in both killing ability and infection load. The analysis was based on a four-step strategy ([Fig. 3a](#) of main text): Firstly, each read was mapped to each of the five reference genomes present in the starting population. Secondly, the edit distance between the reference and the mapped read (NM field in SAM format) was recorded and compared among the five alignments (referring to the five reference genomes). Only reads were considered for further analysis when they produced the lowest Edit distance to the MYBT18679 genome (i.e., they had the highest similarity with MYBT18679 but not the other genomes). Thus, reads with the same or lower Edit distance to the non-MYBT18679 strains were excluded (see mapping statistics in [Supplementary Table 9](#), where reads mapping uniquely to each reference and total reads mapped are reported). Thirdly, SNVer software version 0.4.1¹² was used to identify SNPs and short indels using default parameters except that the strand bias and the fisher exact threshold was set to 20 instead of 30 (-u 20) to avoid frequency bias due to overfiltering¹⁵. Minimum mapping quality and base quality were set to 20 and the results are shown in [Supplementary Table 14](#). Further filtering consisted of: (i) excluding positions for which an identified SNP was below the 2% or above the 98% quantile of the observed coverage distribution; (ii) excluding SNPs and short indels if a significant Fisher exact test on strand bias was inferred (0.05 threshold); (iii) excluding SNPs if an indel is detected at the same position; and (iv) keeping SNPs with a minimum allele frequency (MAF) across the sample above 5%. Finally, we identified structural variations using Pindel version 0.2.4¹⁶ with default parameters except the following: -w 1 (1 million base bins) and -u 0.03 (maximum allowed mismatch rate). The results are summarized in [Supplementary Table 15](#).

3.3.2 Copy number variation and horizontal gene transfer

Several tools have been developed to detect copy number variations (CNVs) using depth of coverage (e.g. CNVnator¹⁷ or Event Wise Testing¹⁸). However, these approaches have not been designed to account for pooled population samples where only some individuals may harbor a CNV, possibly leading to only a proportional coverage change below but not above the value of one. Therefore, we developed our own approach. Firstly, we used the average rank of each position instead of the raw or scale data, in order to account for general coverage variations among samples. Secondly, we calculated the variance at each position for the rank of the depth of coverage across the samples. Thirdly, outliers were extracted using the `getOutliers()` function of the `extremevalues` library in R with the method I and a normal fit¹⁹. Adjacent outlier positions (i.e., with a distance of less than 100 bp) were considered to belong to the same coverage singularity. Fourthly, scale coverage relative to the median coverage of chromosomal contigs was calculated at candidate position to estimate the average copy number in each sample ([Supplementary Table 16](#)).

Following a similar approach, we also assessed copy number variation for each contig within the MYBT679 reference by calculating the ratio of each contig over the average of all chromosomal contigs. The variance was estimated by random sampling of 10000 positions. The results are presented in [Supplementary Table 17](#).

Horizontal gene transfer (HGT) was evaluated by identifying non-MYBT18679 genome regions within the populations dominated by MYBT18679. For this, we extracted reads mapping uniquely and best to one of the non-MYBT18679 reference genomes. We only considered the thus identified putative HGT fragments, for which an indication of HGT from the same reference genome is continuously found across at least 1 kb. The frequency of each putative HGT was then estimated through the ratio of the median coverage of the fragment over the median coverage of the chromosomal contigs of MYBT679 ([Supplementary Table 18](#)).

3.3.3 Population genetic analysis

We calculated three different population genetics statistics in a sliding window approach with 5 kb steps and 10 kb window size, namely Watterson's θ , Tajima's π and Tajima's D. To correct for coverage variation within a window and along the genome, coverage was taken as a proxy for the number of samples and statistics were calculated using the adjusted Watterson's θ and Tajima's π estimates that specifically allow for sample size variation across the genome²⁰. Only polymorphisms showing a frequency above 0.05 were considered. The results are summarized in [Supplemental Table 19](#).

3.3.4 Statistical analyses

The same statistical tests were performed on each dataset, which either contained the identified SNPs, short indels, pindel structural variants, CNVs detected through coverage variation, putative HGTs, or the population genetic characteristics. We excluded coevolution

replicate 3 at transfer 12 from the analysis because it contained two genotypes at higher frequencies (MYBT18679 and MYBT22) and it was thus not directly comparable to the other replicate populations dominated by MYBT18679. Two types of statistical analyses were performed. Firstly, a linear regression analysis between genomic variation and either killing ability or infection load. The linear regression (using R¹⁴) was weighted by the log₁₀(coverage) on each dataset except of the population genetics statistics, because the read depth coverage is directly affecting the variance on frequency estimates. Secondly, an analysis of variance (ANOVA) was performed to compare the difference between treatments. The treatment effect was nested within transfer as follows:

*Variable ~ Transfer + Treatment[Replicate] + Transfer * Treatment[Replicate]*

Significance levels were adjusted using the false discovery rate²¹.

The statistical analysis identified a large number of genome regions ([Supplementary Table 20](#)). At least some of them, but possibly not all, may have influenced pathogen adaptation to either coevolving or non-changing host. In order to identify the most relevant regions for such adaptational processes, we used the following statistical and functional criteria: (i) The relevant genome regions should have been identified through variation in at least four replicate populations (and thus not be the consequence of exceptional events in very few populations; note that under the latter conditions homoscedascity of the data - as required for ANOVA - may also be compromised); (ii) for the ANOVA approach, they should only show a treatment effect, but not a transfer or an interaction effect, the latter of which may both indicate convergent evolution across treatments during the course of the experiment; (iii) for the analysis of horizontal gene transfer treatment variance of the transferred region should excel 0.04; and (iv) the identified variations should be of functional consequence, for example they should influence gene expression levels (i.e., changes in copy number) or directly gene function (non-synonymous or frame-shift mutations, etc). The resulting list of candidate regions is presented below and highlighted in yellow and bold font type in [Supplementary Table 20](#).

3.3.5 Overview of identified genome regions

The linear regression analysis revealed four cases of a significant association between genome and killing ability but none with infection load. Three of the four significant cases may be of relevance for bacterial adaptation to either coevolving or non-changing host as they could have functional consequences (i.e., they affect expression levels of genes or gene function itself). In particular, killing ability was found to correlate positively with the copy number of (i) the plasmid pBT679_22_6, which contains the nematocidal toxin genes *Cry21Aa2* and *Cry14Aa1* (q-value=1.73E-07); and (ii) the plasmid (or plasmid fragment) represented by the contig Bti_GWDALJX04IG4JR_1-226, containing a plasmid recombination enzyme, two hypothetical proteins and Parvulin-like peptidyl-prolyl isomerase (q-value=0.016). Killing ability also correlated negatively with the frequency of a chromosomal deletion of 12 amino acids in a putative virulence factor containing a mvIN domain (gene Bt_01995; q-value=0.038). Taken together, the region with the strongest effect (according to the q-value) refers to the plasmid that contains genes with known nematocidal effect and that is thus

known to have a function in pathogen-host interactions. One other region includes a gene with a suspected function in virulence, whereas it is currently unclear in how far the genes within the third region may contribute to bacterial interaction with a host.

The ANOVA approach yielded a comparatively large list of genome regions with a significant treatment effect, strongly suggesting that the imposed differences in selection conditions lead to changes in the favoured genomic variants and/or promoted horizontal gene transfer. In particular, a total of 53 genome regions were inferred from the SNP analysis, 3 from the Pindel-based structural analysis, 81 from the coverage-based copy number variation analysis, 66 from the assessment of horizontal gene transfer, and 35 from the population genetic analysis. Note that some of these regions overlap as a consequence of the different approaches used during the respective analyses. Based on the above outlined conservative criteria, only few of the identified regions are likely of relevance for adaptation to either coevolving or non-changing hosts ([Supplementary Table 17](#)), including (i) a recombinase/invertase (gene Bti_05865), for which the gain of a stop codon varies among treatments (inferred through SNP analysis); (ii) a predicted acetyltransferase/hydrolase (gene Bti_05100), which shows copy number variation between treatments; (iii) two horizontally transferred gene regions from the *B. thuringiensis* strain MYBT18246 containing a Cysteine protease, a recombinase/invertase, and several hypothetical proteins; (iv) one horizontally transferred gene region from MYBT18247, containing among others a transcriptional antiterminator; (v) one horizontally transferred 16S rRNA gene region from MYBT50 ([Extended Data Fig. 7a](#)); and (vi) an approximately 65 kb region from the contig, possibly a plasmid, Bti_GWDALJX04I0LJH_51-405_fm319.5, consistently identified by the population genetic measures to vary among treatments and containing a variety of different genes such as those encoding toxins (with unknown effects), a membrane protein, a transposase, germination proteins, a secreted acid phosphatase, and others ([Extended Data Fig. 6](#)). None of the above regions contains genes previously implicated in the bacterium's interaction with a host. The only exception may refer to some of the genes found in the 65 kb plasmid region, of which the toxin, the membrane protein, the acid phosphatase, or the germination protein genes could be speculated to contribute to host interactions. The dissection of the above genes' exact role in shaping adaptation to either coevolving or non-changing hosts represents a particular challenge for future research.

Interestingly, 14 of the inferred cases of copy number variations refer to collagen triple helix repeats ([Supplementary Table 20](#)), possibly suggesting a role of these genes in general adaptation to a host environment, irrespective of whether the host is co-adapting or not. It is similarly interesting to note that horizontal transfers mainly originated from two ancestral non-nematocidal *B. thuringiensis* strains that are mainly, yet not exclusively favoured in the absence of the host. Of these, most transfers came from strain MYBT22, encompassing 35 horizontally transferred fragments with a total length of 51 kb, whereas 19 fragments with a total length of 45 kb originated from MYBT50. One of the transferred fragments refers to a phage that originated from MYBT50 and spread through the MYBT18679-dominated populations across time, irrespective of the evolution treatment regime and possibly as a

selfish element that does not contribute to bacterial adaptation to a host ([Extended Data Fig. 7b](#)).

4 Toxin gene screen

To identify genes for crystal toxin proteins that were present in the starting population of *B. thuringiensis*, we performed sequence similarity searches on the draft genome assemblies of the nematocidal strains MYBT18246, MYBT18247 and MYBT18679 using known cry toxin protein sequences as queries. The query sequences were derived from the cry toxin list available on the Bt toxin nomenclature webpage (http://www.lifesci.sussex.ac.uk/home/Neil_Crickmore/Bt/). Based on this analysis, we identified seven genes with high similarity to known cry toxin sequences: *cry13Aa1* in MYBT18246, *cry6Ba1* in MYBT18247, and *cry14Aa1*, *cry21Aa2*, *cry34Aa4*, *cry35Aa4* and *cry38Aa1* in MYBT18679. *Cry14Aa1* and *cry21Aa2* are located 8 kb apart on a 23 kb plasmid, while *cry34Aa4*, *cry35Aa4* and *cry38Aa1* are all located within a 4 kb region on a separate plasmid. We also identified several additional putative cry toxin genes (<60% similarity to query sequences), but for practical reasons they were not considered in subsequent analyses.

To analyse the composition of crystal toxin genes in the evolved *B. thuringiensis* populations, we focused on *cry13Aa1*, *cry6Ba1*, *cry14Aa1*, *cry21Aa2* and *cry35Aa4*. 20 individual clones were isolated from each evolved population from transfer 12 and 20 by plating the population on nematode growth medium (NGM) plates and picking single colonies, resulting in a total of 1200 clones tested. The clones were grown overnight at 28°C in LB medium, then frozen at -20°C. This frozen material was used directly in PCRs with toxin specific primers ([Supplementary Table 11](#)) and 15.6 µl reaction volumes containing 0.39 units GoTaq DNA Polymerase (Promega), 1x Green GoTaq reaction buffer, 0.2mM each dNTP, and 0.4 µM of each primer. Thermal cycling was performed with an initial denaturation step at 95 °C for 2 min followed by 35 cycles of 30 sec 95 °C, 30 sec 57 °C, 90 sec 72 °C, and then a final extension at 72°C for 10 min. *CodY* primers were included in each reaction to ensure integrity of the template. We additionally determined the chromosomal background of each clone by Sanger sequencing of part of the *codY* gene, amplified by PCR as above.

The chromosomal backgrounds were largely consistent with the whole genome data ([Fig. 2c](#) of the main text): the coevolution treatment was dominated by MYBT18679, the control treatment by MYBT22, while the adaptation treatment showed variation between replicates with virulent populations dominated by MYBT18679 and non-virulent populations dominated by MYBT22 or MYBT50 ([Supplementary table 12](#)). The toxin genes *cry14Aa1*, *cry21Aa2*, and *cry35Aa4* were only found in evolved MYBT18679 clones, thus remaining within the same chromosomal background. Their presence varied among these clones, whereby *cry14Aa1* and *cry21Aa2* showed the same pattern (i.e. both present or both absent) for all but seven clones and were both less abundant than *cry35Aa4* ([Extended Data Fig. 5](#)). *Cry13Aa1*

was found only once in a MYBT18246 background, while *cry6Ba1* was absent, consistent with the very low abundance of MYBT18246 and MYBT18247 in the evolved material. The distribution of the MYBT18679 toxin genes differed significantly between coevolution and control conditions and between some of the coevolved and one-sided adapted populations ([Extended Data Fig. 5](#); [Supplementary Table 13](#)).

5. Functional analysis of toxin genes

We used two complementary approaches to assess the nematocidal effect of cry toxin genes from MYBT18679. On the one hand, we expressed one of the toxin genes, *cry2IAa2*, in *E. coli*, followed by *C. elegans* survival analysis. On the other hand, we introduced either *cry14Aa1* or *cry2IAa2* into a MYBT18679 variant that lost the 22.5 kb plasmid carrying these two toxin genes (denoted MYBT18679_Cry-), again followed by analysis of nematode survival.

For the former approach, the entire coding region of *cry2IAa2* was amplified by PCR (see below) and cloned into the expression vector pQE30 using standard procedures. Both the pQE30 with *cry2IAa2* and the empty vector were transferred into *E. coli* JM109 by electroporation and selection on ampicillin-containing medium (100 µg/ml). Prior to nematode survival experiments, *E. coli* was cultured at 37 °C overnight in Luria broth (LB) medium, containing ampicillin (100 µg/ml) and IPTG (200 µg/ml). The bacteria were washed twice and cell density adjusted to OD₆₀₀ = 5. Virulence of the resulting *E. coli* strains was assessed using exactly the same methods as described above for phenotypic analysis of the evolved material (chapter 1.3). The main exception was that we used an isogenic *C. elegans* strain (the standard laboratory strain N2) and standard Petri dishes instead of wormballs. Nematode survival was assessed after 48 h under six treatment conditions: (i) the ancestral MYBT18679 with cry toxins (MYBT18679_Cry+); (ii) the MYBT18679_Cry- strain lacking the two tested toxin genes; (iii) MYBT18679_Cry- combined with a low concentration of the *cry2IAa2*-expressing *E. coli* (a 1:10 dilution of the OD5-concentrated stock); (iv) MYBT18679_Cry- combined with a high concentration of *cry2IAa2*-expressing *E. coli* (the OD5-concentrated stock without any dilution); (v) only the *cry2IAa2*-expressing *E. coli* (at the OD5 stock concentration); and (vi) only the empty vector *E. coli* strain. In all cases, the empty-vector *E. coli* strain was added as food.

For the second approach, we first substituted *gfp* with a multiple cloning site (MCS) in the pHT315 *pAphA-gfp* plasmid that is used as an *E. coli*-*B. thuringiensis* shuttle vector (kindly provided by Christina Nielsen-LeRoux, Guyancourt, France). For this, the MCS of the pUC19 plasmid (Carl Roth, Germany) was amplified by PCR using Phusion High-Fidelity DNA polymerase (Thermo Scientific, Germany) and primers MCS_f and MCS_r ([Supplementary Table 21](#)). The PCR product was gel-purified (QIAquick Gel Extraction Kit and PCR purification kit, both Qiagen, Germany), digested with *Hind*III and *Xba*I, ligated with T4 DNA ligase (Thermo Scientific, Germany) into the respective sites of pHT315_ *pAphA-gfp* to create pHT315_ *pAphA*-MCS. This vector was introduced into *E. coli* Top10 (Invitrogen, US),

grown in LB with ampicillin (100 µg/ml), followed by plasmid isolation (QIAprep Spin Miniprep Kit, Qiagen, Germany). Thereafter, the entire coding regions of *cry2IAa2* and *cry14Aa1* were PCR-amplified using Phusion High-Fidelity DNA polymerase (Thermo Scientific, Germany) and the respective primers ([Supplementary Table 21](#)), digested with *SalI* and *PaeI*, ligated into pHT315_p*AphA*-MCS, followed by transformation into *E. coli* Top10, and plasmid isolation as above. *B. thuringiensis* MYBT18679_Cry- was transformed with three different vectors (containing either *cry14Aa1*, *cry2IAa2*, or the red fluorescent protein (*rfp*) as a control), using electroporation with a Bio-Rad Gene Pulser (Bio-Rad, Germany), as described previously²². Transformants were grown in LB containing erythromycin (10µg/ml) and presence of the correct inserts was confirmed by Sanger sequencing. Prior to survival experiments, the *B. thuringiensis* strains were grown for four days at 19°C on NGM, washed in S buffer, and the concentration adjusted to $1.2 * 10^8$ particles/ml, generally following the procedures outlined above for the evolution experiment. The survival experiment was performed using the same methods as above, including the N2 *C. elegans* strain and Petri dishes for exposure. The empty-vector *E. coli* strain was always added as food. Survival was tested for a total of five treatments: (i) the ancestral MYBT18679 containing all cry toxins (MYBT18679_Cry+); (ii) the MYBT18679_Cry- lacking the two toxin genes; (iii) the MYBT18679_Cry- which contains the *cry14Aa1*-expressing plasmid (MYBT18679_Cry-₊₁₄); (iv) the MYBT18679_Cry- which contains the *cry2IAa2*-expressing plasmid (MYBT18679_Cry-₊₂₁); and (v) and the MYBT18679_Cry- with the *rfp*-expressing plasmid as a control (MYBT18679_Cry-₀).

The results of the two assays are shown in [Fig. 3d](#) of the main text and the statistical results are given in [Supplementary Tables 22 and 23](#).

II. Supplementary Tables

Supplementary Table 1. Comparison between evolved and ancestral host phenotypes¹

Trait	Treatment	Transfer ²	<i>F</i>	df	<i>P</i>
Survival rate	Coevolution	12	7.72	1,12	0.0167
		20	10.79	1,14	0.0054
		28	3.63	1,13	0.0788
	Adaptation	12	0.25	1,15	0.6210
		20	4.28	1,15	0.0562
		28	0.26	1,15	0.6118
	Control	12	0.19	1,14	0.6657
		20	2.52	1,16	0.1315
		28	2.08	1,14	0.1703
Host pop. growth	Coevolution	12	2.26	1,10	0.1633
		20	0.54	1,7	0.4841
		28	4.78	1,8	0.0602
	Adaptation	12	0.99	1,9	0.3445
		20	0.47	1,10	0.5047
		28	0.32	1,11	0.5782
	Control	12	0.00	1,9	0.9372
		20	1.49	1,10	0.2497
		28	0.25	1,10	0.6229
Host body size	Coevolution	12	0.29	1,11	0.5952
		20	0.26	1,14	0.6142
		28	0.04	1,12	0.8380
	Adaptation	12	0.42	1,13	0.5242
		20	0.00	1,14	0.9963
		28	0.19	1,13	0.6638
	Control	12	0.18	1,12	0.6739
		20	0.00	1,15	0.9535
		28	0.02	1,12	0.8752
Host infection load ³	Coevolution	12	1.12	1,12	0.3113
		20	3.37	1,14	0.0877
		28	0.09	1,12	0.7733
	Adaptation	12	3.84	1,12	0.0737
		20	2.39	1,14	0.1447
		28	0.08	1,12	0.7801
	Control	12	1.06	1,11	0.3246
		20	2.23	1,15	0.1562
		28	0.03	1,12	0.8588

¹ Comparison between evolved and ancestral hosts both exposed to ancestral pathogens using an analysis of variance. Degrees of freedom (df) are given for the comparison and the error

(before and after comma, respectively). Significant values after FDR adjustment are given in bold.

² Time point is given as host transfer number.

³ Infection load is adjusted by body size.

Supplementary Table 2. Analysis of changes in host phenotypes across time and treatments¹

Trait	Factor	df	F	P
Host survival	Treatment	2	1.18	0.3155
	Transfer	2	2.91	0.0641
	Treat.*Trans.	4	1.04	0.3941
Host pop. growth	Treatment	2	1.18	0.3191
	Transfer	2	0.09	0.9096
	Treat.*Trans.	4	1.04	0.3635
Host body size	Treatment	2	0.58	0.5613
	Transfer	2	0.48	0.6216
	Treat.*Trans.	4	1.85	0.1392
Host infection load	Treatment	2	0.05	0.9464
	Transfer	2	2.86	0.0699
	Treat.*Trans.	4	0.37	0.8284

¹ The defined models included evolution treatment, transfer, the interaction between the two as fixed factors and replicate nested within treatment as a random factor. The specified models provide a better fit to the data than the corresponding minimal models ($P < 0.0001$). The table shows the results for the factor effect tests, none of which yielded a significant result.

Supplementary Table 3. Comparison between evolved and ancestral pathogen phenotypes¹

Trait	Treatment	Transfer ²	F	df	P
Killing ability	Coevolution	12	0.50	1,16	0.4858
		20	0.79	1,16	0.3869
		28	8.53	1,16	0.0100
	Adaptation	12	4.41	1,16	0.0517
		20	0.46	1,11	0.5086
		28	2.10	1,11	0.1748
	Control	12	215.88	1,15	<0.0001
		20	1715.68	1,15	<0.0001
		28	1542.75	1,14	<0.0001
Pathogen impact on host pop. growth	Coevolution	12	1.02	1,14	0.3200
		20	1.26	1,14	0.2700
		28	2.94	1,14	0.1081
	Adaptation	12	3.20	1,14	0.0949
		20	1.64	1,10	0.2287
		28	0.79	1,8	0.3975
	Control	12	21.89	1,14	0.0004
		20	95.13	1,10	<0.0001
		28	18.70	1,14	0.0007
Pathogen impact on host body size	Coevolution	12	4.89	1,14	0.0440
		20	4.19	1,13	0.0612
		28	11.84	1,15	0.0036
	Adaptation	12	0.00	1,14	0.9623
		20	0.27	1,10	0.6138
		28	0.08	1,10	0.7792
	Control	12	46.68	1,15	<0.0001
		20	111.18	1,11	<0.0001
		28	103.81	1,13	<0.0001
Pathogen infection load ³	Coevolution	12	2.79	1,14	0.1168
		20	1.83	1,14	0.1967
		28	3.95	1,15	0.0653
	Adaptation	12	4.10	1,13	0.0638
		20	3.40	1,8	0.1023
		28	5.18	1,8	0.0523
	Control	12	3.42	1,15	0.0842
		20	2.26	1,11	0.1607
		28	3.2	1,13	0.0966

¹ Comparison between evolved and ancestral pathogens both exposed to ancestral hosts using an analysis of variance. Degrees of freedom (df) are given for the comparison and the error (before and after comma, respectively). Significant values after FDR adjustment are in bold.

² Time point is given as host transfer number.

³ Infection load is adjusted by body size.

Supplementary Table 4. Analysis of the changes in pathogen phenotypes across time and treatments¹

Trait	Factor	df	F	P
Killing ability	Treatment	2	37.4	<0.0001
	Transfer	2	8.07	0.0011
	Treat.*Trans.	4	1.77	0.1577
Pathogen impact on host pop growth	Treatment	2	17.9	<0.0001
	Transfer	2	2.46	0.0984
	Treat.*Trans.	4	0.27	0.5819
Pathogen impact on host body size	Treatment	2	17.3	<0.0001
	Transfer	2	6.08	0.0054
	Treat.*Trans.	4	1.64	0.1857
Infection load	Treatment	2	10.2	0.0003
	Transfer	2	1.05	0.3597
	Treat.*Trans.	4	1.10	0.3679

¹ The defined models included evolution treatment, transfer, the interaction between the two as fixed factors and replicate nested within treatment as a random factor. The specified models provide a better fit to the data than the corresponding minimal models ($P < 0.0001$). The table shows the results for the factor effect tests. Significant probabilities are given in bold.

Supplementary Table 5. Fisher exact test of differences in the number of bacterial populations able to form biofilm¹

Comparison	Transfer	df	N²	P
Coevolution vs. Adaptation	12	1	10,9	0.0031
Coevolution vs. Control	12	1	10,10	<0.0001
Control vs. Adaptation	12	1	10,9	0.0867
Coevolution vs. Adaptation	20	1	10,7	0.0034
Coevolution vs. Control	20	1	10,8	<0.0001
Control vs. Adaptation	20	1	8,7	0.2000
Coevolution vs. Adaptation	28	1	10,4	0.2857
Coevolution vs. Control	28	1	10,8	<0.0001
Control vs. Adaptation	28	1	8,4	0.0182

¹ Time point is given as host transfer number. Significant values after FDR adjustment are given in bold.

² Sample sizes for first and second factor of the comparison, respectively.

Supplementary Table 6. Mann-Whitney U test of differences in bacterial competition

Medium ¹	Comparison ²	<i>U</i>	<i>N</i> ³	<i>P</i> ⁴
NGM	B/B vs. NB/NB	1.06	44, 45	0.2870
	B/B vs. NB/B	5.34	44, 59	<0.0001
	NB/B vs. NB/NB	4.86	59, 45	<0.0001
PF-NGM	B/B vs. NB/NB	1.02	14, 14	0.3071
	B/B vs. NB/B	-2.28	14, 23	0.0221
	NB/B vs. NB/NB	-1.48	23, 14	0.1333

¹ NGM, nutrient-rich Nematode Growth Medium; PFM, nutrient-poor Peptone-Free Medium

² B, biofilm-forming bacterial clone; NB, non-biofilm-forming clone

³ Sample sizes for first and second factor of the comparison, respectively.

⁴ Significant probabilities are given in bold.

Supplementary Table 7. Parameters and symbols of the mathematical model.

Symbol	Parameter
$B_T (B_0)$	number of toxin (non toxin) producing bacteria
$N_u (N_d)$	units of undigestible (digestible) nutrient
$b_T (b_0)$	initial number of toxin (non toxin) producing bacteria
$n_u (n_d)$	initial units of undigestible (digestible) nutrient
$r_{T1} (r_{01})$	growth rate of toxin (non toxin) producing bacteria in first phase
$r_{T2} (r_{02})$	growth rate of toxin (non toxin) producing bacteria in second phase
c	conversion coefficient from digestible nutrient into bacteria
d	host death threshold; measure for strength of host resistance
m	bacterial mortality
g	number of time steps (bacterial generations within a single host)
r	number of selection rounds

Supplementary Table 8. Statistics of the mapping of Illumina reads to the concatenated meta-reference. Table is presented as an Excel file.

Supplementary Table 9. Results for the estimation of ancestral strain frequencies in the evolved populations by mapping of diagnostic polymorphic positions. Table is presented as an Excel file.

Supplementary Table 10. Statistical analysis of the variation in strain composition across evolution treatments and time¹.

Comparison	Factor	Df	F	P
Coevolution vs. Adaptation	Treatment	2	15.5	0.001
	Transfer	1	6.0	0.004
	Treatment * Transfer	2	1.4	0.240
Coevolution vs. Control	Treatment	4	19.8	0.001
	Transfer	1	6.0	0.010
	Treatment * Transfer	3	1.7	0.155
Adaptation vs. Control	Treatment	2	51.3	0.001
	Transfer	1	1.0	0.332
	Treatment * Transfer	2	0.8	0.459

¹ We used an extended AMOVA adonis function in R package vegan. The defined model included evolution treatment, transfer, and the interactions between the two as fixed factors and replicate nested within treatment as random factor. The specified model provided a better fit to the data than the corresponding minimal model ($P < 0.0001$). The table shows the effect tests for the fixed factors. Significant probabilities are given in bold.

Supplementary Table 11. Genes and primers used for PCR-based toxin screen.

Gene	Strain	Forward primer (5'-3')	Reverse primer (5'-3')
<i>cry13Aa1</i>	MYBT18246	AATGTGCTGGGACAATCAGG	TTGGGAATTTTCTGGAACACC
<i>cry6Ba1</i>	MYBT18247	CTGTTCAAGTACAACACTAGCAC	GGCTATCTCTTTCCATTGACC
<i>cry14Aa1</i>	MYBT18679	CTAATAATGCGCGACCTACTG	GTACCAGCTATTGCACAACC
<i>cry21Aa2</i>	MYBT18679	CAACACCTTCAAATCGCATGG	CATAAGTCCTGGTTGTTCTCC
<i>cry35Aa4</i>	MYBT18679	CCAGAAGTAGGAGGAGGTACA	TTCATACCGAATGGTTTGTGAG
<i>codY</i>	all	TGAACACCAGCTTCAAGCAAT	GTTATTACAGAGCGCAGCAGG

Supplementary Table 12. Number of clones with particular chromosomal background in the evolved replicate populations.

Treatment	Transfer	Repl.	MYBT 18246	MYBT 22	MYBT 50	MYBT 18679	Total
Coevolution	12	1	0	1	1	18	20
		2	0	0	0	20	20
		3	0	1	0	19	20
		4	0	0	0	20	20
		5	0	1	0	19	20
		6	0	0	0	20	20
		7	0	0	0	20	20
		8	0	0	0	20	20
		9	0	0	0	20	20
		10	0	0	0	20	20
Coevolution	20	1	0	0	0	20	20
		2	0	0	0	20	20
		3	0	0	0	20	20
		4	0	0	0	20	20
		5	0	0	0	20	20
		6	0	0	0	20	20
		7	1	0	0	19	20
		8	0	3	0	17	20
		9	0	0	0	20	20
		10	0	0	0	20	20
Control	12	1	0	19	0	1	20
		2	0	20	0	0	20
		3	0	19	1	0	20
		4	0	15	0	5	20
		5	0	2	18	0	20
		6	0	9	11	0	20
		7	0	12	8	0	20
		8	0	17	3	0	20
		9	0	11	6	3	20
		10	0	17	3	0	20
Control	20	1	0	20	0	0	20
		2	0	20	0	0	20
		3	0	20	0	0	20
		4	0	20	0	0	20
		5	0	20	0	0	20
		6	0	20	0	0	20
		7	0	20	0	0	20
		9	0	20	0	0	20
		10	0	20	0	0	20
		Adaptation	12	1	0	20	0
2	0			0	0	20	20
3	0			0	0	20	20

		4	0	0	0	20	20
		5	0	20	0	0	20
		6	0	0	0	20	20
		7	0	2	18	0	20
		8	0	1	19	0	20
		9	0	0	12	8	20
		10	0	0	20	0	20
<hr/>							
Adaptation	20	2	0	20	0	0	20
		3	0	0	1	19	20
		4	0	1	0	19	20
		6	0	0	0	20	20
		9	0	0	0	20	20
		10	0	0	20	0	20

Supplementary Table 13. Statistical analysis of the variation in toxin gene composition across evolution treatments and time¹.

Comparison	Factor	df	χ^2	<i>P</i>
Coevolution vs. Adaptation	Treatment	5	< 0.01	>0.99
	Transfer	5	10.9	0.0544
	Treatment * Transfer	5	48.3	< 0.0001
Coevolution vs. Control	Treatment	5	96.3	< 0.0001
	Transfer	5	7.1	0.2129
	Treatment * Transfer	5	54.5	< 0.0001
Adaptation vs. Control	Treatment	4	< 0.01	> 0.99
	Transfer	4	69.6	< 0.0001
	Treatment * Transfer	4	2.55	0.6358

¹ The defined nominal logistic models included evolution treatment, transfer, and the interactions between the two as fixed factors and replicate nested within treatment as random factor. The specified models provided a better fit to the data than the corresponding minimal model ($P < 0.0001$). The table shows the effect tests for the fixed factors. Significant probabilities are given in bold.

Supplementary Table 14. Results of the analysis of SNPs and short indels in the MYBT18679-dominated populations. Table is presented as an Excel file.

Supplementary Table 15. Results of the Pindel analysis of structural variation in the MYBT18679-dominated populations. Table is presented as an Excel file.

Supplementary Table 16. Results of the analysis of copy number variation in the MYBT18679-dominated populations. Table is presented as an Excel file.

Supplementary Table 17. Results of the analysis of horizontal gene transfer to the MYBT18679 genotype. Table is presented as an Excel file.

Supplementary Table 18. Results of the analysis of copy number variation for entire contigs in the MYBT18679-dominated populations. Table is presented as an Excel file.

Supplementary Table 19. Results for the population genetic analysis of the MYBT18679-dominated populations. Table is presented as an Excel file.

Supplementary Table 20. Summary of significant variations in the fine-scale genomic analysis of the MYBT18679-dominated populations. Table is presented as an Excel file.

Supplementary Table 21. Primers used during functional analysis of cry toxins

Primer	Sequence (5'-3')
MCS_f	GATGACGGTGAAAACCTCTG
MCS_r	GCCTTTGAGTGAGCTGATAACC
21clo-Fc	GCGGTCGACgaaaggaggtttataaaATGACAAATCCAAC TATACTATATC
21clo-R	GCGGGGCATGCGATTAAGAAACGAGATGAATAC
14Aclo-Fc	GCGGTCGACgaaaggaggtttataaaATGGATTGTAATTTACAATCAC
14Aclo-R	GCGGGGCATGCTGTATGGTGAGATTTACAAG

Supplementary Table 22. Statistical analysis of nematode survival after exposure to cry-toxin-expressing *B. thuringiensis*¹

Reference	Comparison	Z	P
MYBT18679_Cry-	MYBT18679_Cry+	3.44	0.0023
	MYBT18679_Cry-_+14	3.05	0.0092
	MYBT18679_Cry-_+21	1.62	0.4190
	MYBT18679_Cry-_0	0.04	>0.99
MYBT18679_Cry+	MYBT18679_Cry-_+14	0.35	>0.99
	MYBT18679_Cry-_+21	1.77	0.3045
	MYBT18679_Cry-_0	3.35	0.0032

¹ Non-parametric comparisons with control using Dunn method for joint ranking, as implemented in JMP 9.0.2 (SAS Institute Inc.). Significant probabilities are given in bold. Strain abbreviations: MYBT18679_Cry-, MYBT18679 without plasmid which contains the toxin genes *cry14Aa1* and *cry21Aa2*; MYBT18679_Cry+, MYBT18679 wildtype with the toxin-containing plasmids; MYBT18679_Cry-_+14, MYBT18679_Cry- with a *cry14Aa1*-expressing vector; MYBT18679_Cry-_+21, MYBT18679_Cry- with a *cry21Aa2*-expressing vector; MYBT18679_Cry-_+0, MYBT18679_Cry- with a *rfp*-expressing vector as a negative control.

Supplementary Table 23. Statistical analysis of nematode survival after exposure to cry-toxin-expressing *E. coli*¹

Reference	Comparison	Z	P
MYBT18679_Cry-	MYBT18679_Cry+	3.44	0.0030
	MYBT18679_Cry-+EC21_low	-1.20	>0.99
	MYBT18679_Cry-+EC21_high	2.06	0.1947
	EC21	-3.00	0.0137
	EC0	-3.13	0.0084
MYBT18679_Cry+	MYBT18679_Cry-+EC21_low	4.64	<0.0001
	MYBT18679_Cry-+EC21_high	1.36	0.8722
	EC21	-6.52	<0.0001
	EC0	-6.44	<0.0001

¹ Non-parametric comparisons with control using Dunn method for joint ranking, as implemented in JMP 9.0.2 (SAS Institute Inc.). Significant probabilities are given in bold. Strain abbreviations: MYBT18679_Cry-, MYBT18679 without plasmid which contains the toxin genes *cry14Aa1* and *cry21Aa2*; MYBT18679_Cry+, MYBT18679 wildtype with the toxin-containing plasmids; MYBT18679_Cry-+14, MYBT18679_Cry- with a *cry14Aa1*-expressing vector; MYBT18679_Cry-+21, MYBT18679_Cry- with a *cry21Aa2*-expressing vector; MYBT18679_Cry-+0, MYBT18679_Cry- with a *rfp*-expressing vector as a negative control.

III. References

- 1 Teotonio, H., Carvalho, S., Manoel, D., Roque, M. & Chelo, I. M. Evolution of outcrossing in experimental populations of *Caenorhabditis elegans*. *PLoS One* **7**, e35811, (2012).
- 2 Stiernagle, T. Maintenance of *C. elegans*. in *WormBook* (ed The *C. elegans* Research Community) doi/10.1895/wormbook.1.101.1 (2006).
- 3 Schulte, R. D., Makus, C., Hasert, B., Michiels, N. K. & Schulenburg, H. Multiple reciprocal adaptations and rapid genetic change upon experimental coevolution of an animal host and its microbial parasite. *Proc Natl Acad Sci U S A* **107**, 7359-7364, (2010).
- 4 Masri, L. *et al.* Sex differences in host defence interfere with parasite-mediated selection for outcrossing during host-parasite coevolution. *Ecol Lett* **16**, 461-468, (2013).
- 5 Bentley, D. R. *et al.* Accurate whole human genome sequencing using reversible terminator chemistry. *Nature* **456**, 53-59, (2008).
- 6 Langmead, B., Trapnell, C., Pop, M. & Salzberg, S. L. Ultrafast and memory-efficient alignment of short DNA sequences to the human genome. *Genome Biol* **10**, R25, (2009).
- 7 Li, H. & Durbin, R. Fast and accurate short read alignment with Burrows-Wheeler transform. *Bioinformatics* **25**, 1754-1760, (2009).
- 8 MOSAIK read alignment and assembly program (2009).
- 9 Li, R., Li, Y., Kristiansen, K. & Wang, J. SOAP: short oligonucleotide alignment program. *Bioinformatics* **24**, 713-714, (2008).
- 10 Wu, T. D. & Nacu, S. Fast and SNP-tolerant detection of complex variants and splicing in short reads. *Bioinformatics* **26**, 873-881, (2010).
- 11 Darling, A. E., Mau, B. & Perna, N. T. progressiveMauve: multiple genome alignment with gene gain, loss and rearrangement. *PLoS One* **5**, e11147, (2010).
- 12 Wei, Z., Wang, W., Hu, P., Lyon, G. J. & Hakonarson, H. SNVer: a statistical tool for variant calling in analysis of pooled or individual next-generation sequencing data. *Nucleic Acids Res* **39**, e132, (2011).
- 13 modeest: Mode estimation. (2012).
- 14 Team R. R: A language and environment for statistical computing. R Foundation for Statistical Computing Vienna Austria, www.cran.r-project.org, (2010).
- 15 Kim, S. Y. *et al.* Estimation of allele frequency and association mapping using next-generation sequencing data. *BMC Bioinformatics* **12**, 231, (2011).
- 16 Ye, K., Schulz, M. H., Long, Q., Apweiler, R. & Ning, Z. Pindel: a pattern growth approach to detect break points of large deletions and medium sized insertions from paired-end short reads. *Bioinformatics* **25**, 2865-28671, (2009).
- 17 Abyzov, A., Urban, A. E., Snyder, M. & Gerstein, M. CNVnator: an approach to discover, genotype, and characterize typical and atypical CNVs from family and population genome sequencing. *Genome Res* **21**, 974-984, (2011).
- 18 Yoon, S., Xuan, Z., Makarov, V., Ye, K. & Sebat, J. Sensitive and accurate detection of copy number variants using read depth of coverage. *Genome Res* **19**, 1586-1592, (2009).
- 19 Loo, M. P. J. van der. extremevalues, an R package for outlier detection in univariate data. www.cran.r-project.org, (2010).
- 20 Begun, D. J. *et al.* Population genomics: whole-genome analysis of polymorphism and divergence in *Drosophila simulans*. *PLoS Biol* **5**, e310, (2007).

-
- 21 Benjamini, Y. & Hochberg, Y. Controlling the false discovery rate: a practical and powerful approach to multiple testing. *J. R. Stat. Soc. B* **57**, 289-300, (1995).
- 22 Peng, D. *et al.* Elaboration of an electroporation protocol for large plasmids and wild-type strains of *Bacillus thuringiensis*. *J Appl Microbiol* **106**, 1849-1858, (2009).

Curriculum vitae

Address: Calvinstr. 11, 21114 Kiel, Germany

E-mail: apapkou@zoologie.uni-kiel.de

Phone: +49 431 880 4139

Personal information

Date of birth: 3.11.1985

Place of birth: Segezha, Russia

Marital status: Single

Nationality: Belarusian

Education

since 12/2009: PhD student, Department of Evolutionary Ecology and Genetics, University of Kiel, Germany

9/2008-7/2009: Master in Biology, National Academy of Sciences of Belarus, Minsk, Belarus

9/2003-6/2008: Diploma degree in Biology, Belarus State University, Minsk, Belarus

9/2001-6/2003: Secondary school education, Luzhesna, Belarus

9/1992-6/2001: School education, Barouka, Belarus

Research experience

since 12/2009-2014 PhD student (Supervisor Prof. Hinrich Schulenburg)

DEPARTMENT OF EVOLUTIONARY ECOLOGY AND GENETICS, UNIVERSITY OF KIEL

08/2009-11/2009 Junior scientist

INSTITUTE OF GENETICS AND CYTOLOGY, NATIONAL ACADEMY OF SCIENCES OF BELARUS

9/2008-7/2009 Master student

INSTITUTE OF GENETICS AND CYTOLOGY, NATIONAL ACADEMY OF SCIENCES OF BELARUS

Thesis "Diversity of Y-chromosome molecular markers in Belarusians"

Professional membership

European Society for Evolutionary Biology (since 2013)

Acknowledgments

Finishing my project, I realized that this few years of PhD were much more about studying people than those one-thousand-cell creatures, which always make their best to fool us. This wonderful period of my life was full of ups and downs, and now turning the page I see how much I have changed (and, hopefully, not only got older). If so, all the people who supported me and who were around to share the moments of inspiration and disappointment have made a contribution to what I achieved and who I am now.

First of all, I would like to thank Silvia Dähn, as her warm welcome and hospitality made me feel at home in the very first month abroad.

I am deeply grateful to Hinrich Schulenburg, who gave me such a great opportunity to join the group and to work on the project. Thank you for always offering help and for being patient, for encouraging me and for letting me be creative, for providing everything what a PhD student may need. As your student, I had no chance to be disappointed in science, and especially not in evolutionary biology.

I am very much thankful to many various people from universities of Münster, Osnabrück and Göttingen involved in the Bacillus Cluster for your fantastic feedback and useful discussions, which did improve many aspects of this PhD project. Also I really enjoyed a very productive collaboration with Chaitanya Gokhale, Arne Traulsen and Yixian Song from MPI in Plön.

This project could not be finished without great support from Rebecca Schalkowski, Mike Barg and Ines Braker. I am glad that, having being exposed to each other for hours and hours of lab work, we established very good professional and, most important, friendly relationship.

Dear EvoEcoGen group! I really enjoyed your very vibrant and interactive atmosphere. What is most valuable is the diversity of people interests in our group. I was always fascinated by all of you. Our social events and outdoor activities were particularly exciting and unforgettable. Refreshing walks along the Baltic sea with Christiana Anagnostou; adventurous travels around SH and beyond with Gunther Jansen; short but exhausting volleyball sessions with the “happy three friends”, Carola Peterson, Barbara Pees and Camilo Barbosa. I am very thankful to Philipp Dirksen for always being genuinely concerned with how I was doing and for his spontaneous and brilliant ideas how to spend Friday evenings. I am really grateful to my nice and intelligent office-mates – Charlotte Rafaluk and Wentao Yang, who proved to be reliable companions for any serious scientific dispute in a pub. Charlotte, if not being your office-mate, I would have to write this thesis in Belarusian. Katja Dierking, Tim Moor, Rania Nakad, Alejandra Zárate-Potes, Christina Griebner, Antje Thomas and many students, thank you all for your help and socializing!

As much as I was looking forward to new people joining our group, I felt sad when anyone were leaving. I remember and appreciate the contribution of the former members – Monika Trienens, Aurore Dubuffet, Leila Masri, Anna Sheppard,

Gerrit Joop and, of course, Andreas Mitschke.

This thesis would not have been possible unless the constant support from my friends in Germany, in Belarus and elsewhere, who made my life brighter and eventful. I am greatly indebted to my dear parents and brother, as I left them for my studies, but their love is always reaching me.

I would like to thank my beloved Inga for her understanding and love during the past few years. My life has changed since I met you...

Thank your all!